

**Product Design and Development of Innovative Air Cooler
with Desiccant-based Dehumidification**



Project/Thesis ID. 2023: 111

Session: BSc. Spring 2020

Project Supervisor: Prof. Muzaffar Ali

Submitted By:

**Danyal Iqbal
Muhammad Hassan Ameer
Muhammad Talha Aziz
Abdullah Rafique**

[Mechanical Engineering]

[University of Engineering and Technology Taxila, Pakistan]

Certification

This is to certify that [M. Arshad Naveed], [20-ME-18], [Shahmeer Ahmed] [20-ME-74] [M. Abdullah Khan] [20-ME-94] and [Zain Ul Aabideen] [20-ME-170] have successfully completed the final project **Product Design and Development of Indirect Evaporative Cooler with Desiccant-Based Dehumidifier**, at the **University of Engineering and Technology, Taxila** , to fulfill the partial requirement of the degree **BSc. Mechanical Engineering**.



Neutral Examiner

Dr. Abid Hussain

Assistant Professor



Project Supervisor

Dr. Muzaffar Ali

Professor



Chairman

Prof. Dr. Riffat Asim Pasha

Department of Mechanical Engineering, UET Taxila

Product Design and Development of Innovative Air Cooler with Desiccant-based Dehumidification Sustainable Development Goals

(Please tick the relevant SDG(s) linked with FYDP)

SDG No	Description of SDG	SDG No	Description of SDG
SDG 1	No Poverty	SDG 9	Industry, Innovation, and Infrastructure
SDG 2	Zero Hunger	SDG 10	Reduced Inequalities
SDG 3	Good Health and Well Being <input checked="" type="checkbox"/>	SDG 11	Sustainable Cities and Communities
SDG 4	Quality Education	SDG 12	Responsible Consumption and Production
SDG 5	Gender Equality	SDG 13	Climate Change <input checked="" type="checkbox"/>
SDG 6	Clean Water and Sanitation	SDG 14	Life Below Water
SDG 7	Affordable and Clean Energy <input checked="" type="checkbox"/>	SDG 15	Life on Land
SDG 8	Decent Work and Economic Growth	SDG 16	Peace, Justice and Strong Institutions
		SDG 17	Partnerships for the Goals



Range of Complex Problem Solving		
	Attribute	Complex Problem
1	Range of conflicting requirements	Involve wide-ranging or conflicting technical, engineering and other issues.
2	Depth of analysis required	Have no obvious solution and require abstract thinking, originality in analysis to formulate suitable models.
3	Depth of knowledge required	Requires research-based knowledge much of which is at, or informed by, the forefront of the professional discipline and which allows a fundamentals-based, first principles analytical approach.
4	Familiarity of issues	Involve infrequently encountered issues
5	Extent of applicable codes	Are outside problems encompassed by standards and codes of practice for professional engineering.
6	Extent of stakeholder involvement and level of conflicting requirements	Involve diverse groups of stakeholders with widely varying needs.
7	Consequences	Have significant consequences in a range of contexts.
8	Interdependence	Are high level problems including many component parts or sub-problems
Range of Complex Problem Activities		
	Attribute	Complex Activities
1	Range of resources	Involve the use of diverse resources (and for this purpose, resources include people, money, equipment, materials, information and technologies).
2	Level of interaction	Require resolution of significant problems arising from interactions between wide ranging and conflicting technical, engineering or other issues.
3	Innovation	Involve creative use of engineering principles and research-based knowledge in novel ways.
4	Consequences to society and the environment	Have significant consequences in a range of contexts, characterized by difficulty of prediction and mitigation.
5	Familiarity	Can extend beyond previous experiences by applying principles-based approaches.

Abstract

Demand of air cooling is on-rise due to global warming and increasing population, especially in developing countries, like Pakistan. One of the challenges of the present time is to meet exponentially growing cooling requirements. In this regard, dew point indirect evaporative cooling (DP-IEC) is proposed which is an energy efficient and low operational cost alternative, for space air cooling especially in the dry and hot climate conditions. For this purpose, several design variant prototypes of the DP-IEC are fabricated through the development of heat and mass exchanger (HMX) which has differ in geometries, working air flow patterns, and efficient materials to ensure the high wettability and low weight to volume ratio. The maximum design thermal capacity of the system is achieved up to 1 Ton at maximum flow rate of air around 250 CFM. The resultant maximum dew point and wet bulb effectiveness are 0.76 and 1.11, respectively. Whereas, the coefficient of performance, energy efficiency ratio, and cooling capacities of different design variant prototypes are achieved up to 16.3, 55.7, and 3.3 kW, respectively. In addition, the DP-IEC is evaluated for reduced the water footprint of the prototype. The water footprint analysis indicates that DP-IEC will be used in awater-scarce country. So, this research work shows that DP-IEC which uses significantly lessenergy and improved water footprint is suitable for several areas of the world.

Keywords: Dew Point IEC; Maisotsenko Cycle; Thermal Effectiveness; Energy Efficiency Ratio; Water Recovery; Water Footprint.

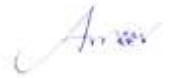
Undertaking

I certify that the project **Product Design and Development of Indirect Evaporative Cooler with Desiccant-Based Dehumidifier** is our own work. The work has not, in whole or in part, been presented elsewhere for assessment. Where material has been used from other sources it has been properly acknowledged/ referred.



Danyal Iqbal

19-ME-42



Muhammad Hassan Ameer

19-ME-47



Muhammad Talha Aziz

19-ME-107



Abdullah Rafique

19-ME-105

Acknowledgement

We truly acknowledge the cooperation and help made by **Dr. Muzaffar Ali**, a professor at the Department of Mechanical and Aeronautical Engineering, UET Taxila for providing us with the opportunity to work on the project titled "Product Design and Development of Indirect Evaporative Cooler with Desiccant Based Dehumidifier". Additionally, we are thankful for his constant guidance and support, which allowed us to learn extensively about the topic and develop a better understanding of the subject matter. We are also grateful to our parents for their assistance in our career progress. We acknowledge the support of everyone who helped us to transform our ideas into reality.

TABLE OF CONTENTS

Certification	ii
Abstract	v
Undertaking.....	vi
Acknowledgement	vii
LIST OF FIGURES	xii
LIST OF TABLES	xvi
List of Acronyms	xvii
Chapter 1	20
1.1 Introduction.....	20
1.2 Problem Statement	20
1.3 Aim and Objectives	21
1.4 Direct evaporative cooler	21
1.5 Maisotsenko cycle (M-cycle).....	22
1.6 Water recovery from exhaust air	22
1.7 Research methods	23
1.8 Report overview	24
Chapter 2	25
2.1 Literature Review.....	25
2.2 Research Gap	28
Chapter 3	29
3.1 Design of multiple configurations of DP-IEC.....	29
3.2 Design of the dry and wet channels	29
3.2.1 Design of the air flow patterns	31
3.3 Design of multiple configurations of DP-IEC.....	32
3.3.1 Design of DP-IEC 01	32
3.3.2 Design of DP-IEC 02	33
3.3.3 Design of DP-IEC 03	34
3.3.4 Design of the DP-IEC for higher capacities.....	35
3.4 Design of the water recovery system	36
3.5 Silica gel	37

3.6 Coating Techniques	39
3.6.1 Dip Coating	39
3.6.2 Spray Coating.....	40
3.6.3 Direct Synthesis	40
Chapter 4.....	42
4.1 Experimental Setup.....	42
4.2 Experimental setups of the design variant prototype (DVP)	42
4.2.1 Design variant prototype 01	42
4.2.1.1 Manufacturing of the HMX	42
4.2.1.2 Experimental setup of DVP 01	44
4.2.2 Design variant prototype 02.....	45
4.2.2.1 Fabrication of the HMX.....	45
4.2.2.2 Experimental setup of DVP 02	45
4.2.3 Design variant prototype 03.....	46
4.2.3.1 Manufacturing of the HMX	46
4.2.3.2 Experimental setup of the DVP 03	49
4.2.4 Design variant prototype 04.....	50
4.2.4.1 Fabrication of the HMX.....	50
4.2.4.2 Experimental setup of the DVP 04	51
4.2.5 Design variant prototype 05	52
4.2.5.1 Manufacturing of the HMX	52
4.2.5.2 Experimental setup of the DVP 05	54
4.2.6 Design variant prototype 06.....	55
4.2.6.1 Fabrication of the HMX.....	55
4.2.6.2 Experimental setup of the DVP 06	56
4.2.6.3 Final product	57
4.2.7 Technical issues	58
4.3 Experimental setups for water recovery	62
4.3.1 Experimental setup of water recovery 01	62
4.3.1.1 Fabrication of the water recovery system	62
4.3.1.2 Experimental setup of water recovery system 01	63
4.3.2 Experimental setup of water recovery system 02	65
4.4 Real-time testing	65
4.4.1 Cloth selection for wettability.....	65

Product Design and Development of Innovative Air Cooler with Desiccant-based Dehumidification

4.4.1.1 Soaking effect on the bonding strength in fabric and plastics sheet	66
4.4.1.2 Cooling/heating effect on bonding strength.....	67
4.4.2 The wettability	68
4.4.2.1 The assessment of wettability in the wet channels	68
4.5 Measuring instruments and procedure	69
4.6 Performance parameters	72
4.7 The CFM assessment	73
4.8 The assessment of pressure losses	74
4.9 Uncertainty Analysis.....	76
4.10 Velocity distributions through channels	77
4.10.1 Velocity distribution through channels of DVP 03.....	77
4.10.2 Velocity distribution through channels of the DVP 06.....	78
4.11 Fabrication of Dehumidification Bed	79
4.11.1. Laser Cutting of Acrylic Sheets to make Ducts.....	79
4.11.2. Silica gel coating on thin Aluminium Sheets using Dip Coating Method.....	80
4.12. Instrumentation and Measurements	82
4.13. Experimental Setup of Dehumidification Bed	83
4.14. Experimental Readings of Dehumidification Bed.....	84
4.15. Experimental Setup of HMX with Dehumidification Bed	85
Chapter 5.....	86
5.1 Results and Discussion	86
5.2 The effect of the ambient air temperature on performing indicators	86
5.2.1 The effect of ambient temperature on temperature difference.....	86
5.2.2 The effect of ambient temperature on dew point effectiveness	87
5.2.3 The effect of ambient temperature on wet bulb effectiveness	87
5.2.4 The effect of ambient temperature on cooling capacity.....	88
5.2.5 The effect of ambient temperature on COP	88
5.2.6 The effect of ambient temperature on energy efficiency ratio (EER).....	89
5.3 Effect of the water temperature on performing indicators.....	89
5.4 Effect of the water flow on performing indicators.....	90
5.4.1 The effect of water flow on supply air temperature.....	91
5.4.2 The effect of water flow on working air temperature	91
5.4.3 The effect of water flow on the effectiveness of the system.....	91
5.4.4 The effect of water flow on cooling capacity	92

Product Design and Development of Innovative Air Cooler with Desiccant-based Dehumidification

5.4.5 The effect of water flow on COP 93

5.4.6 The effect of water flow on EER 93

5.5 Water Recovery 94

5.5.1 Water consumption of the system 94

5.5.2 Water footprint reduction 95

5.6. Water Absorbed by Air Using Psychrometric Chart 95

Chapter 6 1

6.1 Conclusion and Future Recommendations 1

6.1.1 Conclusion 1

6.1.2 Future recommendations 3

Appendix 3

Appendix A: Design specifications and operating parameters of some design variant
prototypes (DVPs) 3

Appendix B: Entrance and exit pressure loss coefficients for multiple square tube core with
abrupt contraction and abrupt expansion (Source: kays and London, 1998.) 5

References 6

Annexure 12

LIST OF FIGURES

Figure 1.1: Schematic diagram of indirect evaporative cooling system, (a) process diagram, (b) process flow on psychrometric chart	20
Figure 1.2: Schematic diagram of the direct evaporative cooling system, (a) process diagram, (b) process flow on psychrometric chart.....	22
Figure 1.3: Process flow of M-cycle on psychrometric chart (source: presentation of Dr. Valeriy S. Maisotsenko in I ² CNER at Kyushu University).....	22
Figure 1.4: Membrane condenser (Source: membrane condenser as emerging technology for water recovery)	23
Figure 1.5: Research methodology	24
Figure 3.1: Working process of dewpoint indirect evaporative cooler (centerline perforated holes); (a) wet channel (b) dry channel.....	31
Figure 3.2: Working process of dewpoint indirect evaporative cooler (extreme left side perforated holes); (a) dry channel (b) wet channel	32
Figure 3.3: Complete design of the DP-IEC 01	33
Figure 3.4: 3D design of DVP-02 (a) front view of the complete design, (b) Labelling of the complete design, (c) HMX assembly with axial fan, pump, and water tank	34
Figure 3.5: Complete design of the DVP-03, (a) cross section view, (b) blur view, (c) complete system with labelled parts of the design	35
Figure 3.6: Multiple stacks design with different views, (a) symmetric view with several HMX stacks, (b) blur view, (c) labelling of multiple stack's complete model	36
Figure 3.7: 3D model of the water recovery system.....	37
Figure 3.8: Silica gel.....	38
Figure 4.1: Different fabrication phases of DVP 01 (a) laser cutting machine, (b) acrylic dividers (c), (d) joining the acrylic dividers with wet and dry channels by silicone, (d) cottoncloth, (e) joining the acrylic dividers with aluminum sheet.....	43
Figure 4.2: Different fabrication phases (a) holes creation in the dry channel, (b) zig zag holes pattern, (c) copper pipes with holes for water flow, (d) pump used for pumping the water in the wet channels.....	44
Figure 4.3: Experimental setup of the design variant prototype 01	44
Figure 4.4: Different fabrication phases (a) aluminum foil, (b) acrylic dividers, (c) joining acrylic dividers and aluminum foil, (d) create holes in zig-zag pattern.....	45
Figure 4.5: The apparatus diagram of the design variant prototype 02	46

Figure 4.6: Different materials used (a) polypropylene nonwoven fabric, (b) A ₃ laminated plastics sheet, (c) holes pattern on sheet, (d) attaching dividers on plastic sheet with sementex bond	47
Figure 4.7: Fabrication phases (a) dry and wet channels after preparation, (b) joining dry and wet channels to fabricate the HMX	47
Figure 4.8: Dry and wet channels of the DVP 03	48
Figure 4.9: Different views of HMX of design variant prototype 03 (a) process air side view, (b) product air side view, (c) top view, (d) working air exhaust side view	48
Figure 4.10: The HMX of the design variant prototype 03 with duct	49
Figure 4.11: Experimental setup of the DVP 03 integrated with ACLU	50
Figure 4.12: Different views of the HMX of DVP 04 (a) working air side view, (b) symmetric view.....	50
Figure 4.13: Assembly phases of DVP 04 (a) axial fan, (b) axial fan with external assembly, (c) HMX with external assembly, (d) fixing HMX and water storage sump.....	51
Figure 4.14: Experimental setup of the design variant prototype 04.....	52
Figure 4.15: Fabrication process of DVP 05, (a) scrubbing of solution with brush, (b) joining non-woven fabric with A ₃ sheet (c) acrylic dividers, (d) applying the primer	53
Figure 4.16: Dry and wet channels of the DVP 05	53
Figure 4.17: Different views of the HMX of DVP 05, (a) front view, (b) back view, (c) top view, (d) bottom view	54
Figure 4.18: The experimental setup of the design variant prototype 05	54
Figure 4.19: Different assembly steps of the HMX of DVP-06, (a) piling up dry and wet channels, (b) channels assembly, (c), channel assembly with supports, (d) symmetric view of HMX.....	55
Figure 4.20: Design variant prototype 06 (a) rear view, (b) front view.....	56
Figure 4.21: The experimental setup of design variant prototype 06 (Internal view).....	56
Figure 4.22: The experimental setup of design variant prototype 06 with measuring sensors (External view).....	57
Figure 4.23: Different assembly steps of the final product, (a) HMX, (b) HMX fixed in external casing, (c) back view of the final product.....	58
Figure 4.24: The materials used for the water recovery system, (a) hydrophobic sheets, (b) mesh cloth, (c) sewing the hydrophobic sheet and mesh cloth, (d) stainless steel mesh...	63
Figure 4.25: Making a filter type arrangement, (a) fixing the hydrophobic sheet by using SS mesh, (b) closing the top and bottom sides, (c) filter type array.....	63

Figure 4.26: Experimental setup of water recovery system with hydrophobic type filter.....	64
Figure 4.27: Experimental system of water recovery with dehumidifier	65
Figure 4.28: Different types of cloths, (a) cotton cloth, (b) fabric cloth, (c) mesh cloth, (d) non-woven cloth.....	66
Figure 4.29: PP sheets dipped in water container, (a) partially dipped, (b) completely dipped	67
Figure 4.30: PP sheet condition after, (a) soaking, (b) evaporation.....	67
Figure 4.31: Cooling and heating effect on bonding strength.....	68
Figure 4.32: Exhaust working air with water droplets from the wet channels	69
Figure 4.33: Top view of the HMX	69
Figure 4.34: Pictures of temperature measuring instruments (a) digital thermometer (TP 300), (b) thermometer type k/j (TM-82N), (c) temperature humidity meter datalogger (TM-182), (d) IR thermometer (FLUKE 62 MAX), (e) thermometer	70
Figure 4.35: Pictures of humidity and velocity measuring instruments, (a) digital humidity meter, (b) mini anemometer (UT363), (c) digital anemometer (MS6252B), (d) hot wire anemometer (AM-4204)	71
Figure 4.36: U-tube barometer.....	71
Figure 4.37: Photograph of water level measurement (a) upper level, (b) lower-level	72
Figure 4.38: Velocity distribution of the process air through channels of DVP 03.....	77
Figure 4.39: The variation of process air velocity through channels of DVP 03	78
Figure 4.40: Velocity distribution of process air through channels of DVP 06.....	79
Figure 4.41: Ducts with Coated Aluminium Sheets.....	80
Figure 4.42: Silica Gel Coating on Aluminium Sheets.....	81
Figure 4.44: Single Channel Digital Thermometer.....	82
Figure 4.43: Two-channel digital thermometer.....	82
Figure 4.45: Relative Humidity Meter.....	82
Figure 4.46: Experimental Setup of Dehumidification Bed.....	83
Figure 4.47: Experimental Setup of HMX with Dehumidification Bed.....	85
Figure 5.1: Temperature difference in dry channels of various DVPs	87
Figure 5.2: Dew point effectiveness of various DVPs.....	87
Figure 5.3: Wet bulb effectiveness of the various DVPs.....	88
Figure 5.4: Variation of CC with ambient air temperature (T_{in}).....	88
Figure 5.5: Coefficient of performance (COP) variation.....	89

Product Design and Development of Innovative Air Cooler with Desiccant-based Dehumidification

Figure 5.6: Energy efficiency ratio (EER) of the systems	90
Figure 5.7: Effect of water temperature on temperature difference	90
Figure 5.8: Supply air temperature with/without water flow in wet channels	91
Figure 5.9: Working air temperature with/without water flow in wet channels	92
Figure 5.10: Effectiveness of the system with/without water flow in wet channels	92
Figure 5.11: Variation in cooling capacity of the system	93
Figure 5.12: COP of the system with/without water flow	93
Figure 5.13: Energy efficiency ratio of the system	94
Figure 5.14: Water consumption of the system	94
Figure 5.15: Amount of water recovery from exhaust air	95
Figure 5.16: Psychrometric Chart Analysis	95

LIST OF TABLES

Table 2.1: Earlier experimental, mathematical, and simulation investigations for DP-IEC....	27
Table 3.1: Specifications of design variant prototypes.....	29
Table 3.2: 2D design of dry and wet channel with dimensions.....	30
Table 3.3: Comparison of three types of Coating Techniques.....	39
Table 4.1: Materials used and technical problems in the development of HMX prototypes...	58
Table 4.2: Different heat and mass exchangers (HMX).....	61
Table 4.3: Design specifications and operating parameters of water recovery system.....	64
Table 4.4: Specifications of the cloth materials.....	65
Table 4.5: Bonding strength of PP sheet with plastics.....	66
Table 4.6: The specifications of the instruments.....	69
Table 4.7: Operating parameters of the design variant prototypes.....	73
Table 4.8: The CFM of different design variant prototypes.....	74
Table 4.9: Operating parameters and conditions.....	74
Table 4.10: Measuring uncertainties of the instruments.....	76
Table 4.11: Uncertainties of performance indicators.....	76
Table 4.12: Experimental Readings of Dehumidification Bed.....	84
Table 5.1: Volumetric flow rates of DVPs.....	86

List of Acronyms

Symbol	Description	Units
ACLU	Air conditioning laboratory unit	–
ACLT	Air conditioning laboratory trainer	–
A	Area	m ²
CC	Cooling capacity	W
CFM	Cubic feet per minute	cu ft/m
CFC	Chlorofluorocarbon	–
COP	Coefficient of performance	–
C_p	Specific heat	kJ/kg
D	Diameter	mm
DEC	Direct evaporative cooler	–
DP-IEC	Dew point indirect evaporative cooler	–
DVP	Design variant prototype	–
EER	Energy efficiency ratio	–
F	Frictional effect	
G	Core mass velocity	kg/m ² s
GHG	Greenhouse gas	–
H	Height	mm
ΔH	Sensible enthalpy	J/kg
HMX	Heat and mass exchanger	–
HVAC	Heating, ventilation, and air conditioning	–
IEC	Indirect evaporative cooler	–
K	Viscous stress	N/m ²
K	Thermal conductivity	W/mK
K_c	Coefficient of contraction	–
K_e	Coefficient of expansion	–
L	Length	mm
ṁ	Mas flow rate	kg/s
M-cycle	Maisotsenko cycle	–
N	Coordinates	–
pA	Absolute pressure	atm
P	Pressure	Pa

PVC	Polyvinyl chloride	–
Q	Heat source	W/m ³
Q_m	Mass source	Kgm ³ s
Q	Absorption coefficient	W/m ³ K
R	Radius	m
R	Gas constant	J/kgK
Re	Reynolds number	–
RH	Relative humidity	–
SS	Stainless steel	–
T	Temperature	°C
ΔT	Temperature difference	°C
Th	Thickness	mm
U	Inflow velocity	m/s
V	Velocity	m/s
V	Volumetric flow rate	m ³ /h
VCS	Vapor compression system	–
W	Width	mm
Ẇ	Total power consumption	W
X	Height of channel	mm
Y	Width of channel	mm

Subscripts	Description
C	Free flow
Dp	Dew point
Fr	Frontal
H	Hydraulic
In	Ambient temperature
M	Mean
P	Power
S	Supply temperature
W	Water
Wb	Wet bulb
Wa	Working air

Product Design and Development of Innovative Air Cooler with Desiccant-based Dehumidification

Greek letters	Description	Units
ρ	Density	kg/m ³ K
Φ	Uncertainty	%
ϵ	Effectiveness	–
Σ	Free flow to frontal area ratio	–
μ	Kinematic viscosity	Pa.s
Ω	Absolute humidity	g/kg

Chapter 1

1.1 Introduction

Indirect evaporative cooling (IEC) system consists of alternative dry and wet channels. In dry channels, ambient air loses sensible heat to evaporate the water in wet channels. While in the wet channels, water and air behaves alike to that of the DEC technique. So, working air takes away the latent heat of vaporized water and sensible heat by direct contact. Therefore, temperature of the supply air in dry channels reduced [1] [2]. The process diagram of IEC as shown in Figure 1.1 (a). The process of IEC on psychrometric chart as shown in Figure 1.1 (b), where the process 1-3 is considered as the process in which the moisture content of the ambient air remains constant while the process 1-2 is for working process in which air is directly contact with water and causes evaporation.

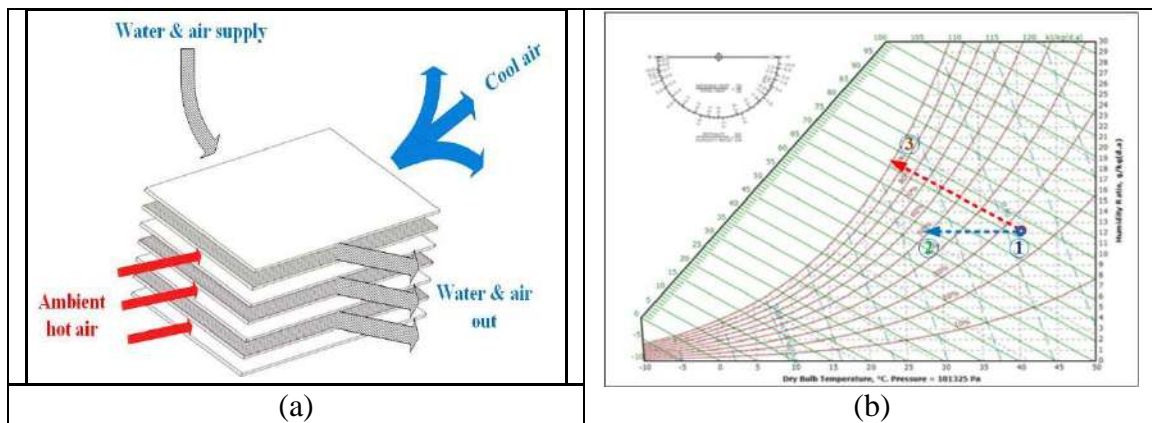


Figure 1.1: Schematic diagram of indirect evaporative cooling system, (a) process diagram, (b) process flow on psychrometric chart

1.2 Problem Statement

The cooling demand increases with the passage of every day, which leads to increase the energy demand. Generally, more than 30% of total overall electricity production is used in building sectors. In typical buildings, approximately 40-60% of primary energy is consumed by air-conditioners. Conventional air-conditioning systems typically consume more electricity because of their reliance on vapor compression system. The conventional vapor compression cycle uses Chlorofluorocarbons, the leakage of these hazardous gases causes depletion of the Ozone layer.

Conventional air cooler (Conv-AC) is the cheap technology in Pakistan till yet and several products are sold yearly. The drawback of Conv-AC is adding the humidity in supply air and does not work in high humidity environment. It is unhealthy for the human immune system and not suitable for patients with asthma. It is also activating the bacteria in the environment if they are not cleaned before used. Therefore, it is necessary to develop an indigenous healthy, efficient, and cost-effective solutions utilizing the local materials, instead of importing on expensive technologies.

The evaporative coolers provide considerable energy savings compared to vapor compression air conditioners, but at the same time, they have high onsite water demand. The water demand in evaporative cooler is the major barrier for implementation in hot and dry areas around the world. A portable evaporative cooler might be used up to 04 litres per hour while a centralized air-cooling system consume around 25 litres per hour. Many countries including Pakistan are considered to be a water-threatened country because the available water for a person is less than thousand cubic meters. So, it is necessary to recover water from exhaust air of the dew point indirect evaporative cooler (DP-IEC).

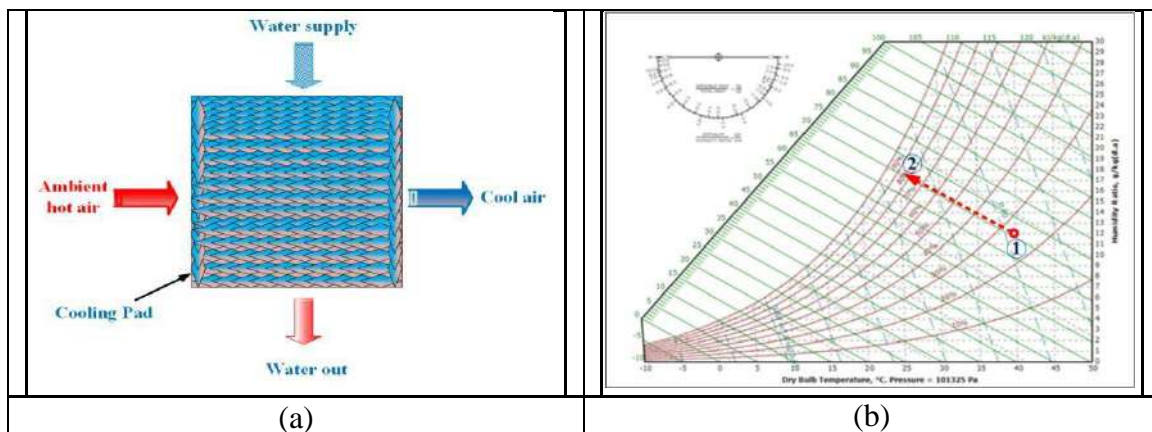
1.3 Aim and Objectives

The aim is to design an energy efficient, low operational cost, and light weight dew point indirect evaporative cooler by using efficient materials, geometries, and working air flow patterns along with improved water footprint technique. The major objectives of the current research work are given below,

- Design a dew point indirect evaporative cooler.
- Efficient materials selection to ensure high wettability.
- Fabrication of several design variant prototypes in term of different geometries, and flow patterns.
- Performing the experimental testing of design variant prototypes under control and real climate conditions.
- Design, fabrication, and implementation of water recovery technique.

1.4 Direct evaporative cooler

Direct evaporative cooling (DEC) system utilize the latent heat of evaporation. The ambient air which is warm interaction with pads that contained water which is at the temperature of wet bulb of the incoming ambient air, released heat [3]. The ambient air goes cool by transferring the heat with water and discharged. The moisture content of the cooled air is higher than ambient air because it absorbed a portion of water vapors by absorbing the latent heat [4]. The working process of DEC as shown in Figure 1.2 (a). The psychrometric representation of the working process of DEC as shown in Figure 1.2 (b).



Product Design and development of Innovative Air Cooler with Desiccant-based Dehumidification.
 Figure 1.2: Schematic diagram of the direct evaporative cooling system, (a) process diagram, (b) process flow on psychrometric chart

1.5 Maisotsenko cycle (M-cycle)

The technique of the M-cycle was developed by Valeriy Maisotsenko. The technique offers cascade of heat and mass exchanges while making it convenient to attain temperature near to its dew point temperature [5]. It uses the energy from the evaporation of water to reduce sensible heat albeit at the cost of reduced mass flow rate at each cascade. It can save up to approximately 80% more energy as compared to conventional systems [6]. The cascade procedure involves pre-cooling of a stream of air using the indirect evaporator cooler concept, which then results in subsequent cooling through evaporation [7][8].

The process 1-5 is considered as the process in which ambient air cools up to dew point temperature of incoming air. While the process 1-6 shows the working air contact with water and causes the evaporation in wet channels. These processes are presented on the psychrometric chart as shown in Figure 1.3.

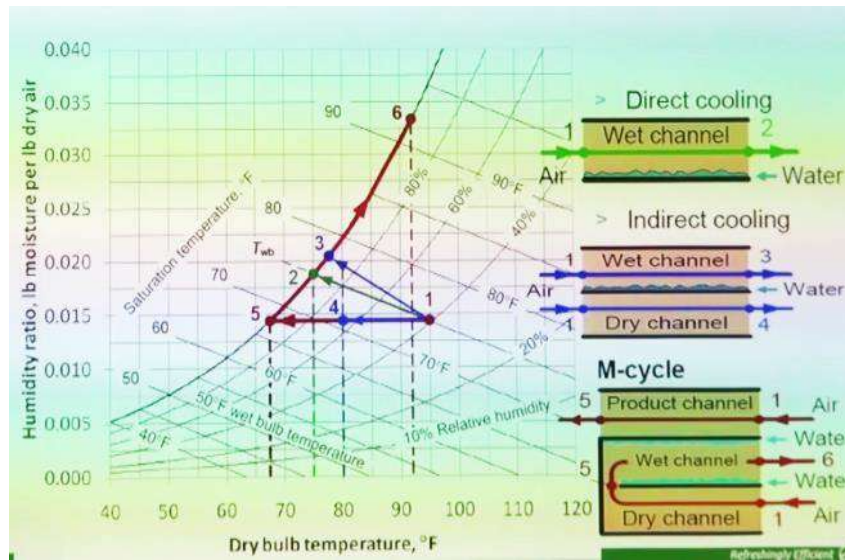


Figure 1.3: Process flow of M-cycle on psychrometric chart (source: presentation of Dr. Valeriy S. Maisotsenko in I²CNER at Kyushu University)

1.6. Water Recovert from exhaust air

A portable evaporative cooler might be used water up to 1 gallon per hour while a centralized air-cooling system consumes around 6.6 gallons per hour. Pakistan is the part of those countries that have faces the water-stressed due to population growth in urban areas, agriculture, climate change and mismanagement of water system. Moreover, the 80 % population of the Pakistan do not access of clean or fresh water [9]. So, it is necessary to save water.

In DP-IEC, some quantities of water are emitted in the air. These quantities of water that are contained in saturated air may be recovered by using the membrane condenser [10] as shown in Figure 1.4.

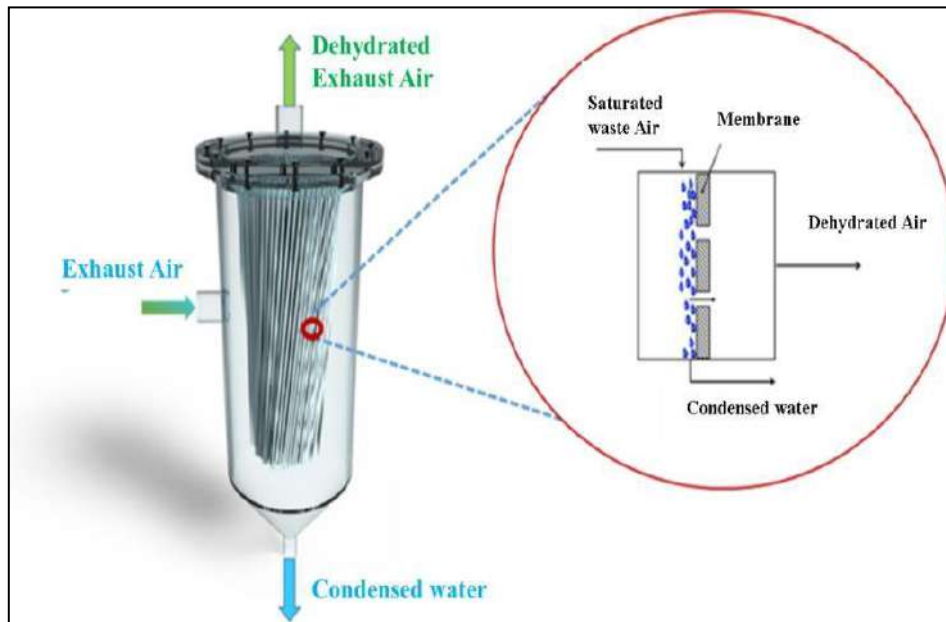


Figure 1.4: Membrane condenser (Source: membrane condenser as emerging technology for water recovery)

1.6 Research methods

The proposed research methodology of the thesis consists of 04 phases as shown in Figure 1.5, which is illustrated below,

Phase 1: Idea development

In this phase, related data is collected from literature review regarding dew point indirect evaporative cooler. DP-IEC consisted of heat and mass exchanger which is compact in design. The desert cooler is not working on hot and humid days. Also, water consumption of the desert cooler is around 04 liters per hour. Particular attention will be given to develop a technology which is efficient, low water consumption and do not added moisture in supply air. Finally, several prototypes will be proposed for DP-IEC.

Phase 2: Design and development

Several design variant prototypes of DP-IEC are fabricated which are differ in size, geometries, and flow patterns. The proposed water recovery system is also developed which are extracted water from exhaust air of DP-IEC.

Phase 3: Experimentations

In this phase, few design variant prototypes of DP-IEC are evaluated under a wide range of controlled as well as actual climate conditions of Mirpur, Gujranwala, and Taxila, Pakistan.

Phase 4: Conclusions and future recommendations

In the final phase, it is concluded that which prototype is viable. Outcomes of the research are then generated with future exploration directions.

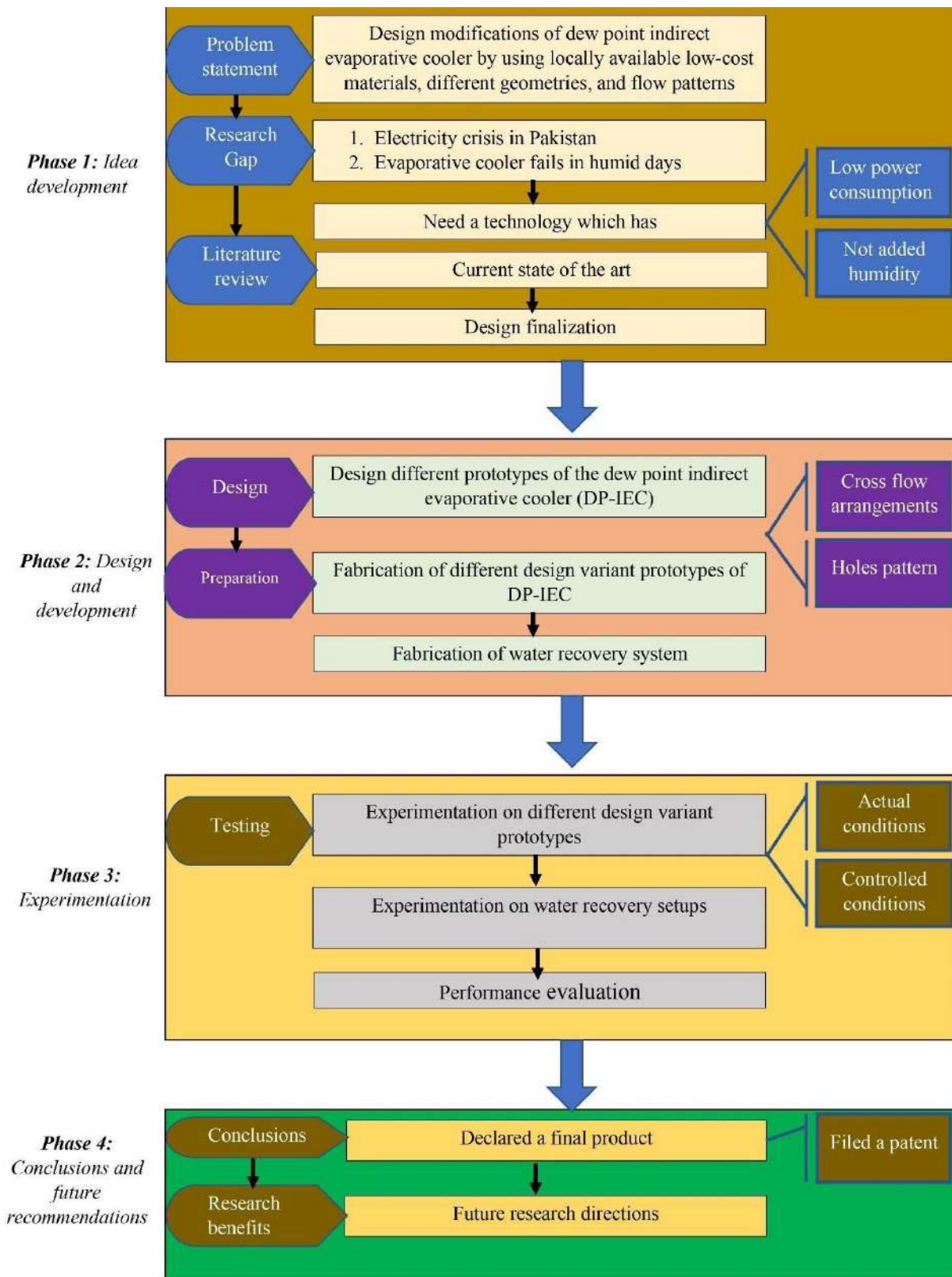


Figure 1.5: Research methodology

1.7 Report Overview

The thesis consists of seven chapters. An overview of these chapters is given below,

Chapter 2 deals with the literature review about cross flow and counter flow indirect evaporative techniques, desiccant based indirect evaporative techniques through various research studies.

Chapter 3 provides the design of several configurations of the design variant prototypes (DVP) of dew point indirect evaporative cooler and water recovery system.

Chapter 4 consists of fabrication process, design specifications, experimental setups and real-time testing of materials of the design variant prototypes with detailed analysis of measurement procedures.

Chapter 5 reports performance analysis of DVPs of dew point indirect evaporative cooler. Real time performance analysis of DVP systems including controlled as well as actual climate conditions. Performance analysis of water recovery systems under actual climate conditions.

Chapter 6 incorporates the key conclusions of this research work and future recommendations for further works.

Chapter 2

2.1 Literature Review

Energy is a fundamental commodity for a comfortable life. Diverse as well as intensifying climate conditions are escalating burden on electricity demand for air cooling purposes, especially for developing and vulnerable countries. The swift rise of thermal comfort requirements in the developing countries due to global warming and frequent temperature peaks are off-shooting energy demand to meet the air conditioning requirements [11]. Global warming and ozone depletion are the one of the concerning disasters of the world right now causing global climatic changes and deviation in weather patterns. A major contribution to this alarming crisis is the gases i.e., CFCs etc. which are emitted by using conventional vapor compression cycle air conditioning units [12].

The energy demand increases because of the prompt growing population, urbanization, and new infrastructure development [13]. Heating, ventilation, and air conditioning (HVAC) systems have an important role in comfort living. HVAC systems are consuming extensive power and energy. Hence, these systems have share of around 40-60% energy in buildings [14]. The decisive goal of HVAC systems is to anticipate the comfort zone for human under steady state conditions [15].

Air conditioning is the process for handling the temperature, humidity, and distribution in a building to sustain a cool atmosphere. Generally, the building sector uses over 30% of total overall electricity generation. In standard buildings, a significant portion of primary energy is used by air-conditioner units [16]. The conventional air-conditioner units, relying on vapor compression systems (VCS), usually use more electrical power and play a major role in global warming with significant carbon dioxide (CO₂) emissions mostly by consuming more electricity whose majority is coming from non-renewable sources [17].

M-cycle is a thermodynamically efficient technique that is becoming popular around the world. This system is environmentally friendly as it does not need any CFCs/HCFCs refrigerants which are causing GHG [18]. Dew point indirect evaporative cooler (DP-IEC) is an efficient technology, delivers fresh air without adding the moisture, having air temperature closed to its dew point temperature or below the wet bulb temperature [19]. It has two basic flow patterns classified as cross flow and counter flow [20]. The process air passes the dry channels, and up to 30-40% of process air is diverted into wet channels, referred to as working air. The working air absorbs heat from the ambient air and it cools process air without the addition of moisture. This cool air is called product air [21]. The effectiveness of DP-IEC is up to 30% more than conventional IEC [22].

Many studies were performed on the structural design of the M-cycle based DP-IEC based on cross flow [23][24], counter flow [25][26], and hybrid configurations [27] of heat and mass exchanger. The effectiveness of cross flow DP-IEC was reported experimentally where dew point and wet bulb effectiveness were 0.67 and 1.2 respectively [28]. Another experimental study was indicated that the efficiency of the system had improved up to 5% by improving the channel width to height ratio and high wettability materials in wet channels [29].

Moreover, the effectiveness of DP-IEC was increased up to 25% by using fins in dry channels [30]. In addition, M-cycle based DP-IEC was examined in terms of effectiveness and cooling capacity. The results indicated that the dew point and wet bulb effectiveness ranged between 0.15-0.78 and 0.85-1.15 respectively. The cooling capacity varied between 1-19 kW [31]. Another study was carried out to investigate the effectiveness of the DP-IEC under various operating conditions. The results showed that the dew point and wet bulb effectiveness varied between 0.58-0.84 and 0.92-1.14 [32].

Moreover, few integrated studies of DP-IEC with desiccant systems were also investigated. In parametric study, holistic integration of counter flow DP-IEC with solar assisted desiccant cooling system was observed that maximum COP value of the system was 0.85. The economic analysis shown that it saved up to 62.9 % energy cost as compared to VCS [33]. In another study, DP-IEC was integrated with a refrigeration cycle to reduce power consumption for an office building that saved up to 38 % electricity [34]. Additionally, a two-dimensional analytical model of DP-IEC was developed by using the finite element method that predicted the latent heat transfer up to 3900 W [35]. Moreover, a numerical model of M-cycle was developed on TRNSYS software, which predicted the highest COP of 0.728 [36].

To enhance the performance of counter flow DP-IEC, the corrugated surface of the system was experimentally and mathematically investigated that resulted 10 % more effectiveness than the flat surface of the systems [22]. To reduce the cost of regenerative counter flow DP-IEC, heat pipe and porous ceramic tube were also integrated, resulting the cooling capacity (CC) of 140 W per m² [37]. In another study, the DP-IEC was integrated with solar-wind catcher system reduced the 70% operational cost of the system than conventional systems [38]. Several researchers have also been contributing with their untiring efforts to cope with this problem over the past decade. They have set different geometries and volumetric flow rates of air to optimize the performing parameters of the DP-IEC systems. Earlier experimental, numerical and simulation investigations for dew point indirect evaporative cooler are given below in Table 2.1.

Table 2.1: Earlier experimental, mathematical, and simulation investigations for DP-IEC

Ref.	Materials	Geometry mm	Method	V m ³ /h	m _w Kg/s	P Pa	ΔT °C	ε _{dp}	ε _{wb}	CC kW	COP	EER
[30]	Aluminum Sheet	Cross flow	Exp	–	–	–	25	0.93	1.43	0.69	11.24	–
[39]	Cotton sheet coated with polyurethane	Counter flow	Exp	130	–	–	–	0.78	1.05	0.43	–	10.6
[31]	Plastics	Cross flow	Model	600	–	–	20	0.74	1.05	1.5	–	–
[40]	Aluminum	Cross flow	Exp	400	–	–	7	0.65	0.8	–	14	–
[28]	Aluminum Sheet	Cross flow	Exp	512	–	27	17	0.67	1.2	1.8	–	–
[41]	–	Counter flow	Model/Simu	–	–	–	14	0.65	1.06	–	–	–

[22]	Product Design and development of Innovative Air Cooler with Desiccant-based Dehumidification.	Corrugated Plate	Counter flow	Exp/Model	2014	1.3	0.77	1.05	8.6	30.1	-	
[42]	Aluminum foil + Hydrophilic membranes	Cross flow	Exp	73.5	-	-	10	-	-	0.2	78	-
[35]	-	Cross flow	Exp	400	0.08	-	13	-	0.83	-	-	-
[43]	-	Counter flow	Model	130	-	-	13	-	1.16	-	-	-
[44]	Corrugated Sheet	Counter flow	Model/Simu	-	-	-	19	0.78	1.15	-	-	-
[32]	Polymer Sheets + fabric	Counter flow	Exp	-	1.6×10^{-5}	-	14	0.76	1.02	-	-	-
[45]	Corrugated Sheet	Counter flow	Exp	120	-	-	13	1.06	1.13	0.74	-	15.5
[24]	-	Cross flow	Model/Simu	130	-	-	15	0.63	1.05	0.38	-	19
[26]	-	Counter flow	Model	-	-	-	13	-	1.05	-	-	-
[25]	-	Counter flow	Model	208	-	40	-	0.82	1.1	0.45	-	11.22
[46]	Al Sheet + Kraft Paper	Counter flow	Exp	-	-	-	22	0.93	1.3	-	-	-
[47]	-	-	Model	-	-	-	10	0.78	1.15	0.64	2.3	19.8
[48]	-	Counter flow	Model	-	-	-	-	0.9	1.3	-	-	-
[27]	-	Counter flow/ Cross flow	Model	800	-	-	12/ 11	0.92/0.8	-	1.7	-	-
[49]	Plastics	Cross flow	Exp/Model	300	3×10^{-4}	-	23.7	0.73	1.17	1.5	14.2	-
[50]	-	Cross flow	Exp	1700	0.3	-	16	-	1.11	-	-	30.9

2.2 Research Gap

In view of the above literature review, it is observed that DP-IEC is a complicated structure as it has consisted of alternative dry and wet channel arrangements and flow diversions along with channels. Although, this technology is well-established, however, such technology should be tailored in terms of few design modifications and available localized efficient materials which help to develop indigenous cost-effective solution. In addition, performance of DP-IEC system strongly influenced by local climate conditions as well. Therefore, the current research work is based on design and development of localized solution with efficient materials that have enhanced heat and mass transfer characteristic and have almost comparable performance with international standardized system. In this work, initially, several design variant miniature heat and mass exchangers are designed ensuring uniform air distribution throughout all channels of the stack. These design variant HMX are fabricated with locally available efficient polymeric materials ensuring high wettability and also which makes it lightweight and low cost. The high wettability is ensured through attachment of the non-woven fabric with polypropylene sheets with heat press laminator. Moreover, few published literatures are found that improved water footprint. Therefore, it is necessary to reduce the water footprint of the dew point indirect evaporative cooler. So, this study is also aim for optimum water-energy nexus. Moreover, the viability of the proposed DP-IEC needs to assess in terms of energy savings and reduced the water footprint so that the choices of most efficient formation in different climates might be possible.

Chapter 3

3.1 Design of multiple configurations of DP-IEC

In this chapter, design variant prototypes are designed. Several design variant prototypes of dew point indirect evaporative cooler are designed to obtain the compact most effective model. These designs are differed from each other by geometry, sizing, holes spacing, holes position, channel spacing, flow patterns, and number of dry and wet channels.

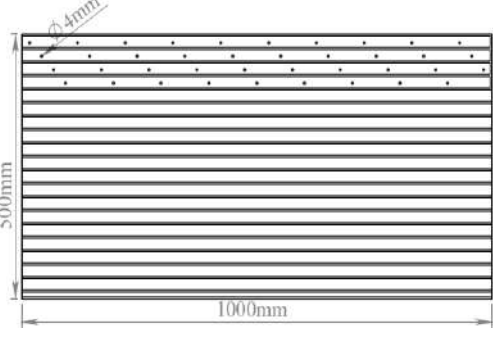
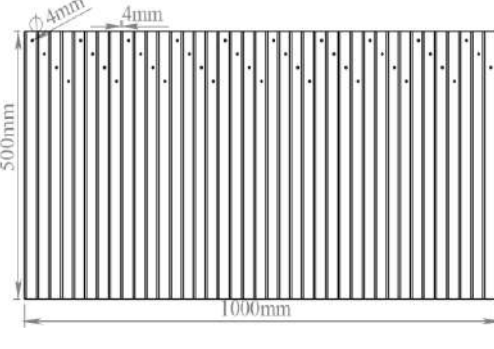
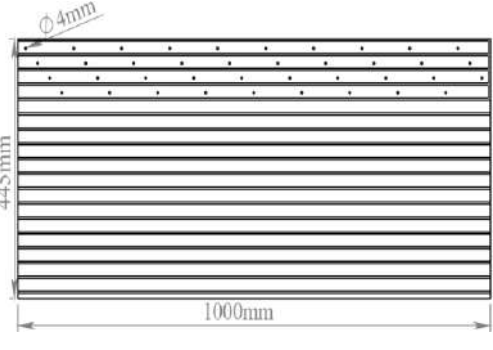
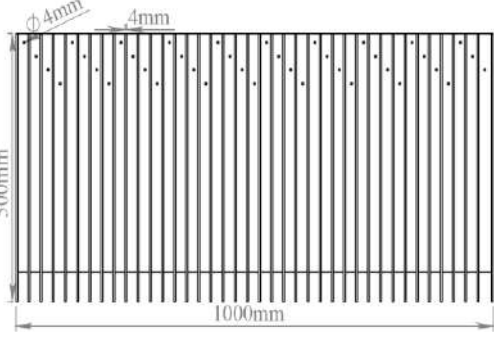
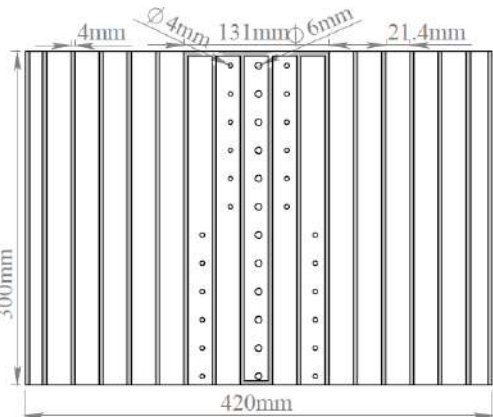
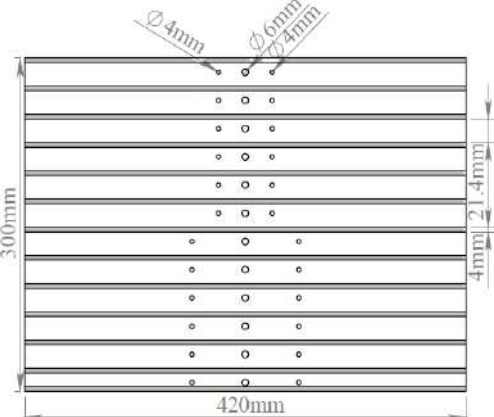
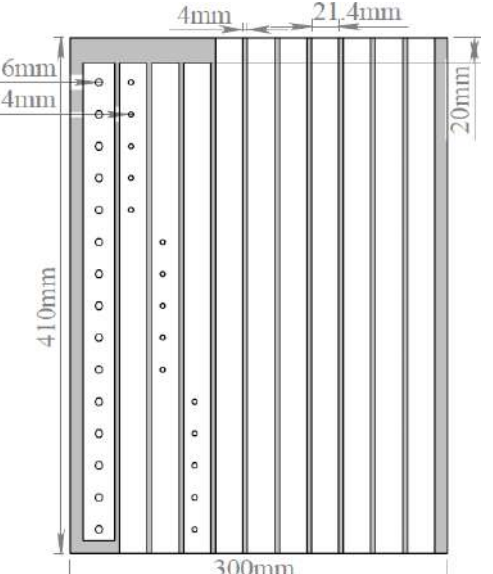
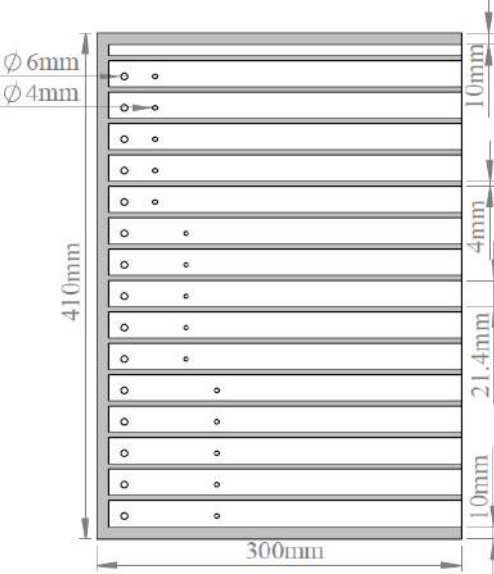
3.2 Design of the dry and wet channels

The dry and wet channels of the HMX designed which are differed in geometries, holes spacing, and holes positions. The specifications of each design variant prototype are given in Table 3.1. The 2D design of dry and wet channels with dimensions of each DVP are given in Table 3.2.

Table 3.1: Specifications of design variant prototypes

Design variant prototypes (DVP)	Length mm	Width mm	Height mm	Channel spacing mm	Water holes mm	Air holes mm
DVP-01	1000	17	500	25.4	06	04
DVP-02	1000	12.4	445	25.4	06	04
DVP-03	300	420	152	21.4	06	04
DVP-04	300	420	300	21.4	06	04
DVP-05	410	300	65	21.4	06	04
DVP-06	410	300	204	21.4	06	04
Final product	410	300	170	21.4	06	04

Table 3.2: 2D design of dry and wet channel with dimensions

DVP	Dry Channel	Wet Channel
DVP-01		
DVP-02		
DVP-03 and 04		
DVP-05 and 06		

3.2.1 Design of the air flow patterns

There are two types of flow patterns are designed. In the first design, the water holes are created in between the channels. The air holes are created on both sides of the water holes as shown in Figure 3.1. While, in the second design, the water holes are created at extreme left side of the channels. The air holes are created on the right side of the water holes as shown in Figure 3.2.

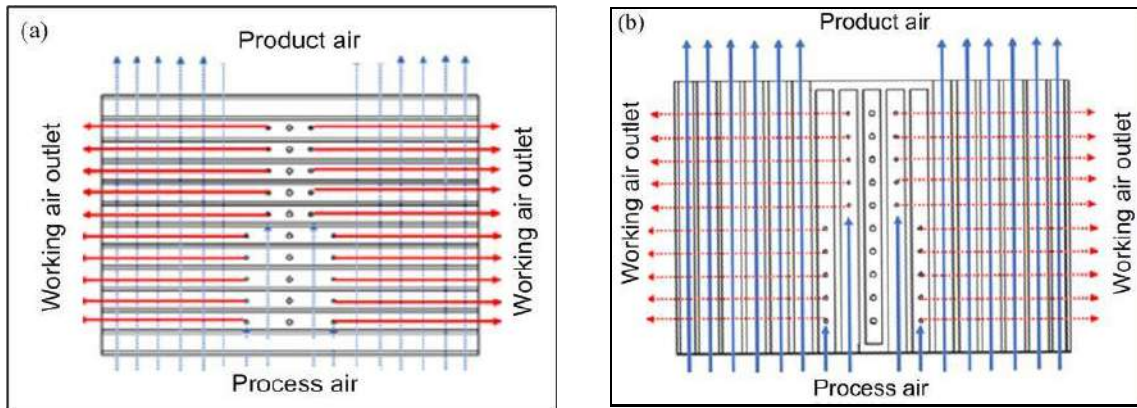


Figure 3.1: Working process of dewpoint indirect evaporative cooler (centerline perforated holes); (a) wet channel (b) dry channel

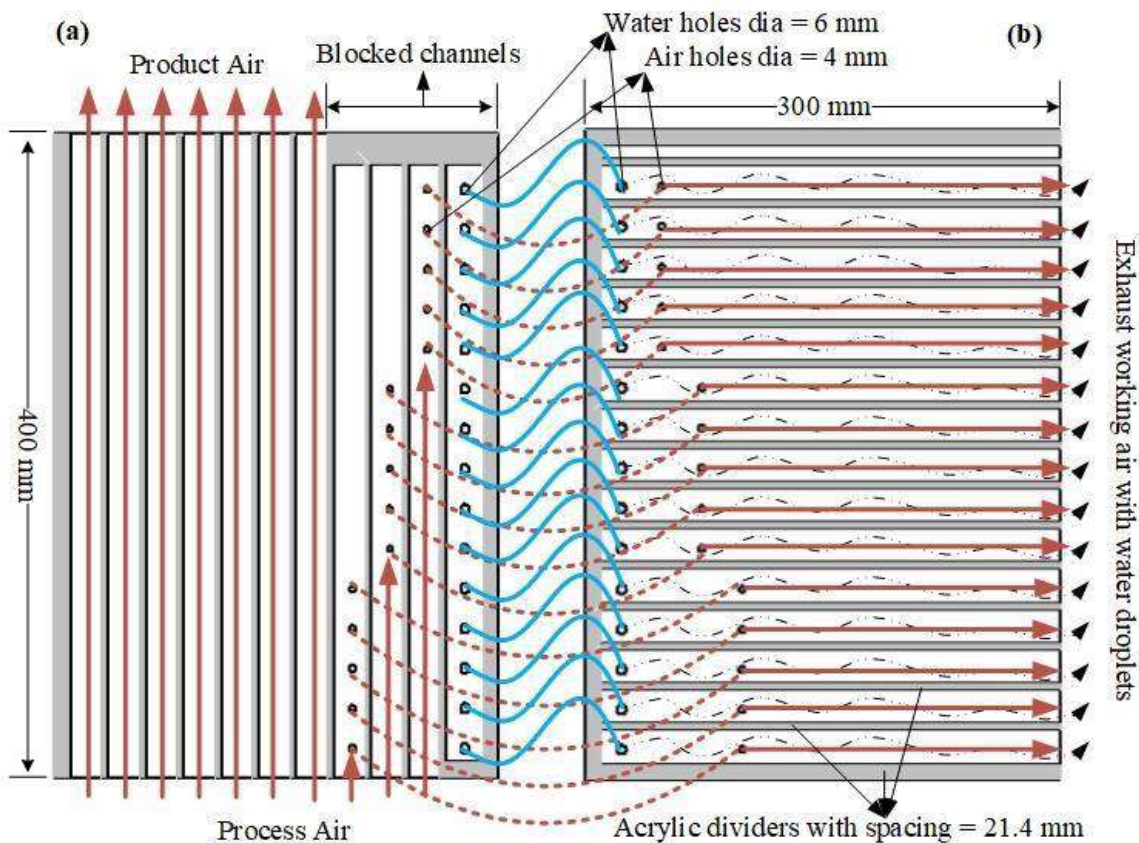


Figure 3.2: Working process of dewpoint indirect evaporative cooler (extreme left side perforated holes); (a) dry channel (b) wet channel

Product Design and development of Innovative Air Cooler with Desiccant-based Dehumidification.
3.3 Design of multiple configurations of DP-IEC

3.3.1 Design of DP-IEC 01

After the completion of different heat and mass exchanger (HMX), the next step is the design of the proper/complete system of the prototype. The design of DP-IEC 01 is consisted of HMX, water pump, water supplying pipe etc. The direction of the water and air flow are shown with arrows. The water holes are presented on the top of the HMX design. Figure 3.3 (a) and (b) shows the process side, product side as well as working air side of the HMX. Figure 3.3 (c) shows the complete design of the DVP-01 along with water storage tank and pump.

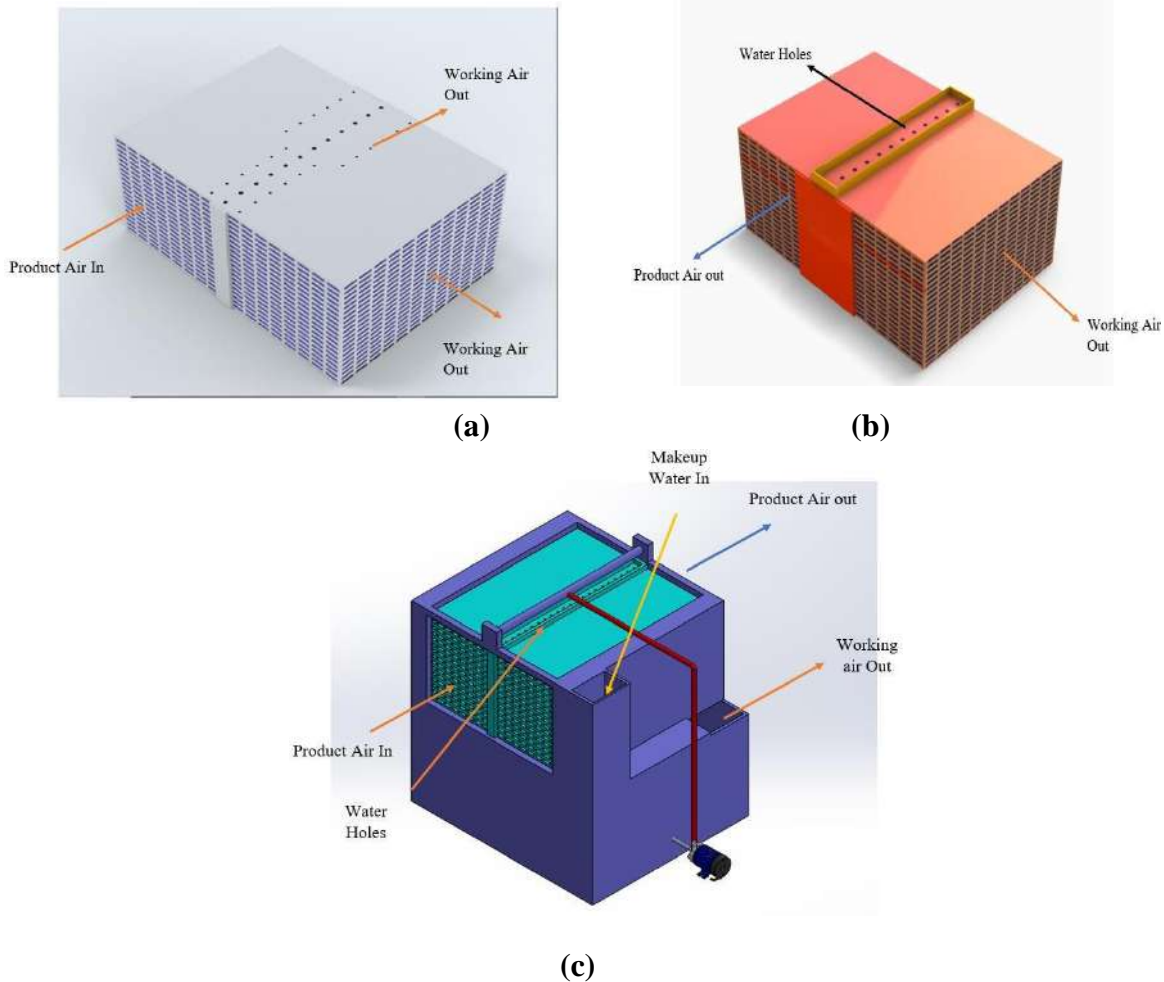
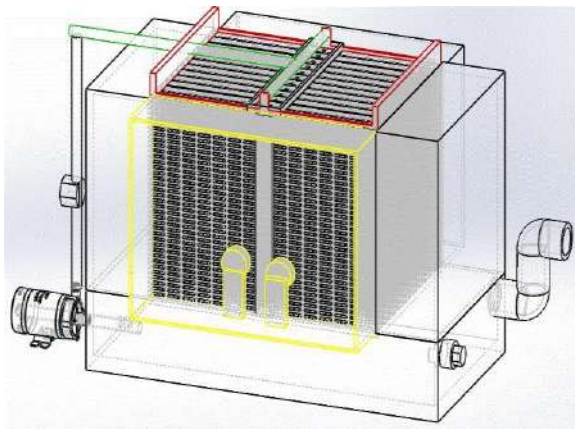


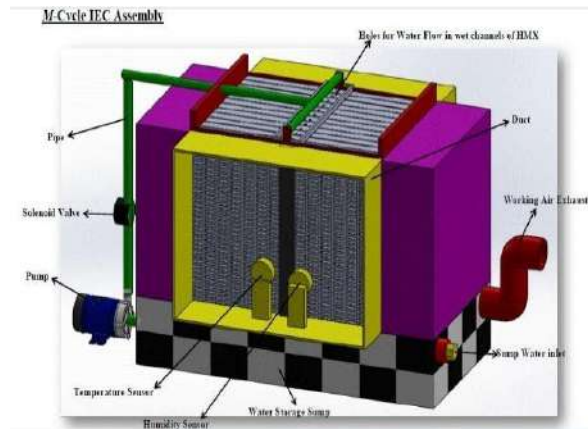
Figure 3.3: Complete design of the DP-IEC 01

3.3.2 Design of DP-IEC 02

The design of the DP-IEC 02 is also consisted of axial fan, HMX, water pump, and water supplying pipe etc. In this design, the water holes are created in the center of the HMX, and air holes are created on both left and right sides of water holes. Figure 3.4 shows the complete assembly of the DVP-02, (a) blur view of the HMX with pump, (b) HMX with water pump and water supplying system, (c) complete 3D design of the DVP-02 with labelled parts of the system.



(a)



(b)

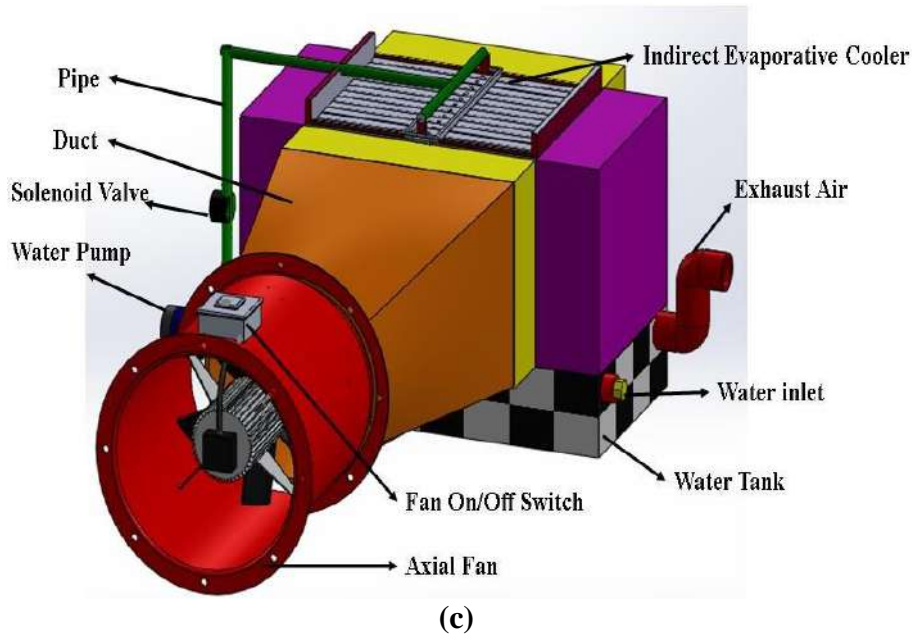
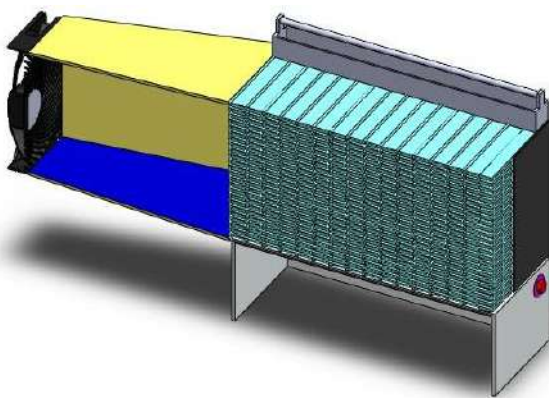


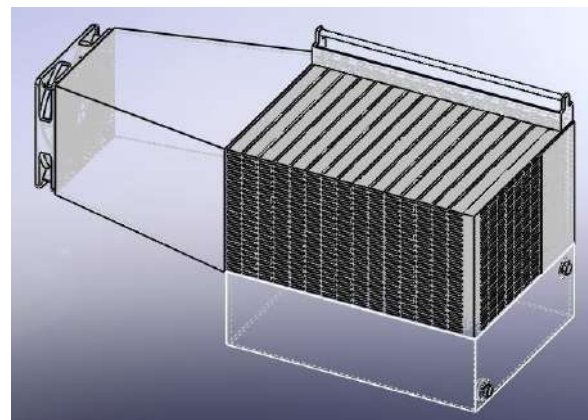
Figure 3.4: 3D design of DVP-02 (a) front view of the complete design, (b) Labelling of the complete design, (c) HMX assembly with axial fan, pump, and water tank

3.3.3 Design of DP-IEC 03

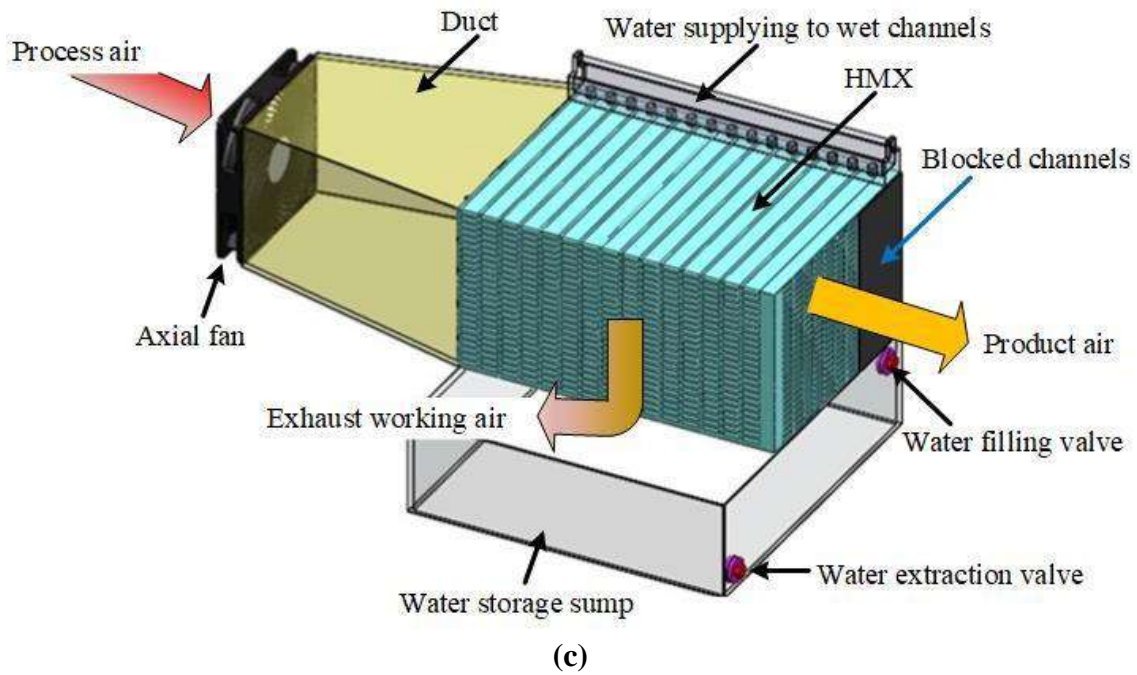
Design of the DP-IEC 03 is consisted of HMX, axial fan, and water pump etc. In this design, the water holes are created on the extreme left side of the HMX, and air holes are created on right side of the water holes. Figure 3.5 shows the complete assembly of DVP-03, (a) cross section view, (b) blur view, (c) complete assembly with labelled parts of the system.



(a)



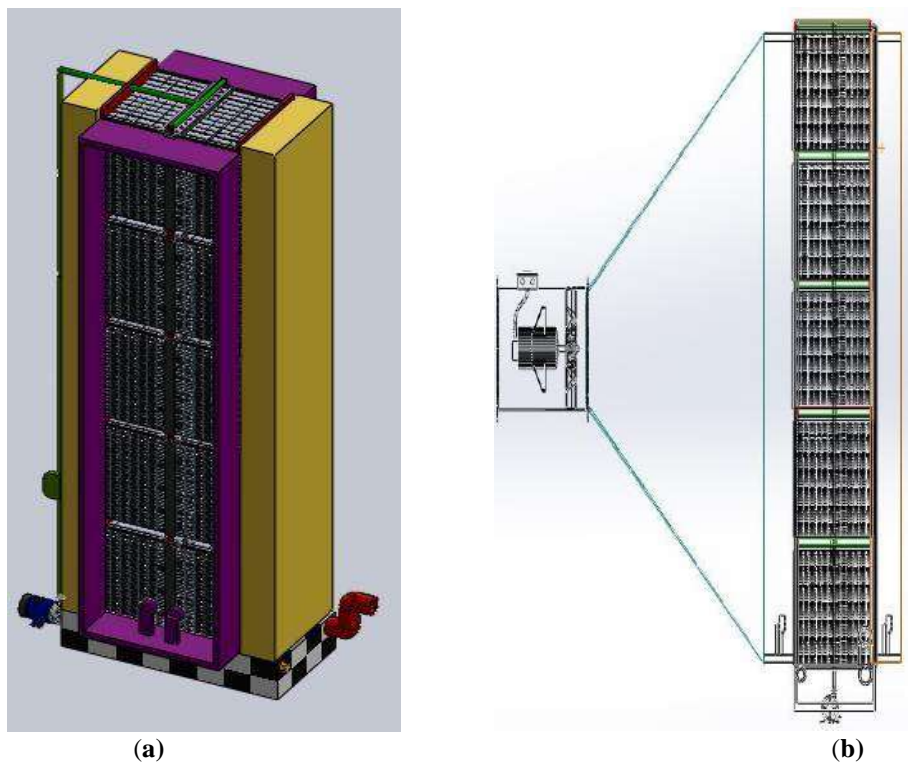
(b)

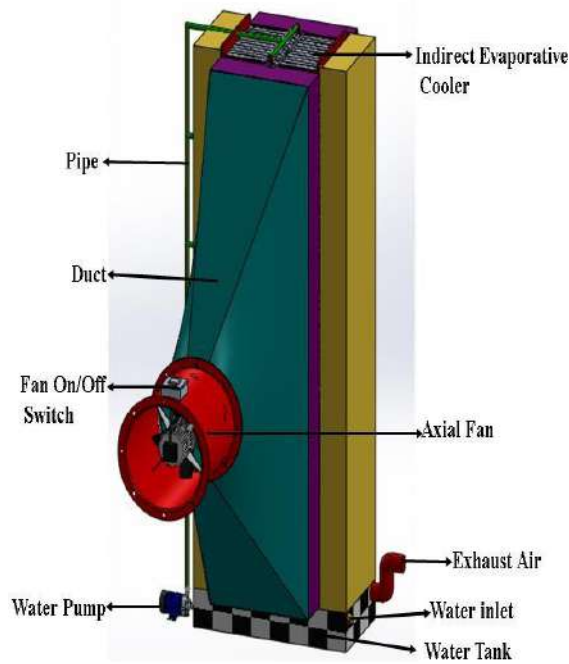


(c)
Figure 3.5: Complete design of the DVP-03, (a) cross section view, (b) blur view, (c) complete system with labelled parts of the design

3.3.4 Design of the DP-IEC for higher capacities

Multiple stacks assembly is designed for the higher capacities of CFM. The range of the CFM will be 1.5-2 Ton. The complete design consists of several HMX stacks along with axial fan, water supplying pipes, water storage tank, and water pump. Figure 3.6 shows the different views of multiple stacks assembly, (a) symmetric view with several HMX stacks, (b) blur view, (c) complete design of the multiple stack assembly with labelled parts.





(c)

Figure 3.6: Multiple stacks design with different views, (a) symmetric view with several HMX stacks, (b) blur view, (c) labelling of multiple stack's complete model

3.4 Design of the water recovery system

For water recovery from the exhaust working air, the wet side of the HMX is connected to filter type arrangement of hydrophobic sheets. Another duct is used to connect the working side of the HMX with filter. A water bottle is used to collect the recovered water from exhaust air. Complete design assembly of water recovery system as shown in Figure 3.7.

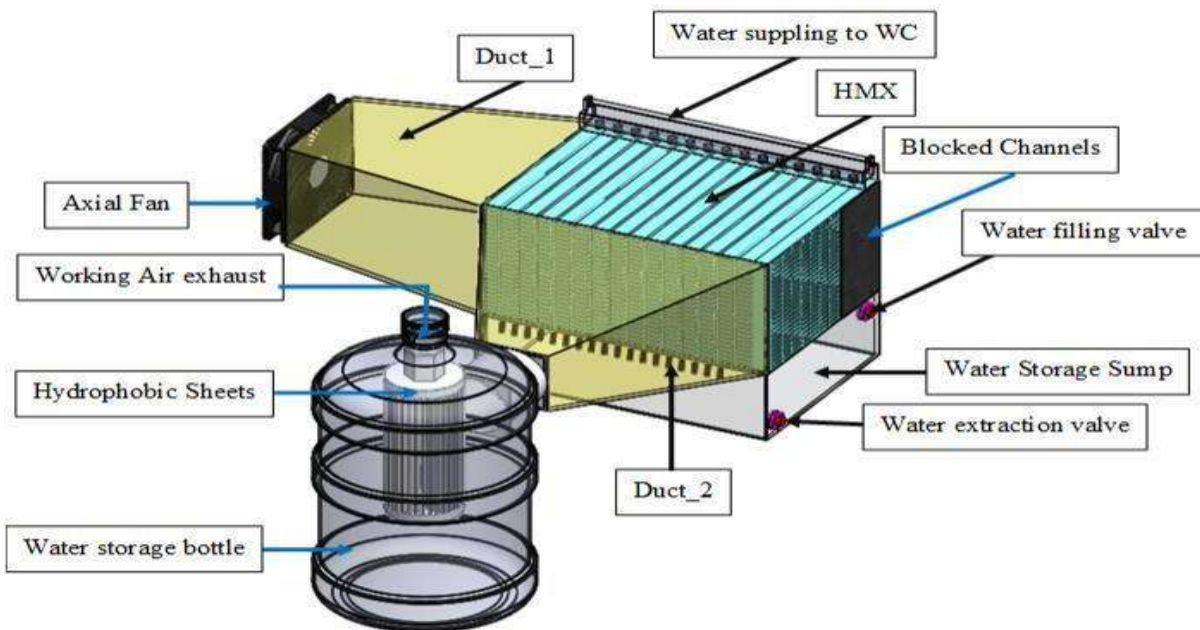


Figure 3.7: 3D model of the water recovery system

3.5 Silica gel

Silica gel as shown in Figure 3.10 is a type of silicon dioxide (SiO_2), which is a compound comprised of silicon and oxygen atoms. This material is porous and consists of tiny crystals or beads that possess a large surface area, allowing them to adsorb and retain moisture within their structure. Additionally, when heated, the beads can release moisture, which is why silica gel is often utilized in products that require dryness. Chemical modification of silica gel can produce various types with diverse properties.

For instance, the addition of aluminum ions to silica gel can result in a form that can adsorb specific organic compounds. Furthermore, adding titanium ions to silica gel can create a form that functions as a catalyst. Silica gel with different specifications and costs are available for purchase on Daraz



Figure 3.8: Silica gel

The specifications of silica gel powder as described on Daraz are as follows:

Water absorbability: 35%

Type: These heat transfer sheets are waterproof and even oil proof.

Reusable: Need to be regenerated by using heat up to 10°C .

Material: A3 silica gel

Size: 40-63 μm

Quantity: 1kg

Cost: Rs.1090 and shipping charges of Rs. 175

3.6 Coating Techniques

To achieve a consistent and long-lasting coating of desiccants on metal surfaces, it is essential to carefully select appropriate desiccants and binders, and to employ an appropriate coating method. Various methods have been used by researchers to achieve this goal, including dip coating, spray coating, and direct synthesis. The advantages and disadvantages of each of these methods are discussed in the following Table 3.2

Table 3.3: Comparison of three types of Coating Techniques

Properties	Dip coating	Spray coating	Direct synthesis
Reaction conditions	Mild	Mild	Severe
Coating thickness (μm)	120	120	10 to 15
Possibility of serial production	Easy	Easy	Very difficult
Price	Cheap	Slightly Expensive	Expensive
Maintenance	Easy	Difficult	Difficult

3.6.1 Dip Coating

The process for applying a coating to a metal fin involves several steps. First, the fin must be cleaned by soaking it in an alkali solution for one hour, followed by a rinse with distilled water. Next, a solution of desiccant and binder is prepared and stirred thoroughly to prevent clumping. The cleaned and dried fin is then dipped multiple times into this solution, with each dip being followed by placement in an oven at 120°C for 1-2 hours, depending on the desired thickness of the coating. This process is repeated 5-6 times until a uniform coating of the desired thickness is achieved.[25] However, it is important to note that dip coating has some potential disadvantages, such as weak mechanical strength, increased volatility, and high heat and mass transfer resistance. Additionally, achieving a thin and uniform coating requires multiple dips, which can lead to uneven distribution of the desiccant and blockage of gaps between the fins. Despite these challenges, dip coating is often preferred due to its simplicity and low cost.

3.6.2 Spray Coating

Product Design and Development of Innovative Air Cooler with Desiccant-based Dehumidification.

An effective way to apply desiccant powder onto fins is using an electrostatic spray coater, which employs an intense electrostatic field to spray a mixture of desiccant and binder onto the metal surface. The coating powder is first prepared and loaded into the electrostatic spray coating device, where it is fluidized in the hopper, conveyed through hoses by injectors, and then sprayed onto the fins. Fang et al. [26] reported that a coating thickness of 120 μm can be achieved using SEM and XRD techniques without cracking.

However, it is important to note that while spray coating is more specialized than dip coating, its effectiveness compared to dip coating is still unclear. In addition, spray coating requires frequent maintenance of the specialized device, and the high initial investment required for the process are some of its disadvantages [27].

3.6.3 Direct Synthesis

Extensive research has been conducted on synthesizing zeolites directly on the surface of heat exchanger fins. In-situ hydrothermal synthesis processes have been used to coat different metal substrates, including copper and aluminum foams, with zeolites. [28,29]. The duration of the synthesis process depends on the type of zeolite particles and can range from a few hours to several days. The synthesis of zeolites on metal substrates takes place in a closed hydrothermal system at high pressure (around 1 kbar) and high temperature (around 450°C). [30].

While the direct synthesis process provides stable coatings, Freni et al. [31] have argued that the synthesis conditions are too extreme compared to the dip coating process. Additionally, the direct synthesis process yields coating thicknesses of only 10-50 μm , making it difficult to implement for industrial production. In contrast, dip coating offers milder reaction conditions and a more straightforward implementation process in industry. Furthermore, dip coating can coat heat exchangers of any complex shape while maintaining a uniform coating thickness. Therefore, most researchers prefer to use the dip-coating process to coat desiccants onto metal fins

Chapter 4

4.1 Experimental Setup

The experimental setups of the different design variant prototypes are discussed in this chapter. The focus of this work is to fabricate the low cost, energy efficient, environmentally friendly, and less water footprint dew point indirect evaporative cooling system that can provide cooler product air than either direct evaporative cooling or conventional indirect evaporative cooling systems, without increasing the moisture content of the supply air. Moreover, the real-time experimentations of some design variant prototypes are performed in actual as well as controlled climate conditions of Pakistan. In addition, the real time testing of the materials, the performance investigation of the systems, instrumentations, and measuring procedures are described in detail. Further, the CFM of the systems and pressure drop calculations of the systems are explained.

4.2 Experimental setups of the design variant prototype (DVP)

4.2.1 Design variant prototype 01

4.2.1.1 Manufacturing of the HMX

Design variant prototype 01 consists of heat and mass exchanger (HMX), blower, duct, water pump, and copper pipes. The HMX is the key part of the system, and it is made with dry and wet channels which are arranged in cross flow position. Dry and wet channels are made of aluminum sheets, cotton cloth, and acrylic dividers. The acrylic dividers are prepared by using laser cutting machine, into specific patterns to make the air and water passages more prone to heat transfer and maintained the equal and proper distance along the whole sheet. The width and height of each divider is 04 mm. For dry and wet channels, 1000 mm and 500 mm long dividers are prepared respectively. The dividers are joined with aluminum sheet and cotton cloth with the help of white transparent silicone sealant bond. The cotton cloth is on one side of the sheet and the dividers are fixed on both sides of sheet. The acrylic dividers are fixed vertically on cotton side and fixed horizontally on other side of the sheet. The distance is 25.4 mm with each divider. After that, all the dry and wet channels are assembled in such a way that dry channel came after the wet channel to fabricate the HMX.

The heat and mass exchanger of the design variant prototype 01 is consisted of 03 channels (one dry and two wet channels). The height, width, and length of the HMX is 500 mm, 17.4 mm, and 1000 mm, respectively. The holes of 4 mm are created on copper pipe so that water is flown in wet channels. In the dry and wet channels, air holes are created in four sub-channels in zig-zag pattern. In the dry channel, four sub-channels are blocked at output side and the air is transferred into the wet channels through these holes for evaporation. The different fabrication phases of design variant prototype 01 as shown in Figures 4.1 and 4.2.

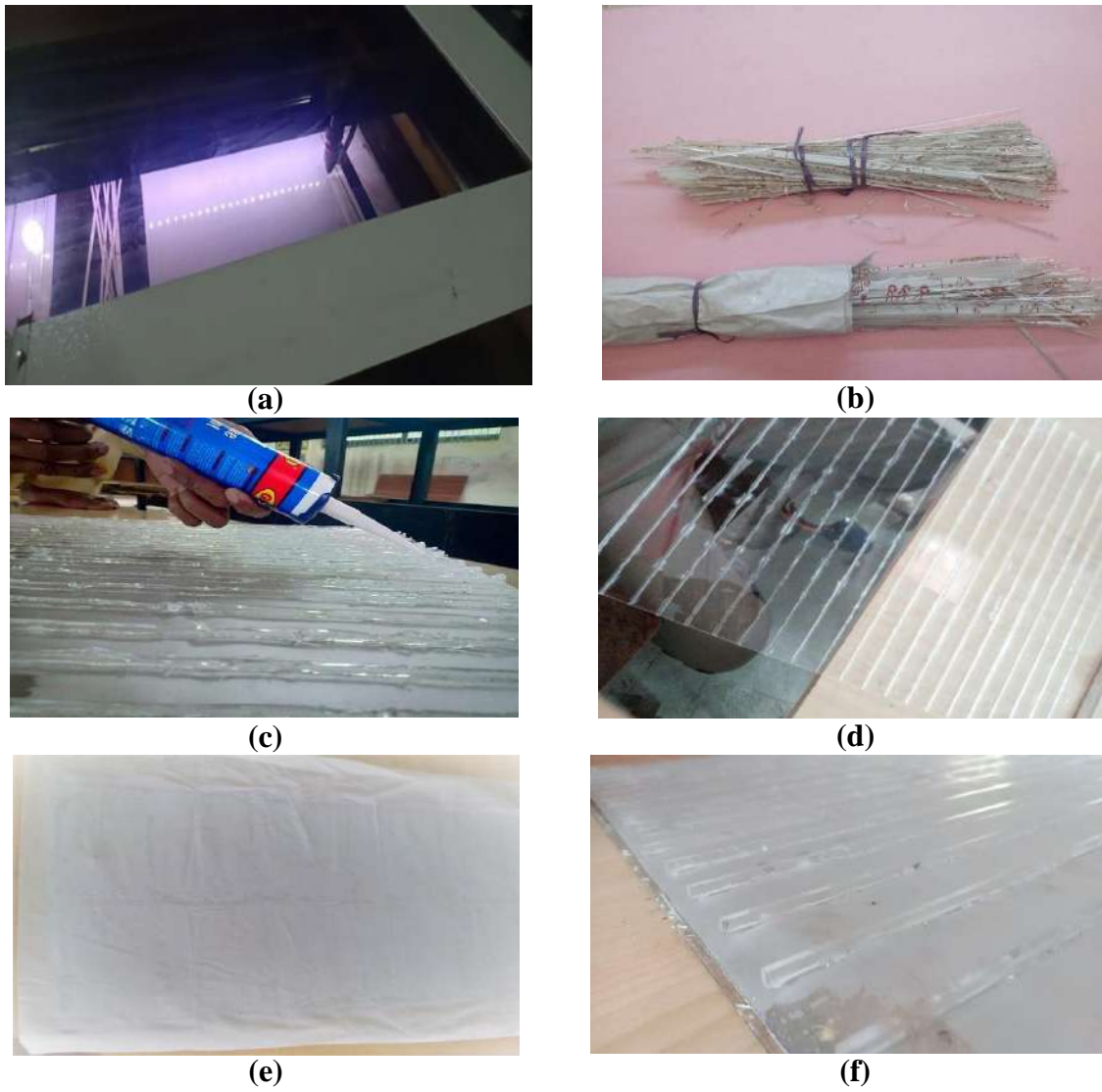


Figure 4.1: Different fabrication phases of DVP 01 (a) laser cutting machine, (b) acrylic dividers (c), (d) joining the acrylic dividers with wet and dry channels by silicone, (d) cotton cloth, (e) joining the acrylic dividers with aluminum sheet





Figure 4.2: Different fabrication phases (a) holes creation in the dry channel, (b) zig zag holes pattern, (c) copper pipes with holes for water flow, (d) pump used for pumping the water in the wet channels

4.2.1.2 Experimental setup of DVP 01

The locally developed design variant prototype 01 consists of the HMX, blower, water pump, water pipe, and water storage tank. The ambient air is supplied to dry channels which is divided into two passages, one is the working air and the other is the product air. The product air is the useful cool air that is used for desired purposes. Also, the ambient air that is flown in the blocked dry channels is forwarded into the wet channels through the holes along dry channels. This working air is exhausted into the atmosphere after engrossing heat and water droplets due to the evaporation in wet channels. The water is entered into the wet channels from the top of the HMX by the force of gravity. The copper pipes are used for water supplied to HMX while water storage tray below the HMX is used to collect the water and transport it back to copper pipes by using the water pump. This water flows through wet channels of the HMX which cools the incoming ambient air in dry channels that is supplied to the conditioned space. The design specifications of the DVP 01 are given in Appendix A. The experimental setup of the DVP 01 as shown in Figure 4.3.

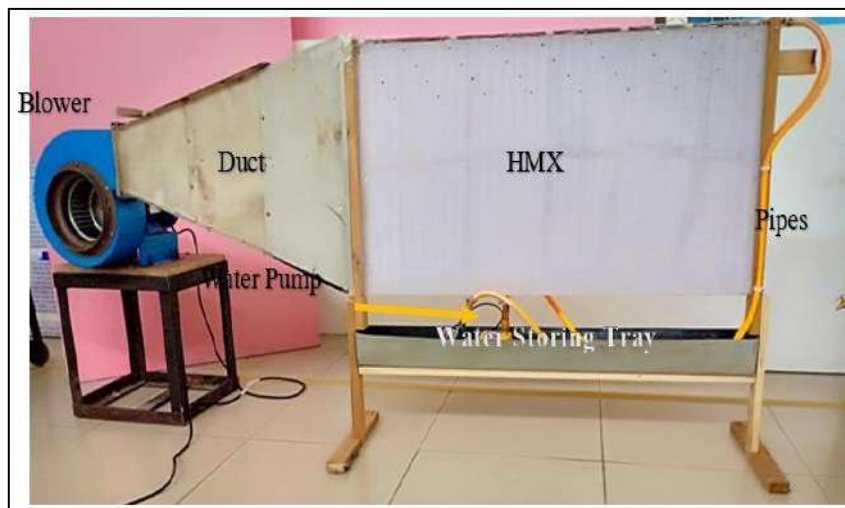


Figure 4.3: Experimental setup of the design variant prototype 01

4.2.2 Design variant prototype 02

4.2.2.1 Fabrication of the HMX

Design variant prototype 02 consists of the heat and mass exchanger, blower, duct, pump, and copper pipes. In this DVP, aluminum sheet is replaced with aluminum foil for the fabrication of the heat and mass exchanger. So, the dry and wet channels are made with aluminum foil, acrylic dividers, and cotton cloth. Moreover, the size of the acrylic dividers is changed for the wet channels. The length of the dividers are 445 mm for the wet channels. The manufacturing process of the DVP 02 is the same as DVP 01.

The HMX of the design variant prototype 02 also consisted of 03 channels (one dry and two wet channels). The height, width, and length of the HMX is 445 mm, 12.4 mm, and 1000 mm respectively. The different fabrication phases of design variant prototype 02 as shown in Figure 4.4.

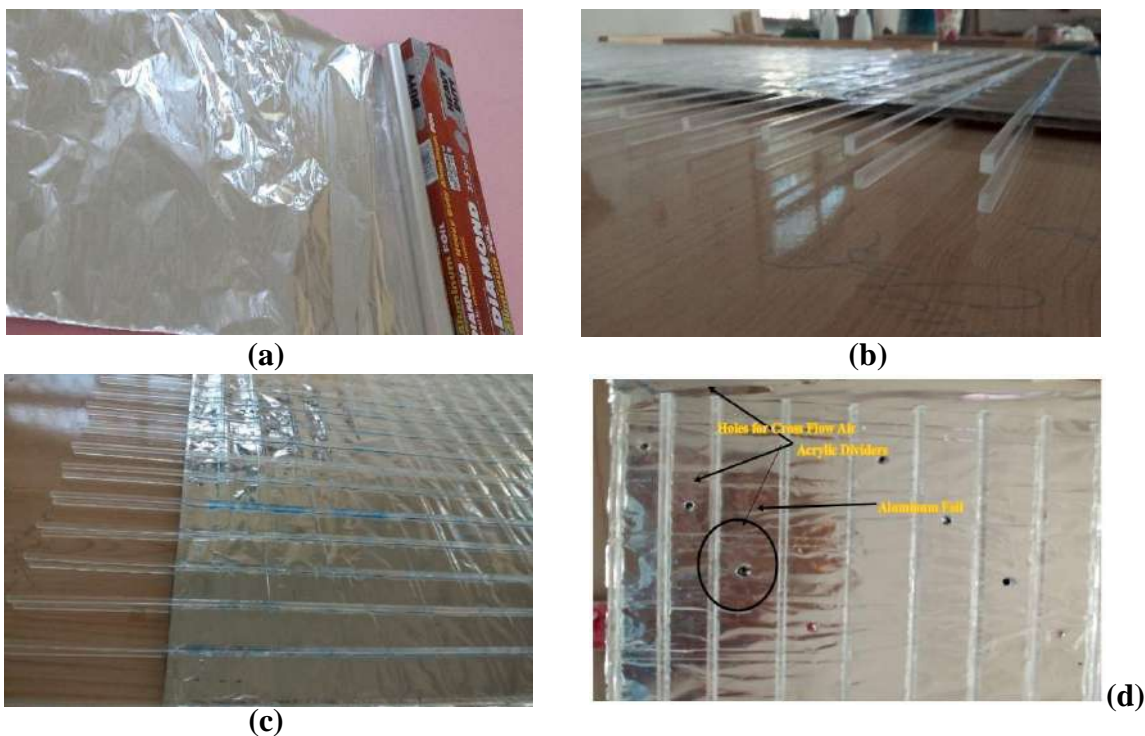


Figure 4.4: Different fabrication phases (a) aluminum foil, (b) acrylic dividers, (c) joining acrylic dividers and aluminum foil, (d) create holes in zig-zag pattern

4.2.2.2 Experimental setup of DVP 02

The locally developed design variant prototype 02 consists of the HMX, blower, water pump, water pipe, and water storage tank. The difference in this system is the dimensions and materials used for the fabrication of the HMX. The working principle of DVP 02 is the same as DVP 01. The design specifications of the DVP 02 are given in Appendix A. The complete experimental setup of the design variant prototype 02 in which aluminum foil is coupled with cotton cloth as shown in Figure 4.5.5.

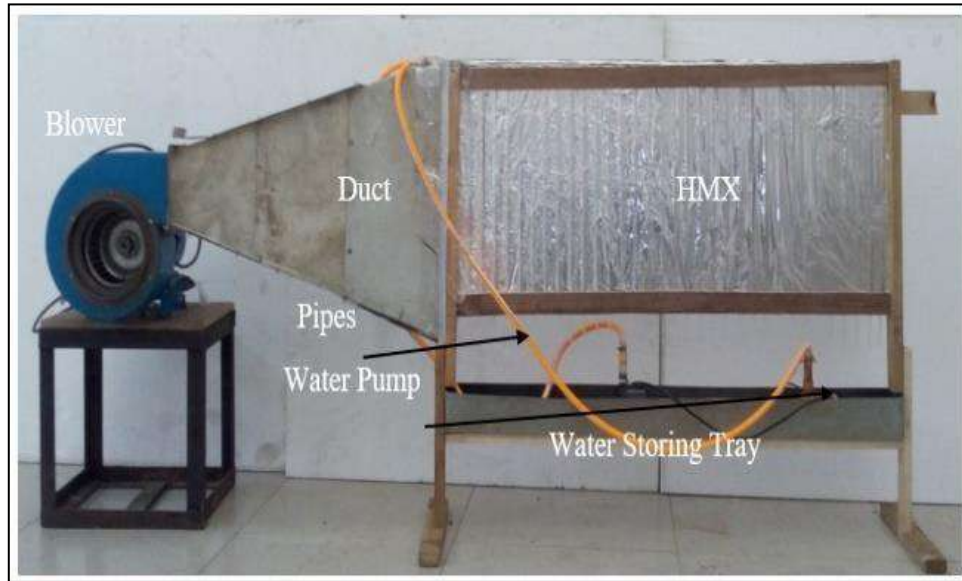


Figure 4.5: The apparatus diagram of the design variant prototype 02

4.2.3 Design

variant prototype 03

4.2.3.1 Manufacturing of the HMX

Design variant prototype 03 is consisted of blower, HMX, and water pump. The dry and wet channels of the HMX are made with A₃ laminated plastics sheets, acrylic dividers, and non-woven fabric. The laminated plastics sheets are cut by using appropriate tools so that there is no sharp edges or any embossed edges. These A₃ laminated sheets are attached with non-woven fabric to increase the wettability in the wet channels of the HMX. The acrylic dividers are joined with A₃ laminated plastics sheets and non-woven fabric with the help of sementex bond. The distance is 21.4 mm with each divider.

The HMX of the design variant prototype 03 is made with 18 dry and 19 wet channels. So, the height, width, and length of the HMX is 152 mm, 420 mm, and 300 mm respectively. In dry and wet channels, air and water holes are created in five sub-channels. So, the working air and water is moved through these holes into the wet channels. In dry channel, four sub-channels are blocked at output side and air is transferred into the wet channels through these holes for the evaporation. The different materials and fabrication phases of design variant prototype 03 as shown in Figures 4.6 and 4.7. The dry and wet channels of the design variant prototype 03 as shown in Figure 4.8.

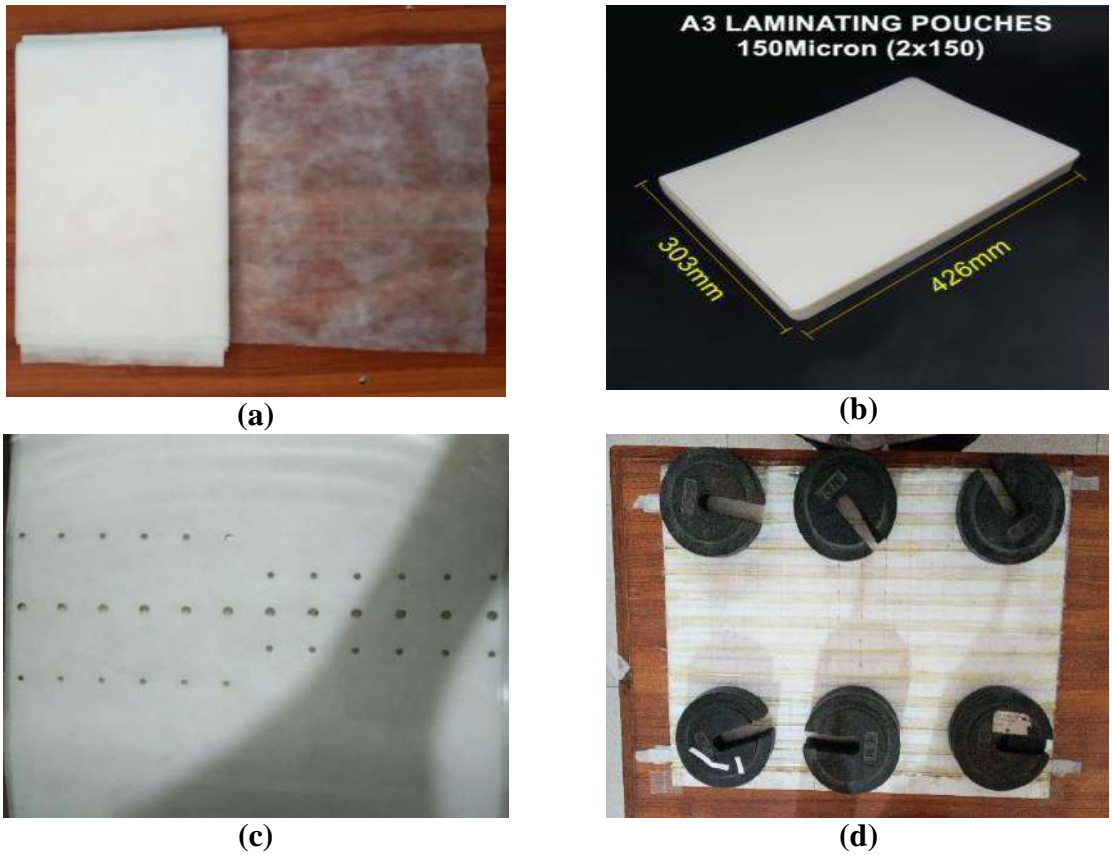


Figure 4.6: Different materials used (a) polypropylene nonwoven fabric, (b) A3 laminated plastics sheet, (c) holes pattern on sheet, (d) attaching dividers on plastic sheet with sementex bond

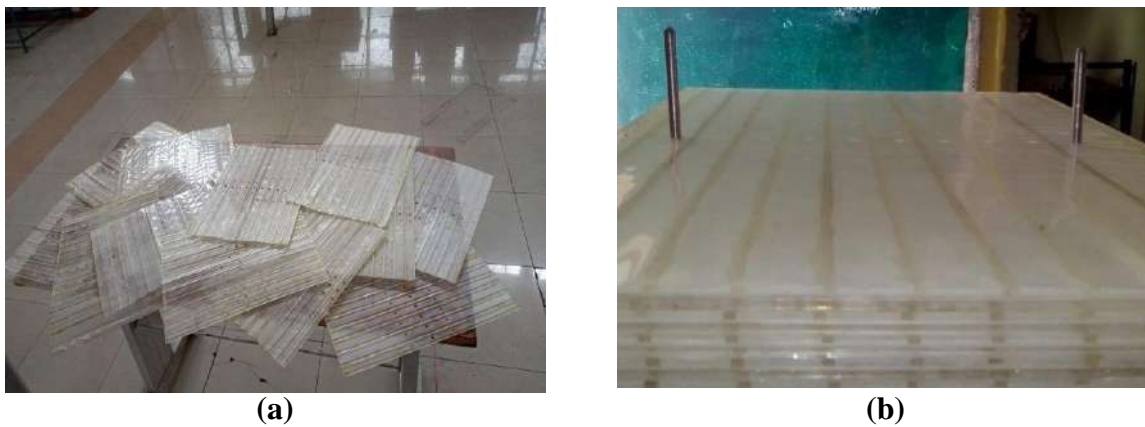


Figure 4.7: Fabrication phases (a) dry and wet channels after preparation, (b) joining dry and wet channels to fabricate the HMX

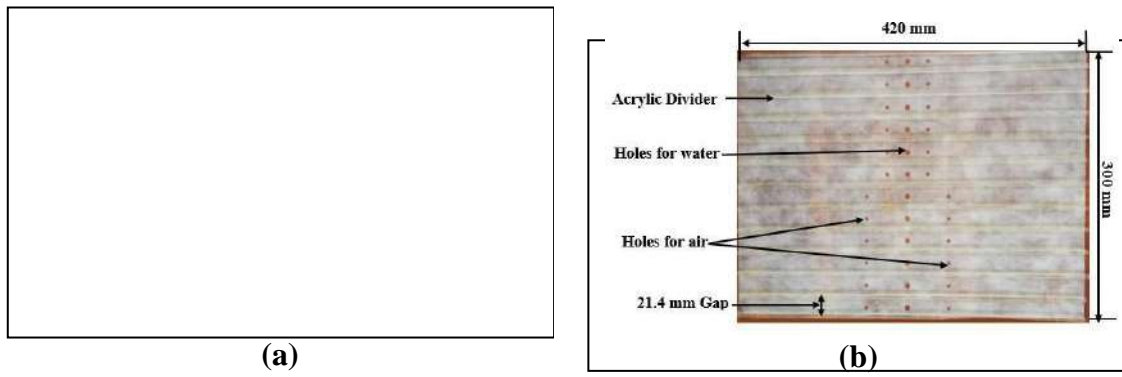


Figure 4.8: Dry and wet channels of the DVP 03

The different views of the HMX of

design variant prototype 03 (a) process air side view, (b) product air side view, (c) top view, (d) working air exhaust side view as shown in Figure 4.9. The HMX of the design variant prototype 03 with duct as shown in Figure 4.10.

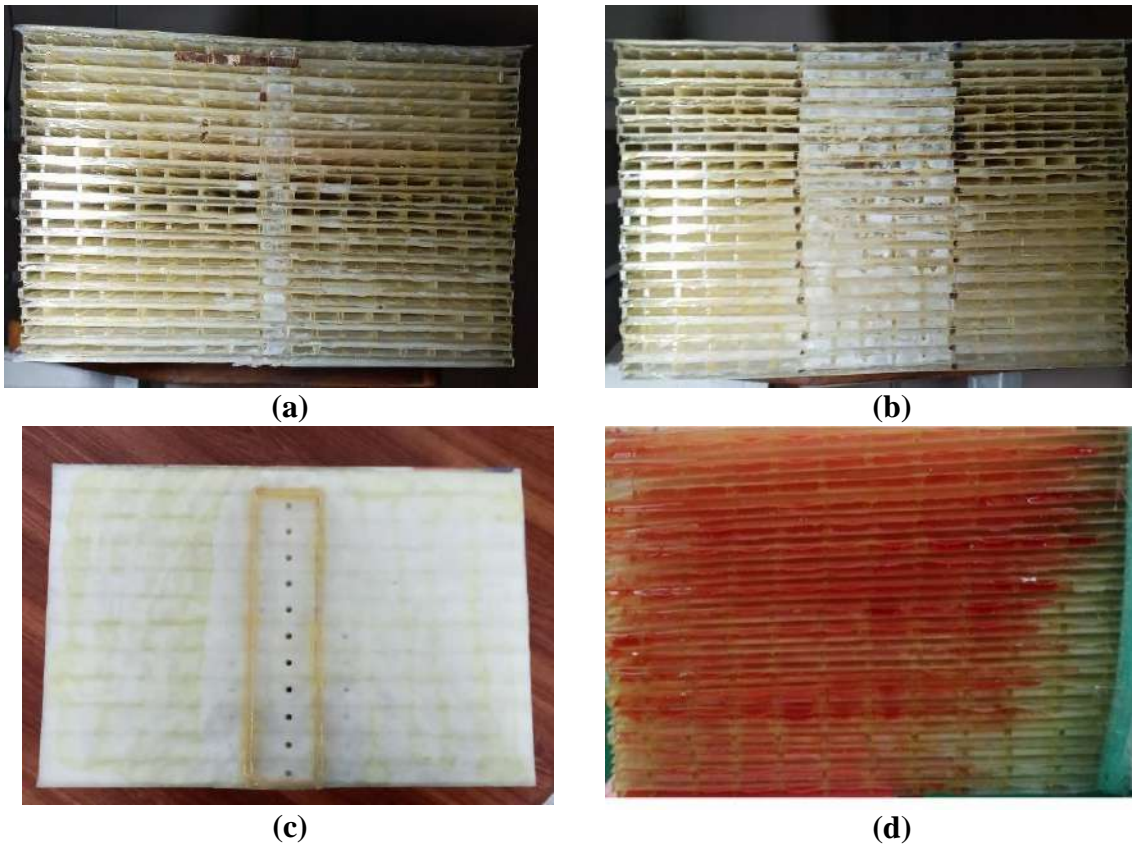


Figure 4.9: Different views of HMX of design variant prototype 03 (a) process air side view, (b) product air side view, (c) top view, (d) working air exhaust side view

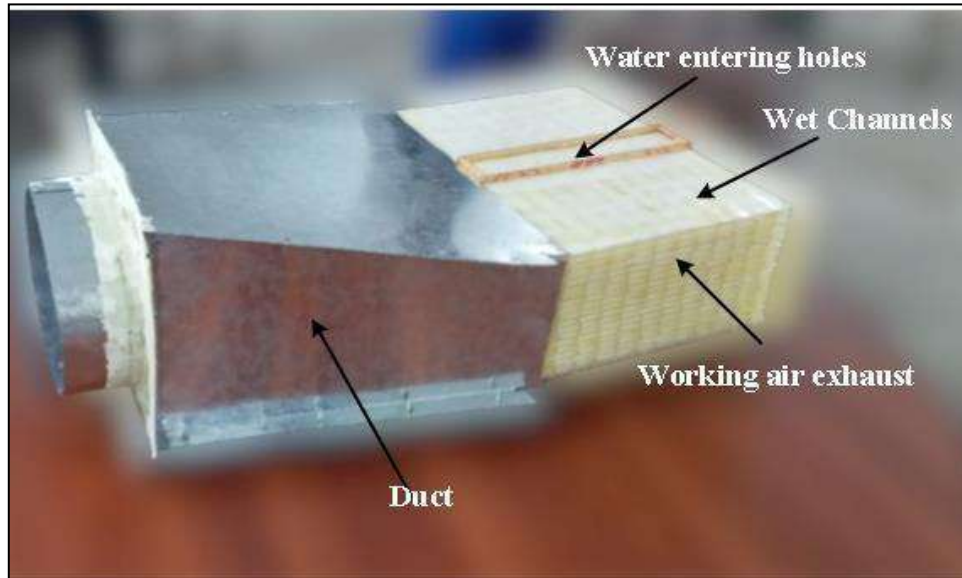


Figure 4.10: The HMX of the design variant prototype 03 with duct

4.2.3.2 Experimental setup of the DVP 03

Locally developed design variant prototype 03 consists of air conditioning laboratory unit (ACLU), HMX, and water pump. ACLU is used to testify the DVP-03. ACLU is an autonomous training system for the experimentation on cooling, refrigerating, air handling, heating, humidifying, and de-humidifying system. It is designed to create various conditions and environments. It is also designed for investigating the primary factors that have been controlled in a conventional air-cooling system. Using ACLU, they have set required values of ambient temperature and humidity. This system is tested under a wide range of temperatures which is varying T_{in} from 30-49 °C and RH varying from 13-20% while the other parameters like velocity (6.1 m/s) and water temperature (20 °C) are fixed. The design specifications of the DVP 03 are given in Appendix A. The air conditioning laboratory unit coupling with the HMX at the outlet of the unit as shown in Figure 4.11.

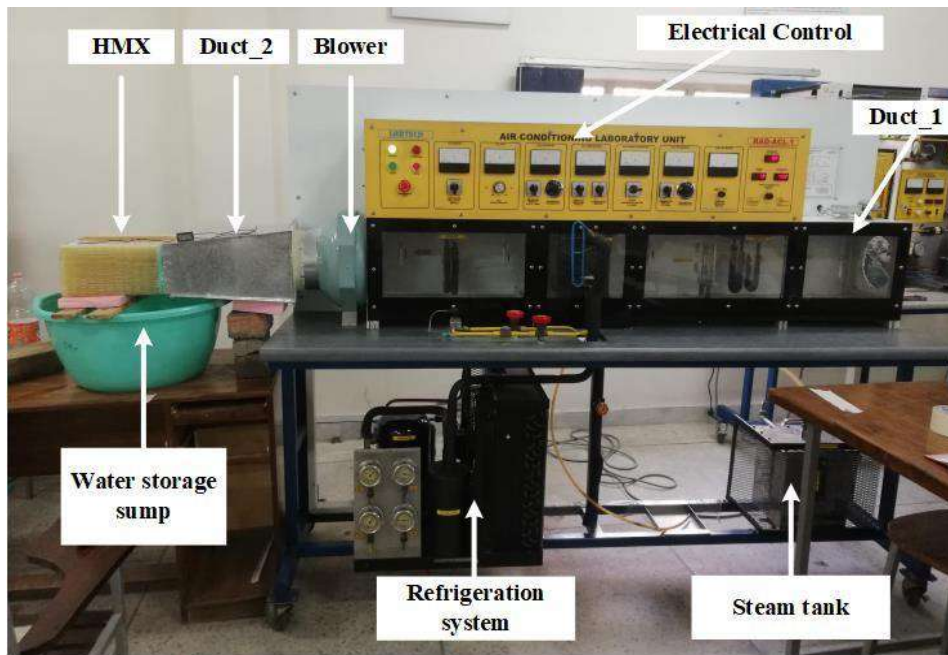


Figure 4.11: Experimental setup of the DVP 03 integrated with ACLU

4.2.4 Design

variant prototype 04

4.2.4.1 Fabrication of the HMX

In design variant prototype 04, the sementex bond is replaced with the desmocoll adhesive bond while the remaining fabrication process is same as DVP 03. Moreover, height of the HMX is also increased by increasing the number of dry and wet channels. The HMX of the design variant prototype 04 is made with 36 dry and 37 wet channels. The height, width, and length of the HMX is 300 mm, 420 mm, and 300 mm respectively. The different views of the HMX of DVP 04 as shown in Figure 4.12. The assembly phases of the DVP 04 (a) axial fan, (b) axial fan with external assembly, (c) HMX with external assembly, (d) fixing HMX, water storage sump in external assembly as shown in Figure 4.13.



Figure 4.12: Different views of the HMX of DVP 04 (a) working air side view, (b) symmetric view

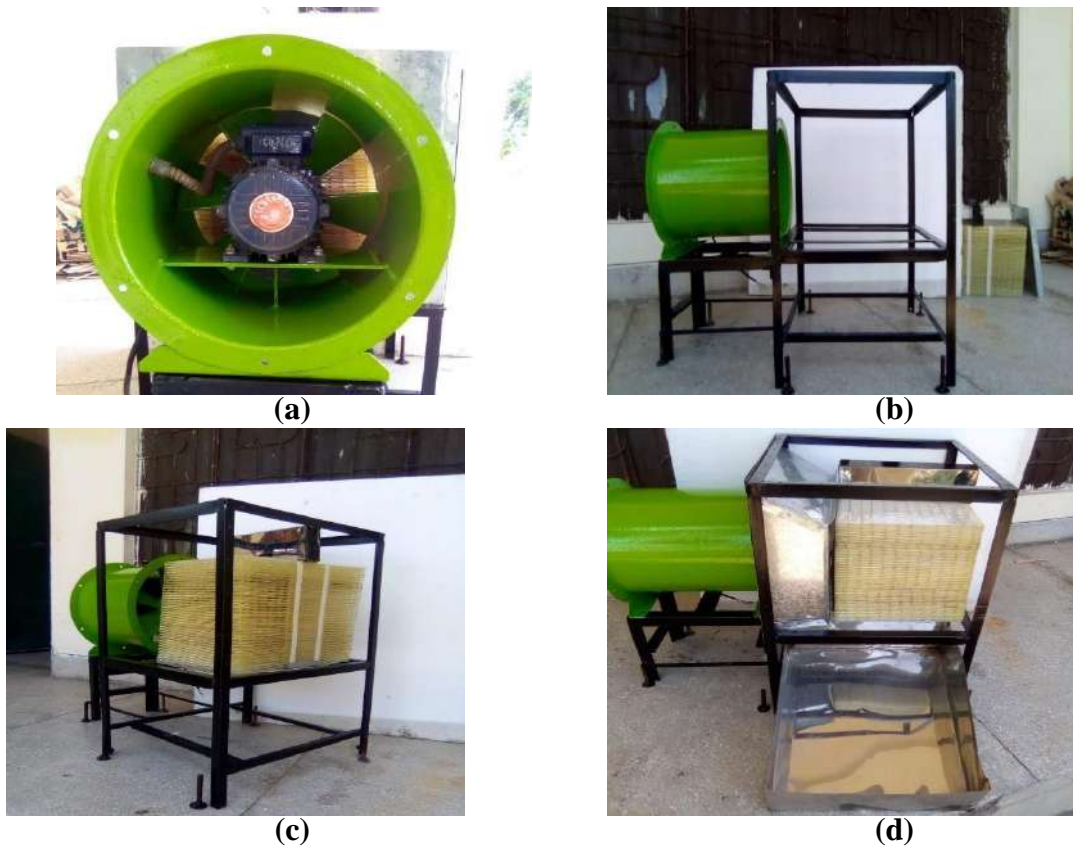


Figure 4.13: Assembly phases of DVP 04 (a) axial fan, (b) axial fan with external assembly, (c) HMX with external assembly, (d) fixing HMX and water storage sump

4.2.4.2 Experimental setup of the DVP 04

Locally developed design variant prototype 04 consists of the HMX, axial fan, duct, and water storage tank. In this system, the water is entered into the wet channels of the HMX from holes that are created at the top of the HMX. This water flows through wet channels of HMX which is cooled the incoming process air in the dry channels that is supplied to conditioned space. The water bucket is used for water supplied to the HMX while the water storage tray below the HMX is used to collect the water and transport it back to the water bucket using a water pump. Moreover, an axial fan is used for supplying the ambient air to the system. The power consumption of the axial fan is 550 W. The design specifications of DVP-04 are given in Appendix A. The experimental setup of design variant prototype 04 as shown in Figure 4.14.

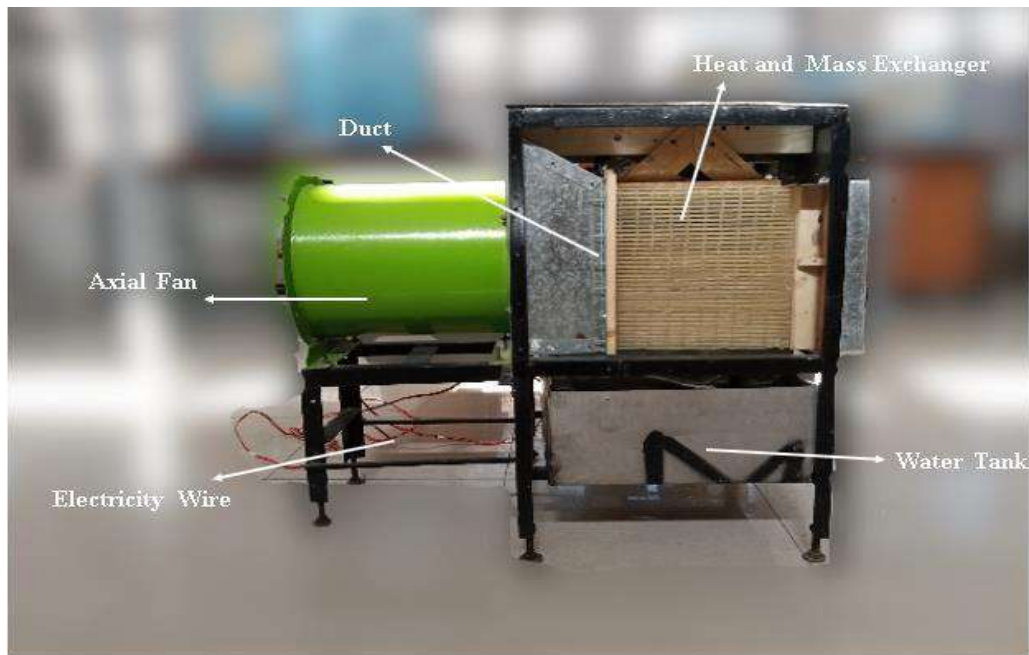


Figure 4.14: Experimental setup of the design variant prototype 04

4.2.5 Design variant

prototype 05

4.2.5.1 Manufacturing of the HMX

In design variant prototype 05, the position of the water and air holes are changed. For water flow, holes are created at extreme left side of the sheets and the air holes are created on right side of the water holes. In design variant prototype 05, A₃ laminated plastics sheets are scrubbed to remove a certain type of solution to get rid of the leakage problems. With the use of brush, this layer is removed, A₃ sheets with no layer of any type of adhesive which further resulted in leakage problem. Ethylene is used to remove the laminated solution from the plastics sheet. After that plastics sheets are attached to non-woven fabric using an adhesive bond. While the remaining fabrication process of DVP 05 is the same as DVP 04. The different fabrication process of DVP 05, (a) scrubbing of solution with brush, (b) joining non-woven fabric with A₃ laminated sheet (c) acrylic dividers cut by laser cutting, (d) using primer before applying adhesive bond as shown in Figure 4.15. The dry and wet channel of DVP 05 as shown in Figures 4.16.

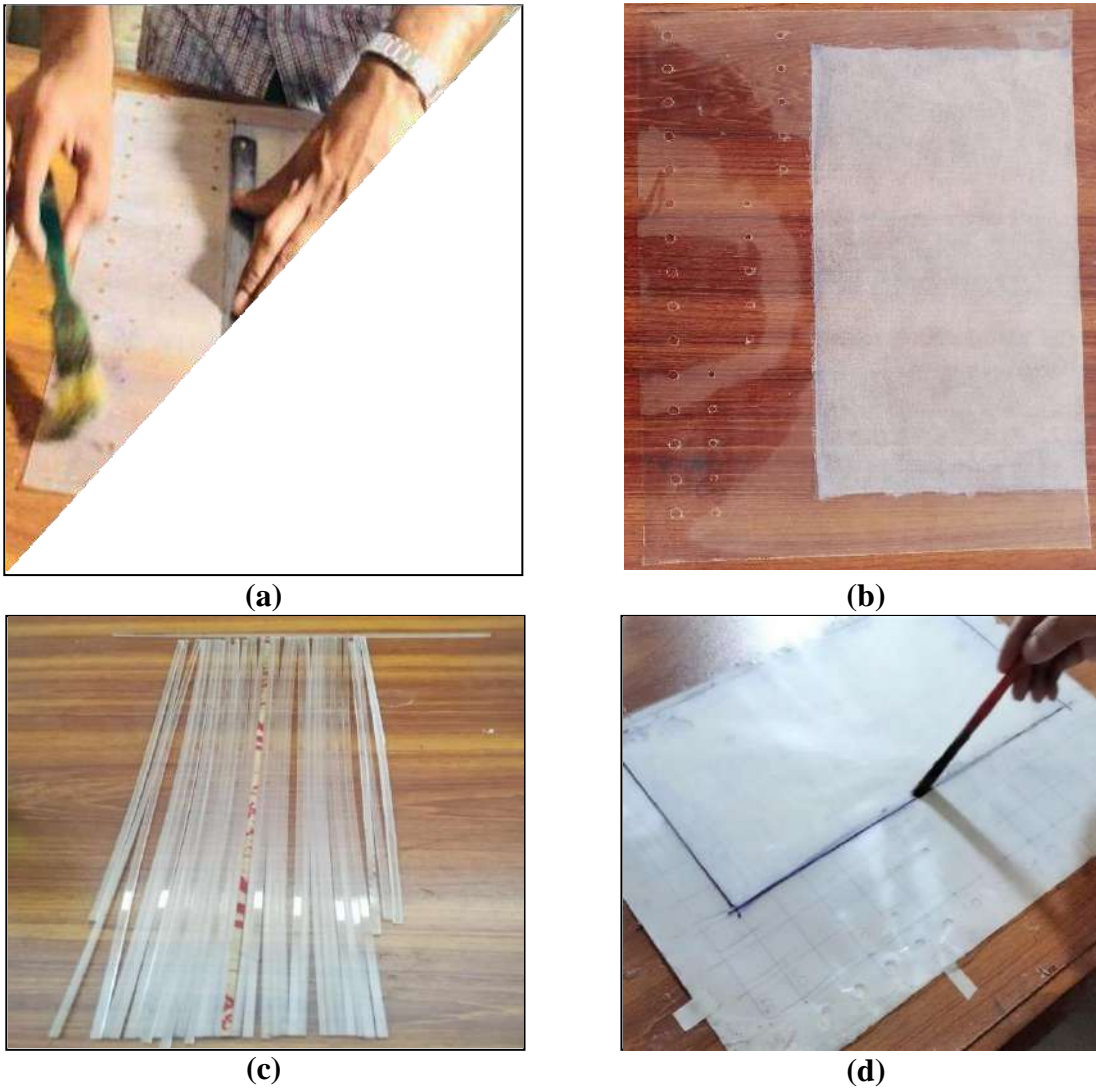


Figure 4.15: Fabrication process of DVP 05, (a) scrubbing of solution with brush, (b) joining non-woven fabric with A₃ sheet (c) acrylic dividers, (d) applying the primer

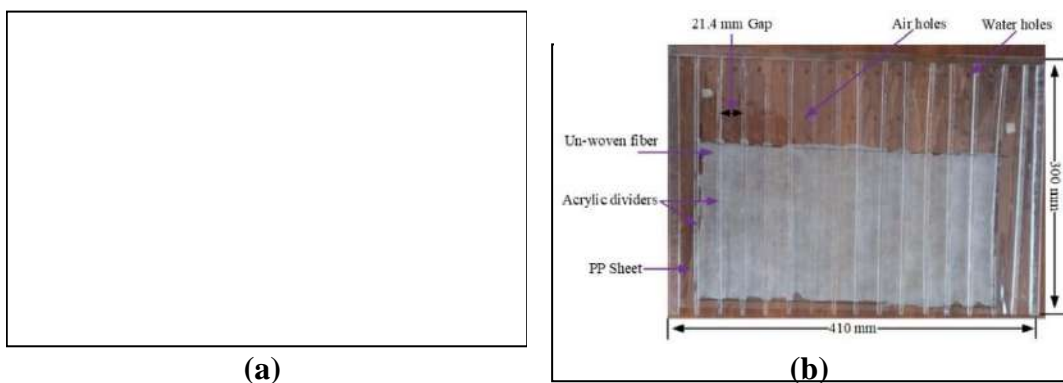


Figure 4.16: Dry and wet channels of the DVP 05

After that, all the dry and wet channels are assembled in such a way that dry channel came after the wet channels to fabricate the HMX. In this design variant prototype, there are 07 dry channels and 08 wet channels. The different views of the HMX

Product Design and development of Innovative Air Cooler with Desiccant-based Dehumidification.

as Shown in Figure 4.17.

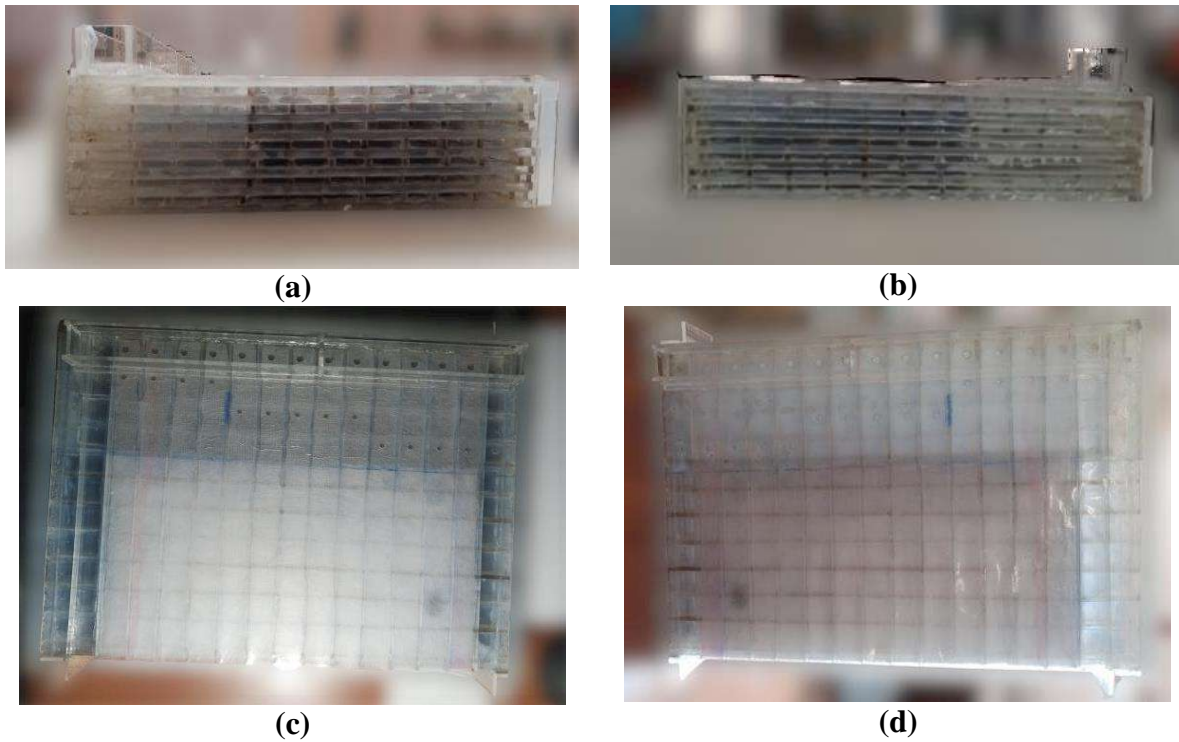


Figure 4.17: Different views of the HMX of DVP 05, (a) front view, (b) back view, (c) top view, (d) bottom view

4.2.5.2 Experimental setup of the DVP 05

Locally developed design variant prototype 05 consists of HMX, axial fan, heating fan, duct, and water storage tank. The ambient air is heated and then supplied in dry channels while the remaining working procedure is same as previous. The design specifications of the DVP 05 are given in Appendix A. The experimental setup of the DVP 05 as shown in Figure 4.18.

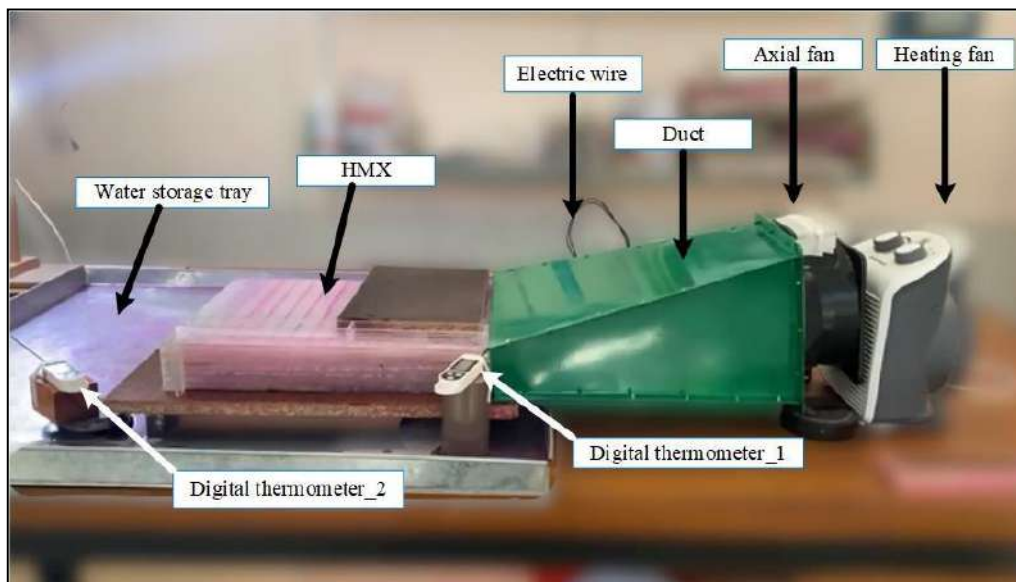


Figure 4.18: The experimental setup of the design variant prototype 05

4.2.6 Design variant prototype 06

4.2.6.1 Fabrication of the HMX

In design variant prototype 06, the height of the HMX is increased by increasing the dry and wet channels. The HMX is consisted of 22 dry and 23 wet channels. The height, width, and length of the HMX are 204 mm, 300 mm, and 410 mm, respectively. The different assembly steps of the HMX as shown in Figure 4.19.

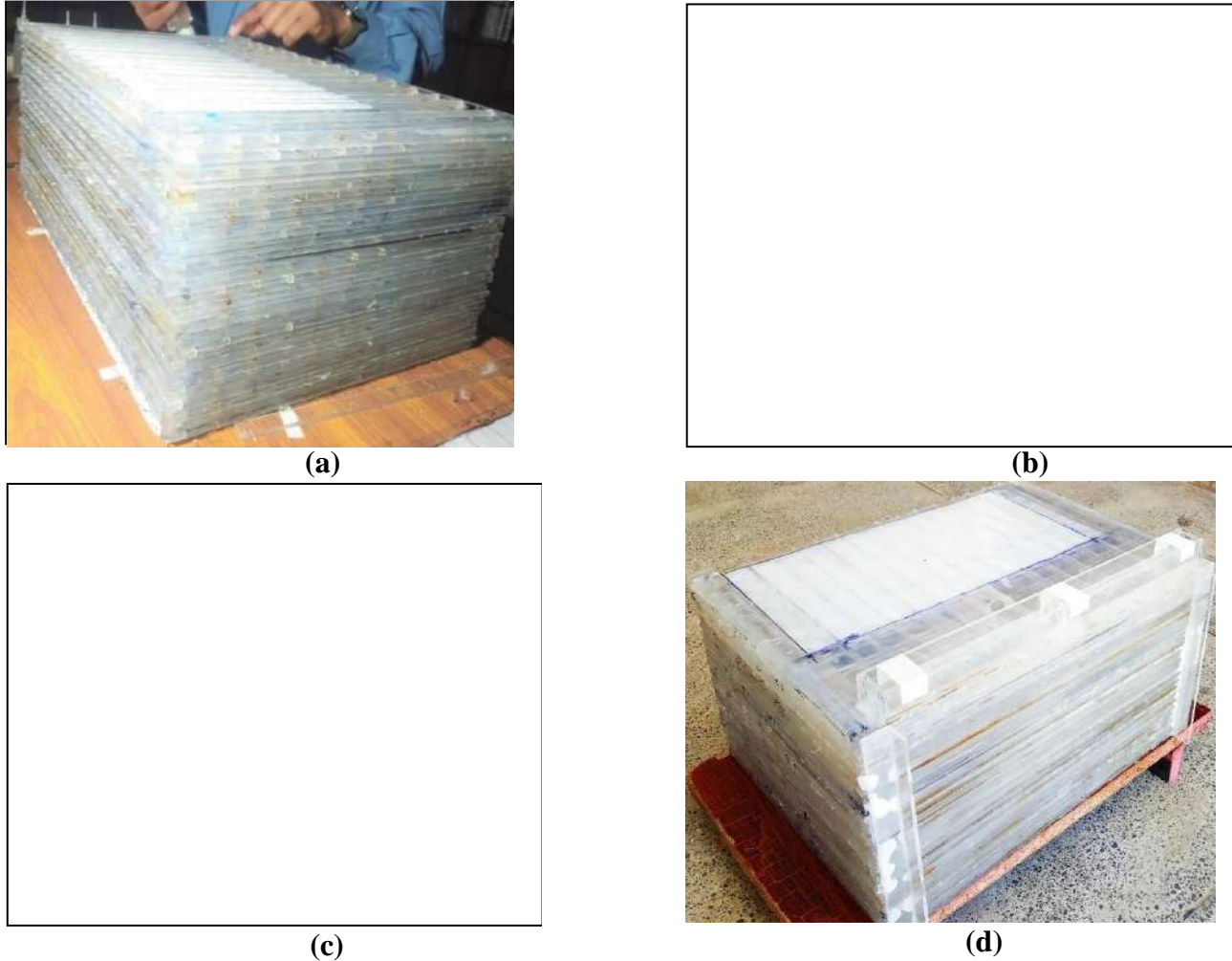


Figure 4.19: Different assembly steps of the HMX of DVP-06, (a) piling up dry and wet channels, (b) channels assembly, (c), channel assembly with supports, (d) symmetric view of HMX

In the DVP 06, the fan is attached with duct which is integrated with the HMX. The water from the tank is pumped to the water bucket. The rear view of the HMX with the fan as shown in Figure 4.20 (a) and the front view showing working air and product air outlet as shown in Figure 4.20 (b).



Figure 4.20: Design variant prototype 06 (a) rear view, (b) front view

4.2.6.2 Experimental setup of the DVP 06

The locally developed design variant prototype 06 consists of HMX, axial fan, water pump, water storage tank, and measuring instruments. The working principal of the DVP 06 is the same as previous. The design specifications of DVP 06 are given in Appendix A. The experimental setup of DVP 06 as shown in Figures 4.21 and 4.22, respectively.

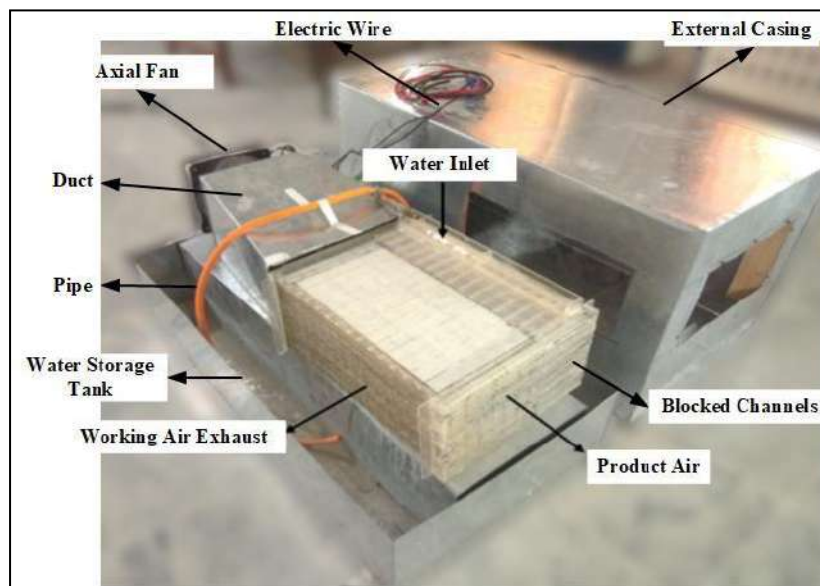


Figure 4.21: The experimental setup of design variant prototype 06 (Internal view)



Figure 4.22: The experimental setup of design variant prototype 06 with measuring sensors (External view)

4.2.6.3 Final product

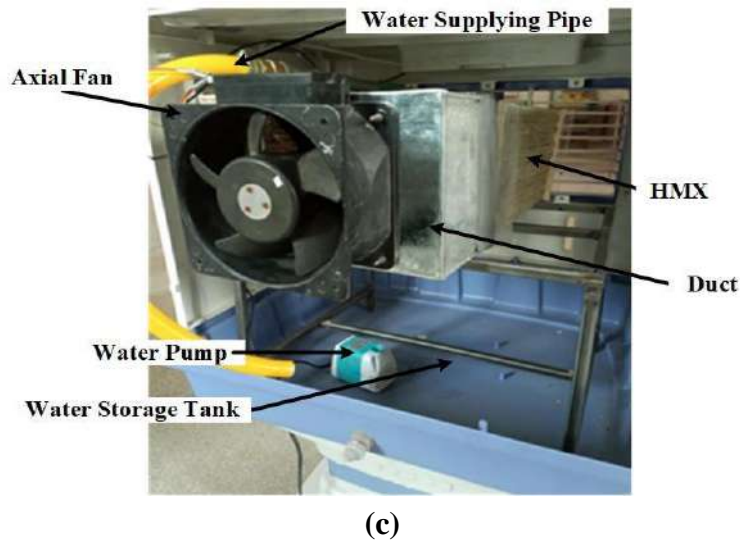
The fabrication process of the final product is the same as previous. In the final product, there are also 19 dry channels and 20 wet channels. So, the height of the HMX of the final product is 176 mm. The HMX is fixed in the external casing. The different assembly steps of the final product as shown in Figure 4.23.



(a)



(b)



(c)
Figure 4.23: Different assembly steps of the final product, (a) HMX, (b) HMX fixed in external casing, (c) back view of the final product

4.2.7 Technical issues

Heat and mass exchanger (HMX) is the key part of the DP-IEC. There are facing many technical problems to develop the efficient heat and mass exchanger and solved them to fabricate the final version of HMX. These technical issues are given below Table 4.1. Moreover, the pictures of the HMXs are given in Table 4.2.

Table 4.1: Materials used and technical problems in the development of HMX prototypes

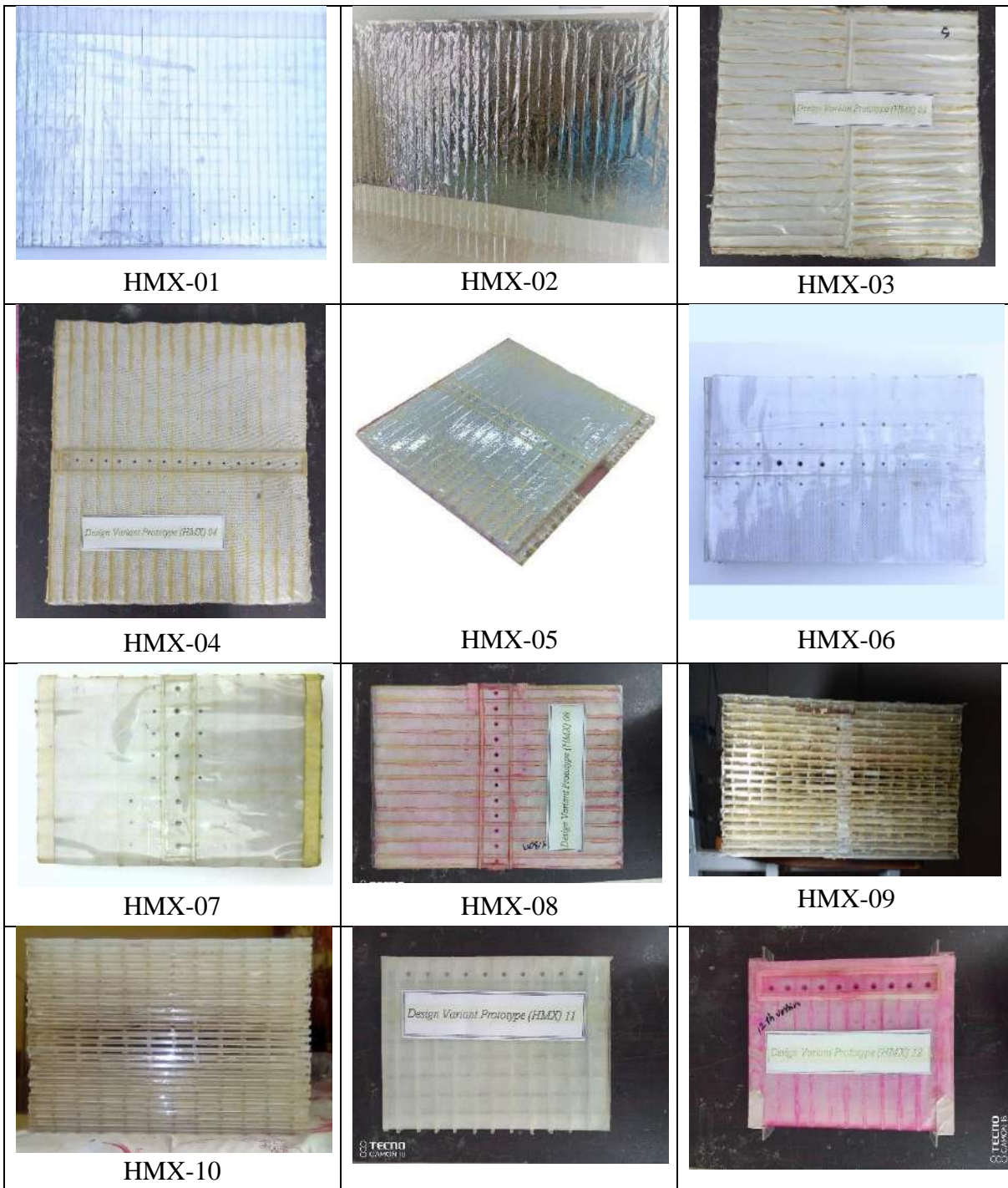
HMX	Materials	Technical issues
HMX-01	Aluminum sheet, acrylic dividers, cotton cloth, Elfie, silicon sealant, copper pipes, and externally supported by acrylic sheet.	In HMX-01, one dry channel is merged between two wet channels in vertical design, the air is diverted from dry channel to wet channels for the evaporation. In wet channels, the flow direction of the air is downward as well as the flow of water droplets are also downwards. But most of the working air is moved upward due to free spaces. On the other hand, air is resisted to water flow, which is necessary for wetting. The copper pipes are used for the supply of water in wet channels, which are assisted in the pressure of water in the wet channels.

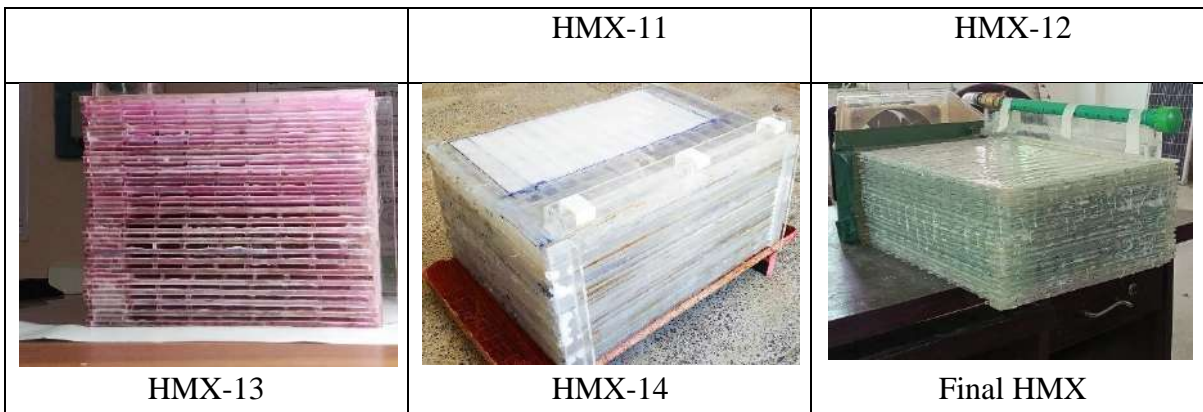
HMX-02	Aluminum foil, cotton cloth, Elfie, silicon sealant, copper pipes and acrylic dividers.	In HMX-02, when the air is moved in the dry channel, the dividers are detached from aluminum foil resultantly. So, the aluminum foil-based channel is inflated. Inside the wet channels, there is the approximately zero flow of the air due to the expand of the channels.
HMX-03	Polythene plastic sheets, cotton cloth, sementex bond, acrylic dividers, and pipes	In HMX-03, the wettability in the wet channels is inadequate due to low water flow. The flow of pressurized water is impossible even using the PVC pipes inside the wet channels.
HMX-04	Polythene sheets, cotton cloth, sementex bond and acrylic dividers.	In HMX-04, the wetting in wet channels is also inadequate due to the use of cotton cloth, because it has not capillary action. On the other hand, water and air holes are manually punched which are resisted the water flow in column by gravity. Moreover, insufficient air is flown from the dry channel to wet channels. Also, cloth is not properly joined with polythene sheets.
HMX-05	Plastic sheets, sementex bond, acrylic dividers, and mesh cloth.	In HMX-05, improper water flow in wet channels because the water holes are punched manually that are produced pressure drops.
HMX-06	A4 size laminated sheets, mesh cloth, acrylic dividers, and double side transparent tape.	In HMX-06, acrylic dividers are not fixed at their positions when the air is flown through the dry channels, because they are joined with double solution transparent tape. The double solution transparent tape is detached due to the air pressure. Also, water and air holes are punched manually that produce pressured drop of the air and improper water flow in wet channels.
HMX-07	Non-woven fabric, A4 size laminated plastic sheets,	In HMX-07, acrylic dividers are not fixed with polypropylene plastic sheets properly. Acrylic

	acrylic plastics, and double side transparent tape.	dividers are detached from their positions due to the pressure drop of the air.
HMX-08	A ₃ size laminated plastic sheets, non-woven fabric, cementex bond, and acrylic dividers.	In HMX-08, there have not observed any significant technical issues.
HMX-09	A ₃ size laminated plastics sheet, non-woven fabric, cementex bond, and acrylic dividers.	In HMX-09, also, there have not observed any significant technical issues.
HMX-10	A ₃ size laminated plastics sheet, non-woven fabric, cementex bond, and acrylic dividers.	In HMX-10, As the size of the HMX increases, the water leakages are started from the wet channels. In the wet channels, cementex bond is not joined the acrylic dividers with non-woven fabric. So, the water leakages are started from the wet channels with passage of times.
HMX-11	A ₃ Laminated plastics sheet, non-woven fabric, adhesive bond (Sample of servis shoes bond) and acrylic dividers.	In HMX-11, also, there have not observed any significant technical issues.
HMX-12	A ₃ size laminated plastic sheets, non-woven fabric, adhesive bond (Sample of servis shoes bond), and acrylic dividers.	In HMX-12, same technical issues are facing as HMX-10. In the wet channels, adhesive bond is not joined the acrylic dividers with non-woven fabric. Water leakages are started in the wet channels with the passage of times.
HMX-13	A ₃ laminated plastic sheets, non-woven fabric, acrylic dividers, and adhesive bond (intra-mer primer, intradur AC hardener, and intra Lowe FW).	In HMX-13, same technical issues are facing as HMX-12.

<p>HMX-14</p>	<p>A₃ laminated plastic sheets, non-woven fabric, acrylic dividers, and adhesive bond (intra-mer primer, intradur AC hardener, and intra Lowe FW).</p>	<p>In HMX-13 identifying the all-technical issues and solved them so that the HMX-14 has no technical issue.</p>
---------------	---	--

Table 4.2: Different heat and mass exchangers (HMX)





4.3 Experimental setups for water recovery

4.3.1 Experimental setup of water recovery 01

4.3.1.1 Fabrication of the water recovery system

The water recovery system is consisted of the hydrophobic sheets, mesh cloth, duct, heat and mass exchanger (HMX), blower, water pump, and water supplying pipes. The hydrophobic sheets and mesh cloth are sewed and then made a filter type array. The stainless steel (SS) mesh sheet is used to support the hydrophobic sheets. This filter type array is blocked from top and bottom sides with the acrylic sheets. The hole is created in the bottom side of the filter for water collection and a water bottle is fixed in the bottom of the filter. The materials used for the fabrication of the water recovery system as shown in Figure 4.24. The different fabrication processes of the water recovery system as shown in Figure 4.25.



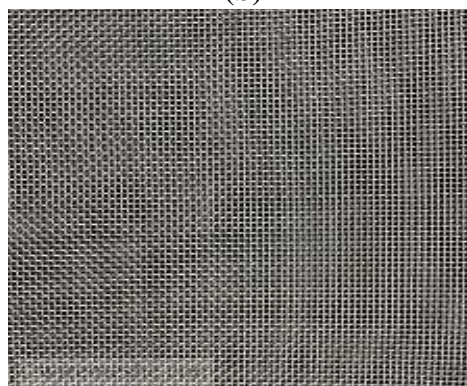
(a)



(b)



(c)



(d)

Figure 4.24: The materials used for the water recovery system, (a) hydrophobic sheets, (b) mesh cloth, (c) sewing the hydrophobic sheet and mesh cloth, (d) stainless steel mesh

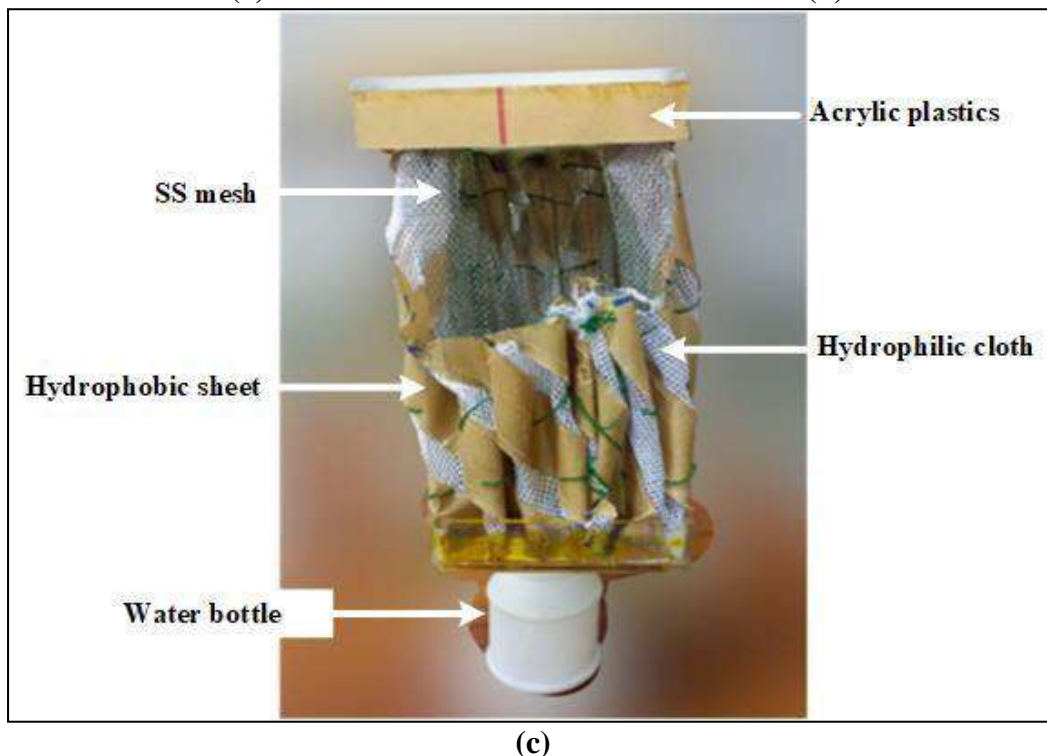
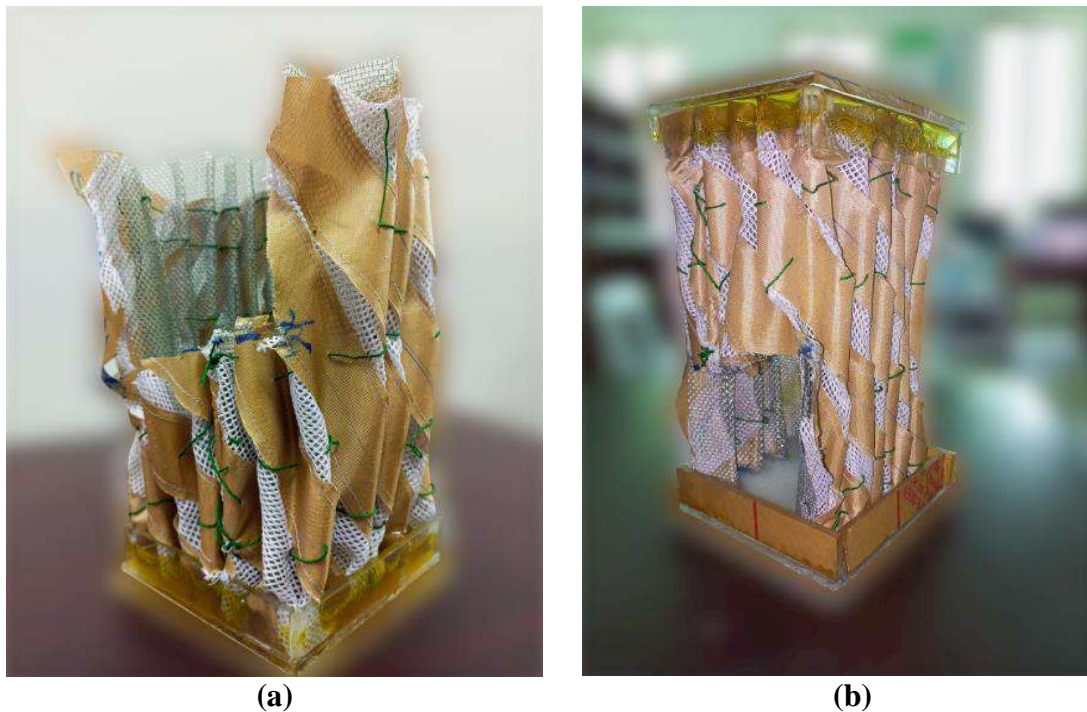


Figure 4.25: Making a filter type arrangement, (a) fixing the hydrophobic sheet by using SS mesh, (b) closing the top and bottom sides, (c) filter type array

4.3.1.2 Experimental setup of water recovery system 01

The locally developed water recovery system consists of the HMX, blower, water pump, water pipe, hydrophobic filter, ducts, and water storage tank. The key part of the system is water recovery filter which is made with hydrophobic and hydrophilic (mesh cloth) sheets. The hydrophobic sheets are water retained sheets

while the hydrophilic are water absorbing sheets. The working air is exhausted after engrossing heat and water droplets due to evaporation in wet channels. This exhaust air is passing through filter where the water droplets are retained on hydrophobic sheets and air is moved to atmosphere. The water bottle at the bottom of the filter is used to collect the extracted water from the working air. The design specifications of water recovery setup are given in Table 4.3. The experimental setup of water recovery system as shown in Figure 4.26.

Table 4.3: Design specifications and operating parameters of water recovery system

Parameter	Value	Parameter	Value
HMX width	300 mm	Hydrophilic sheet Thickness	0.2 mm
HMX length	410 mm	Water hole diameter	06 mm
HMX height	204 mm	No. of holes in working Channel	20
Height of channel	04 mm	Air hole's diameter	04 mm
Width of channel	21.4 mm	Dry channels	22
Type of channel	Rectangular	Wet channels	23
Non-woven fabric thickness	0.08 mm	Product to working air Ratio	30-70%
Polypropylene sheet thickness	0.08 mm	Hydrophobic sheet Thickness	0.15 mm
Axial fan	65 W	Water pump	25 W

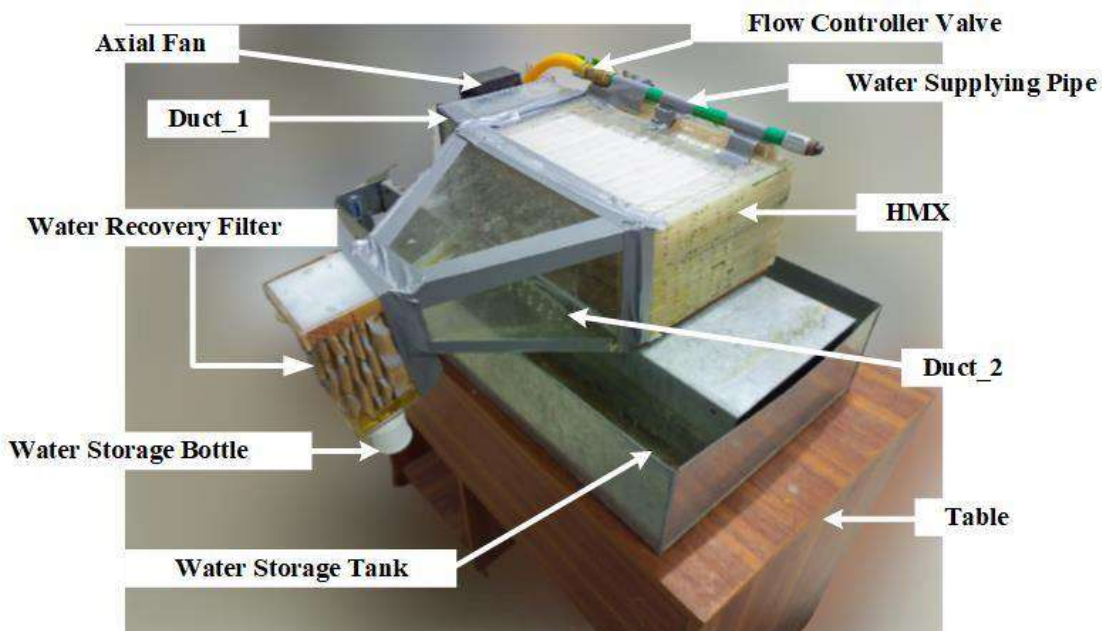


Figure 4.26: Experimental setup of water recovery system with hydrophobic type filter

4.3.2 Experimental setup of water recovery system 02

This water recovery system consists of HMX, blower, water pump, water pipe, ducts, and dehumidifier. The key part of this water recovery setup is the dehumidifier. The working air is exhausted after engrossing heat and water droplets due to evaporation in wet channels, is passing through dehumidifier. The dehumidifier extracted the water from the moist air. These extracted water from working air is collected in dehumidifier bucket and then reused it again in the system. The experimental setup of water recovery system as shown in Figure 4.27.

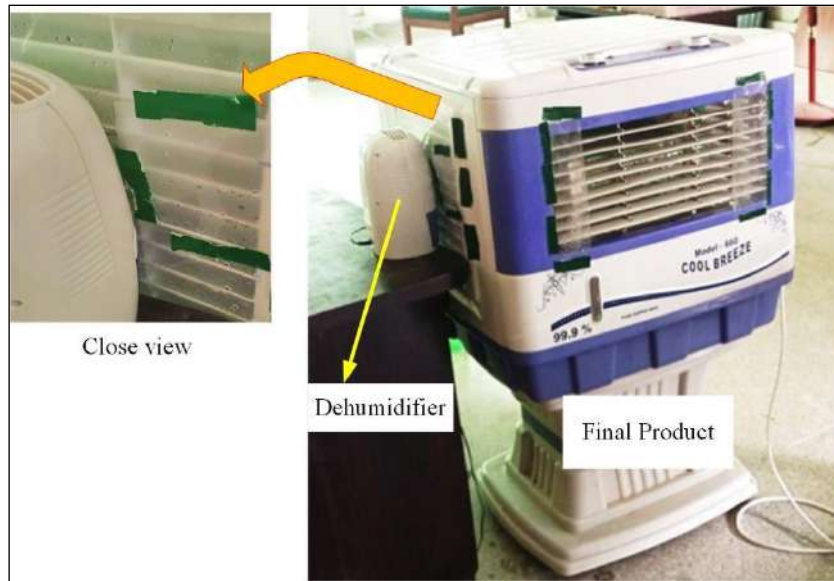


Figure 4.27: Experimental system of water recovery with dehumidifier

4.4 Real-time testing

The real testing is helped to select the more appropriate materials for the fabrication of HMXs (Key part of the DP-IEC). The selection of required materials is based on parameters like durability, life span, bonding strength, cost, and moisture absorbing ability etc.

4.4.1 Cloth selection for wettability

The cloth is used to improve the wettability in the wet channels. The water is flown in wet channels, contact with the working air and created the vapors which is sustained on the cloth surface, which is causing the heat absorption from the dry channels. The specifications of the different cloths as shown in Table 4.4. the different types of cloths or fabrics are trialed in the wet channels as shown in Figure 4.28, observed their capillary actions.

Table 4.4: Specifications of the cloth materials

Sr. No	Type	Thickness	Capillary action	Estimated cost (01 ft HMX)
1	Cotton cloth	0.8 mm	No	Rs 9000
2	Fabric cloth	0.25 mm	No	Rs 3000
3	Mesh cloth	0.9 mm	No	Rs 1050
4	Non-woven fabric	0.1 mm	Yes	Rs 500

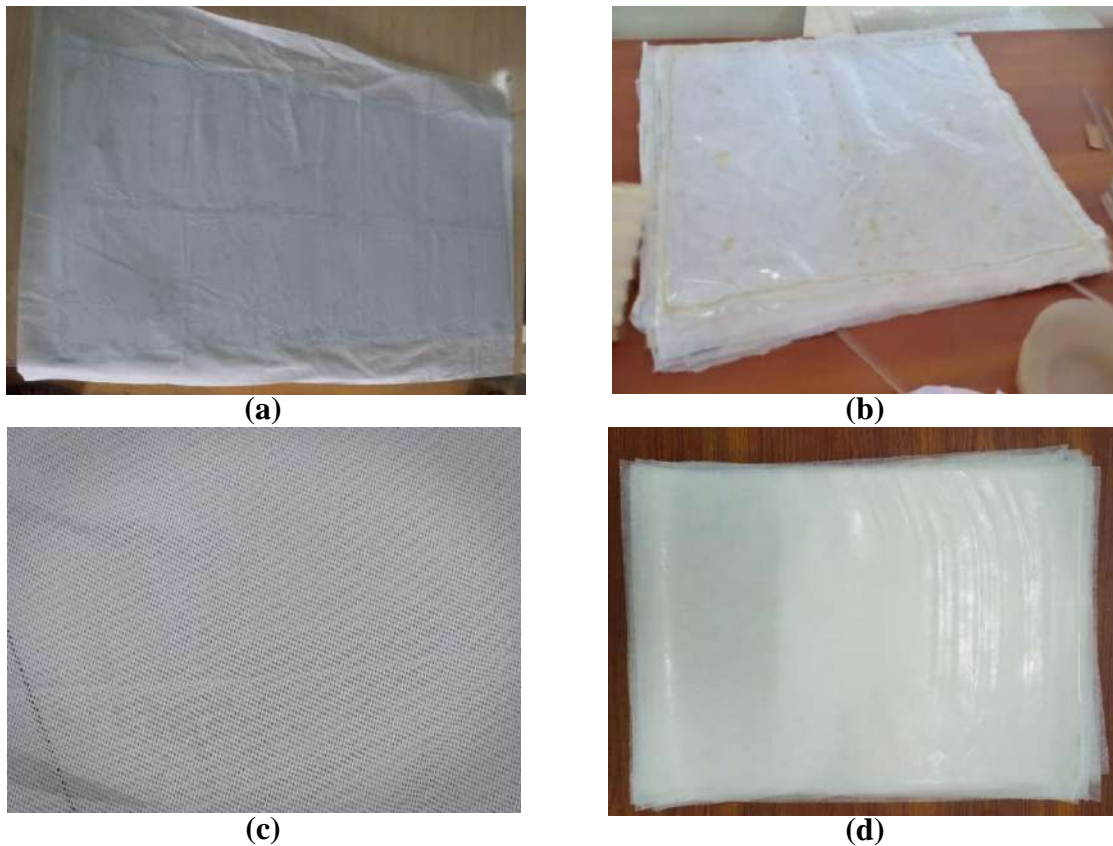


Figure 4.28: Different types of cloths, (a) cotton cloth, (b) fabric cloth, (c) mesh cloth, (d) non-woven cloth

4.4.1.1 Soaking effect on the bonding strength in fabric and plastics sheet

The polypropylene sheet was soaked in water container and for proper time span so it could attain the maximum amount of water. Then, it was kept from water container at room conditions and note down the time taken by sheet to complete evaporation. The bonding strength between the non-woven fabric and plastics as given in Table 4.5. Partially and completely dipped PP sheets in water container as shown in Figure 4.29. The sheet conditions after soaking and evaporating as shown in Figure 4.30.

Table 4.5: Bonding strength of PP sheet with plastics

Sr. No	Soaking time (h)	Complete evaporation (h)	Bonding strength
1	4	1.25	Same as previous
2	5	1.3	Same as previous
3	7	1.2	Same as previous
4	16	1	Same as previous
5	21	1.3	Same as previous



Figure 4.29: PP sheets dipped in water container, (a) partially dipped, (b) completely dipped

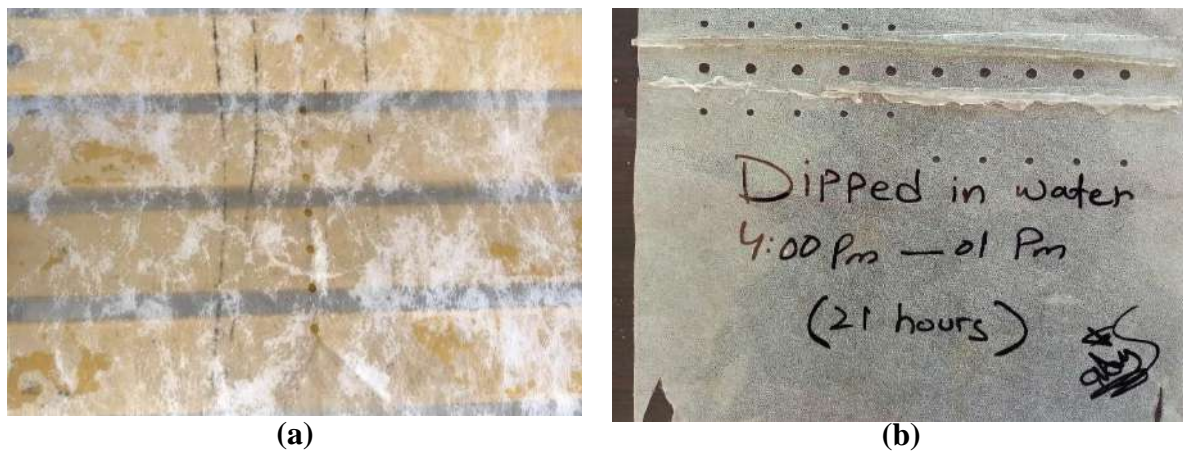


Figure 4.30: PP sheet condition after, (a) soaking, (b) evaporation

4.4.1.2 Cooling/heating effect on bonding

strength

The polypropylene sheets were joined with non-woven fabric and acrylic dividers. After preparing the sheets, some of the sheets were laid in freezer and some of the sheets were dipped in the hot water container. It is observed that the bonding strength of the sheets with non-woven fabric and acrylic dividers remains the same as previous. The prepared sample sheets of polypropylene sheets as shown in Figure 4.31.



Figure 4.31: Cooling and heating effect on bonding strength

4.2.2. The wettability.

The degree of wetting is known as wettability. It is determined by the force balance between cohesive and adhesive forces. The wetting governs the important phenomenon called capillary action, is the capability of a liquid to uphold its contact with solid surface, resulting because of intermolecular interaction between the solid surface and liquid molecules. The wettability depends on the contact angle that liquid molecule makes with the solid surface, less the contact angle the higher will be saturating of the liquid.

4.4.2.1 The assessment of wettability in the wet channels

To examine the wettability of wet channels, filling the plastics bottle with fresh water. Two tablets surf excel, and a small amount of color (pink) were mixed in the water bottle and shaking it so that it has mixed completely. The water bottle turned pink color. When the blower was switched on, air with high pressure came from the blower and started to pass through the open channels of the dry channel and the product air was received from the outlet. The working air was also passing through the wet channels. After that, the color water has been pouring into the wet channels from top of the HMX. A few minutes later, colored water was filled in wet channels and evaporation started. It is observed that working air was made more clusters with water as shown in Figures 4.32 and 4.33.

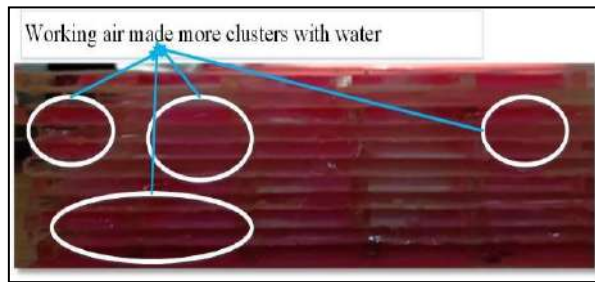


Figure 4.32: Exhaust working air with water droplets from the wet channels

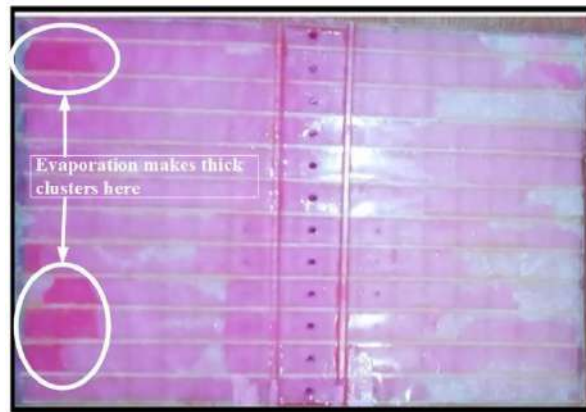


Figure 4.33: Top view of the HMX

4.5 Measuring

instruments and procedure

The temperature of the product and working air was measured with the help of digital thermometers, IR thermometer, and wall thermometer that were fixed at the inlet and outlet of dry channels and wet channels with accuracy ($\pm 0.1^\circ\text{C}$). Relative humidity of the ambient and working moist air was measured with humidity meter datalogger which has the accuracy ($\pm 3\%$). The velocity of the product air and exhaust air were measured with different anemometers with accuracy ($\pm 1-5\%$). Rotameter was used to measure the feed water flow. Feed water temperature was measured at the inlet and outlet of wet channels. The pressure losses of the system were measured with U-tube barometer. Two taps were fitted in the extension of duct and product side of the HMX. Taps were connecting with u-tube barometer tubes which have consisting of water fluids. Water consumption of the DP-IEC system was calculated by measuring the heights level of the water storage tank before and after using the system. Different instrument's specifications are given in Table 4.6. Figure 4.34-4.37 shows the photographs of the measuring instruments.

Table 4.6: The specifications of the instruments

Instrument	Variable Measured	Uncertainty
Digital thermometer	Temperature	0.1 °C
Thermometer	Temperature	0.8% °C
Temperature humidity meter datalogger	Humidity, Temperature	3% RH, 0.8% °C

IR thermometer	Temperature	0.05 °C
Wall thermometer	Temperature	0.2 °C
Digital humidity meter	Humidity	1%
Mini anemometer	Velocity	5% m/s
Digital anemometer	Velocity	1% m/s
Hot wire anemometer	Velocity	5% m/s
Rotameter	Water flow	1% l/m
U-tube barometer	Pressure	1% Pa



(a)



(b)



(c)



(d)



(e)

Figure 4.34: Pictures of temperature measuring instruments (a) digital thermometer (TP 300), (b) thermometer type k/j (TM-82N), (c) temperature humidity meter datalogger (TM-182), (d) IR thermometer (FLUKE 62 MAX), (e) thermometer



(a)



(b)



(c)



(d)

Figure 4.35: Pictures of humidity and velocity measuring instruments, (a) digital humidity meter, (b) mini anemometer (UT363), (c) digital anemometer (MS6252B), (d) hot wire anemometer (AM-4204)

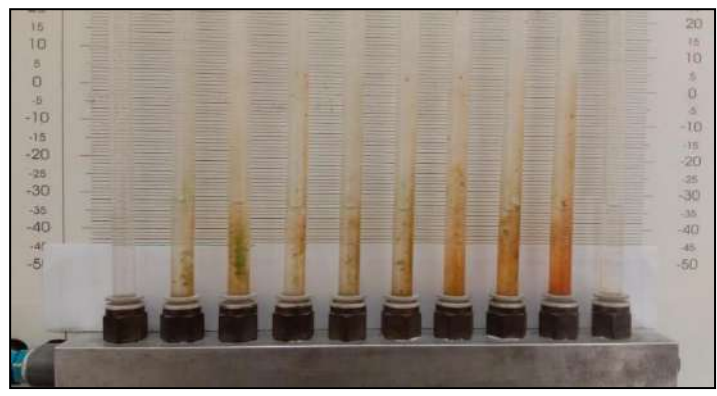


Figure 4.36: U-tube barometer

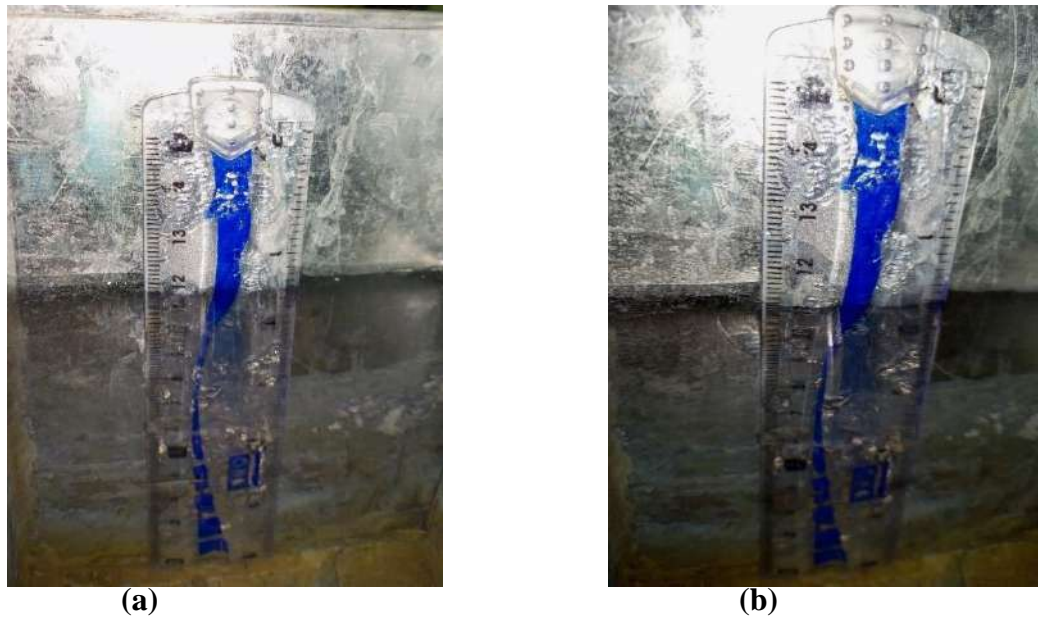


Figure 4.37: Photograph of water level measurement (a) upper level, (b) lower level

4.6 Performance Parameters

The temperature drop of the process air in the dry channel is the key parameter of design variant prototypes. So, temperature drop in the dry channel is measured by taking the difference of ambient temperature (T_{in}) and supply temperature (T_s).

$$\Delta T = (T_{in} - T_s) \quad (4.1)$$

Although cooling capacity (CC) shows the system's ability to handle the cooling load. CC is calculated by the temperature difference product and mass flow rate of air (\dot{m}).

$$\text{Wet } CC = \dot{m} C_p (T_{in} - T_s) \quad (4.2) \quad \text{bulb}$$

effectiveness (ϵ_{wb}) indicates up to what extent cooling effect is produced relative to wet bulb temperature of incoming process air. Similarly, dew point effectiveness (ϵ_{dp}) shows that to which extent cooling is achieved relative to the dew point of the incoming air. These effectiveness's are calculated using relations 4.3 and 4.4 respectively.

$$\epsilon_{wb} = \frac{\Delta T}{\Delta T_{wb}} = \frac{T_{in} - T_s}{T_{in} - T_{wb}} \quad (4.3)$$

$$\epsilon_{dp} = \frac{\Delta T}{\Delta T_{dp}} = \frac{T_{in} - T_s}{T_{in} - T_{dp}} \quad (4.4)$$

Coefficient of performance is a performance rating, which indicates how efficient a cooling system is at transferring heat versus total power consumed. So, it is calculated by dividing the cooling capacity (CC) with the total power consumption (\dot{W}_p) of the system [51].

$$COP = \frac{CC}{\dot{W}_p} \quad (4.5)$$

The energy efficiency ratio (EER) is the efficiency rating of the system in Btu/h per watt of total power consumption. So, it is calculated through multiplying the COP by a factor of 3.413 as given in Equation 4.6 [52]. When the energy efficiency ratio rating is higher, the air cooler is more efficient. A DP-IEC 12 EER rating is considered a better energy efficiency rating [53].

$$EER = 3.413 * COP \quad (4.6)$$

4.7 The CFM assessment

The CFM stands for cubic feet per minute. It is the air flow measurement into the sample analysis. So, the CFM determines how much cubic feet air can be moved in each minute. The CFM of the system is calculated by multiplying the free flow area of the system with average air velocity. The operating parameters are given in Table 4.7.

Table 4.7: Operating parameters of the design variant prototypes

Parameter	Value				
	DVP-01	DVP-02	DVP-03	DVP-04	DVP-06
Length of HMX (mm)	1000	1000	300	300	410
Width of HMX (mm)	17.4	12.4	420	420	300
Height of HMX (mm)	500	445	152	152	204
Height of sub-channel (mm)	04	04	04	04	04
Width of sub-channel (mm)	25.4	25.4	21.4	21.4	21.4
Number of sub-channels	13	11	216	432	184
Air velocity (m/s)	7.94	6.4	6.1	3.7	6.3

The measuring process of the CFM of the design variant prototype 01 is detailed below.

Total frontal area of the HMX,

$$A_{hmx} = H \times W = 500 \text{ mm} \times 17.4 \text{ mm} = 8700 \text{ mm}^2 = 0.094 \text{ ft}^2$$

Free flow area of sub-channel

$$A_{free} = a \times b = 25.4 \text{ mm} \times 4 \text{ mm} = 101.6 \text{ mm}^2 = 0.0011 \text{ ft}^2$$

Free flow area of the HMX

$$A_{total} = n \times (a \times b) = 13 \times (0.0011 \text{ ft}^2) = 0.0143 \text{ ft}^2$$

Average velocity of the DVP

$$V_{avg} = \frac{7.7 + 6.9 + 9.8 + 8.8 + 6.5}{5} = 7.94 \frac{m}{s} = 1563 \text{ ft/m}$$

CFM of the design variant prototype 01

$$CFM = A_{total} \times V_{avg} = 0.0143 \text{ ft}^2 \times 1563 \frac{ft}{m}$$

$$CFM = 22.35 \text{ cu ft/m}$$

Similarly, the CFM of several design variant prototypes are given in Table 4.8.

Table 4.8: The CFM of different design variant prototypes

CFM of the system (Cu ft/m)	Design variant prototype				
	DVP 01	DVP 02	DVP 03	DVP 04	DVP 06
CFM	22.35	15.16	239	290	210

4.8 The assessment of pressure losses

The measurement of the pressure drop in the heat and mass exchanger is necessary mainly for two reasons: (1) Driving power is required to pump the fluid into heat and mass exchanger. The pressure drop of the heat and mass exchanger is directly proportional to the driven power of fluid. (2) The heat transfer rate of fluid is significantly affected by the saturation temperature change if there is a large pressure drop related with the fluid flow. For pressure drop analysis, there should be assumed that fluid is treated as an ideal gas, flow is steady, isothermal, not irrotational, independent on time, fluid density depends on local temperature, fluid pressure is independent of direction, constant friction factor, no energy sinks along a streamline, and body forces are caused by gravity. So, pressure drop in the heat and mass exchanger of prototype 04 is calculated from the Equation 4.7 [54]. The operating parameters and conditions are given in Table 4.9.

$$\frac{\Delta p}{p_i} = \Delta p_{(1-a)} + \Delta p_{core(a-b)} - \Delta p_{(b-2)} \quad (4.7)$$

Which can be written as

$$\frac{\Delta p}{p_i} = \frac{G^2}{2\rho_1 P_1} \left[(k_c + 1 - \sigma^2) + 2 \left(\frac{\rho_1}{\rho_2} - 1 \right) + f \frac{L \rho_1}{r_h \rho_m} - (1 - k_e - \sigma^2) \frac{\rho_1}{\rho_2} \right] \quad (4.8)$$

Table 4.9: Operating parameters and conditions

Parameters	Symbol	Units	Value
Length of HMX	L	Mm	300
Width of HMX	W	Mm	420
Height of HMX	H	Mm	300
Height of channel	X	Mm	04
Spacing of channel	y	Mm	21.4
Number of sub-channels	n	-	432
Air inlet temperature	T ₁	K	322
Air outlet temperature	T ₂	K	297
Inlet air velocity	V	m/s	6.1

Consider that air is an ideal gas, the inlet, outlet, and mean air densities are given by

$$\rho_{1=H} = \frac{p_1}{R T_1} = \frac{101325}{287 \times 322} = 1.096 \frac{kg}{m^3 K}$$

Similarly, the air density is given by

$$\rho_2 = \frac{p_1}{R T_2} = \frac{101325}{287 \times 297} = 1.188 \frac{kg}{m^3K}$$

The mean air density is given by

$$\frac{1}{\rho_m} = \frac{1}{2} \left(\frac{1}{\rho_1} + \frac{1}{\rho_2} \right) = \frac{1}{2} \left(\frac{1}{1.096} + \frac{1}{1.188} \right) = 0.877 \frac{m^3K}{kg} = \frac{1}{1.14} \frac{m^3K}{kg}$$

The hydraulic diameter is given by [24][55].

$$D_h = \frac{4 \times \text{cross sectional area}}{\text{perimeter}} = \frac{4 \times 21.4 \times 4}{2(21.4 + 4)} = 6.740 \text{ mm} = 0.00674 \text{ m}$$

$$\text{Hydraulics radius} = r_h = 1.685 \text{ mm} = 0.001685 \text{ m}$$

Since the volumetric flow (0.157 m³/s) of the air is given as airflow at inlet, the mass velocity is given by

$$G = \frac{V \times \rho_i}{\text{Free flow area}} = 9.3 \text{ kg/m}^2\text{s}$$

Now, entrance and exit pressure loss coefficients are calculated from a Figure as given in Appendix B. These coefficient values are dependent on σ . So, calculating the value of σ which So, σ is the ratio of minimum free flow area to frontal area of HMX.

$$\text{Frontal Area} = W \times H = 420 \times 300 = 124640 \text{ mm}^2 = 0.125 \text{ m}^2$$

$$\text{Free flow Area} = n \times b \times a = 432 \times 21.4 \times 4 = 36979.2 \text{ mm}^2 = 0.037 \text{ m}^2$$

$$\sigma = \frac{\text{Free flow Area}}{\text{Frontal Area}} = 0.296$$

Hence,

$$\text{Coefficient of contraction} = k_c = 0.44$$

$$\text{Coefficient of expansion} = k_e = 0.58$$

The fanning friction factor is calculated by

$$f = \frac{72}{R_e}$$

The Reynold number is calculated by given equation [56].

$$\text{Reynold number} = R_e = \frac{\rho V D_h}{\mu} = 2317.71$$

Where μ is the kinematic viscosity of air ($\mu = 19.54 \times 10^{-5}$ Pa.s). Putting the value of Reynold number in formula to calculate the fanning friction factor.

$$f = \frac{72}{R_e} = 0.0314$$

All the parameters are calculated. Put all values in Equation 7.8 and get

$$\Delta P = 2.42 \times 10^{-3} \times P_1$$

Change in pressure = 2.42×10^{-3} x initial pressure

$$\Delta P = 245 \text{ Pa}$$

Hence, the pressure drop of heat and mass exchanger on dry channel side is 0.24 percent of initial pressure.

4.9 Uncertainty Analysis

In this study, the uncertainty analysis of the DVP 03 is also done. The inlet temperature is varied to observe their effect on the product air temperature of the ambient air. The ambient air temperature varies from 33-49 °C. The relative humidity also varied with two fixed values i.e., 13 % and 20 %. Whereas the remaining parameters are fixed throughout the experiment. The product air temperature is measured after achieving the steady state conditions. The minimum and maximum deviations in the data set is measured using the uncertainties of each instrument. The uncertainties of performance indicators are presented in Table 4.10

Table 4.10: Measuring uncertainties of the instruments

Instruments	Measured Variable	Instrument's Uncertainty	Measured Values		% Uncertainty	
			Min	Max	Max	Min
Digital thermometer	T	0.1 °C	12.95	26.04	0.769	0.385
Digital thermometer	T _{dp}	0.1 °C	25.90	35.67	0.386	0.280
Thermometer	T _{wb}	0.1 °C	15.39	24.31	0.649	0.411
Anemometer	V	0.01 m/s	6.10	6.10	0.167	0.167

The minimum and maximum uncertainties in the experimental results are given in Table 4.11. It can be noted that the overall uncertainties range of all indicators is within the satisfactory limit.

Table 4.11: Uncertainties of performance indicators

Sr. No	Performance Parameters	Minimum Uncertainty %	Maximum Uncertainty %
1	Dew Point Effectiveness $\varepsilon_{dp} = \frac{T_{in} - T_s}{T_{in} - T_{dp}}$	$\frac{\varphi \varepsilon_{dp}}{\varepsilon_{dp}} = \sqrt{\left(\frac{\varphi_{T_{in}-T_s}}{T_{in} - T_s}\right)^2 + \left(\frac{\varphi_{T_{in}-T_{dp}}}{T_{in} - T_{dp}}\right)^2}$ $= \sqrt{(0.385)^2 + (0.280)^2}$ = 0.48 %	$\frac{\varphi \varepsilon_{dp}}{\varepsilon_{dp}} = \sqrt{\left(\frac{\varphi_{T_{in}-T_s}}{T_{in} - T_s}\right)^2 + \left(\frac{\varphi_{T_{in}-T_{dp}}}{T_s - T_{dp}}\right)^2}$ $= \sqrt{(0.769)^2 + (0.386)^2}$ = 0.86 %
2	Wet Bulb Effectiveness $\varepsilon_{wb} = \frac{T_{in} - T_s}{T_{in} - T_{wb}}$	$\frac{\varphi \varepsilon_{wb}}{\varepsilon_{wb}} = \sqrt{\left(\frac{\varphi_{T_{in}-T_s}}{T_{in} - T_s}\right)^2 + \left(\frac{\varphi_{T_{in}-T_{wb}}}{T_{in} - T_{wb}}\right)^2}$ $= \sqrt{(0.385)^2 + (0.649)^2}$ = 0.56 %	$\frac{\varphi \varepsilon_{wb}}{\varepsilon_{wb}} = \sqrt{\left(\frac{\varphi_{T_{in}-T_s}}{T_{in} - T_s}\right)^2 + \left(\frac{\varphi_{T_{in}-T_{wb}}}{T_{in} - T_{wb}}\right)^2}$ $= \sqrt{(0.769)^2 + (0.411)^2}$ = 1 %
3	Mass Flow Rate $\dot{m} = \rho AV$	$\frac{\varphi \dot{m}}{\dot{m}} = \sqrt{\left(\frac{\varphi_V}{V}\right)^2 + \left(\frac{\varphi_A}{A}\right)^2}$ $= \sqrt{(0.167)^2 + (0.009)^2}$ = 0.167 %	$\frac{\varphi \dot{m}}{\dot{m}} = \sqrt{\left(\frac{\varphi_V}{V}\right)^2 + \left(\frac{\varphi_A}{A}\right)^2}$ $= \sqrt{(0.167)^2 + (0.009)^2}$ = 0.167 %
4	Cooling Capacity $CC = \dot{m} C_p \Delta T$	$\frac{\varphi CC}{CC} = \sqrt{\left(\frac{\varphi_{\dot{m}}}{\dot{m}}\right)^2 + \left(\frac{\varphi_T}{T}\right)^2}$ $= \sqrt{(0.167)^2 + (0.385)^2}$ = 0.42 %	$\frac{\varphi CC}{CC} = \sqrt{\left(\frac{\varphi_{\dot{m}}}{\dot{m}}\right)^2 + \left(\frac{\varphi_T}{T}\right)^2}$ $= \sqrt{(0.167)^2 + (0.769)^2}$ = 0.785 %

5	Co-efficient of Performance $COP = \frac{CC}{We}$	$\frac{\varphi_{COP}}{COP} = \sqrt{\left(\frac{\varphi_{CC}}{CC}\right)^2 + \left(\frac{\varphi_{We}}{We}\right)^2}$ $= \sqrt{(0.42)^2 + (1.81)^2}$ $= \mathbf{1.93\%}$	$\frac{\varphi_{COP}}{COP} = \sqrt{\left(\frac{\varphi_{CC}}{CC}\right)^2 + \left(\frac{\varphi_{We}}{We}\right)^2}$ $= \sqrt{(0.785)^2 + (1.81)^2}$ $= \mathbf{2.04\%}$
6	$EER = 3.413 * COP$	$\frac{\varphi_{EER}}{EER} = \frac{\varphi_{COP}}{COP}$ $= \mathbf{1.93\%}$	$\frac{\varphi_{EER}}{EER} = \frac{\varphi_{COP}}{COP}$ $= \mathbf{2.04\%}$

4.10 Velocity distributions through channels

4.10.1 Velocity distribution through channels of DVP 03

In the current study, the system is designed and fabricated in such that uniform air distribution is achieved by appropriate number and positions of water and air holes. The velocity profile of this system shows how airflow is processed in dry and wet channels as shown in Figure 4.38. It is measured with anemometers at different points in the dry and wet channels. Process air is supplied to DVP 03 which is divided into two passages as supply air and working air. About 30% of the process air moves to wet channels, becomes saturated with water and is returned to the atmosphere. Water holes can be seen on the extreme left side of the system, supplying water to wet channels. The remaining process air entering the system is cooled without adding moisture. It is noted that uniform velocity is distributed in dry and wet channels. This is possible due to the less pressure losses and smooth air flow patterns in dry and wet channels. The variation of supplied velocity through channels are shown in Figure 4.39.

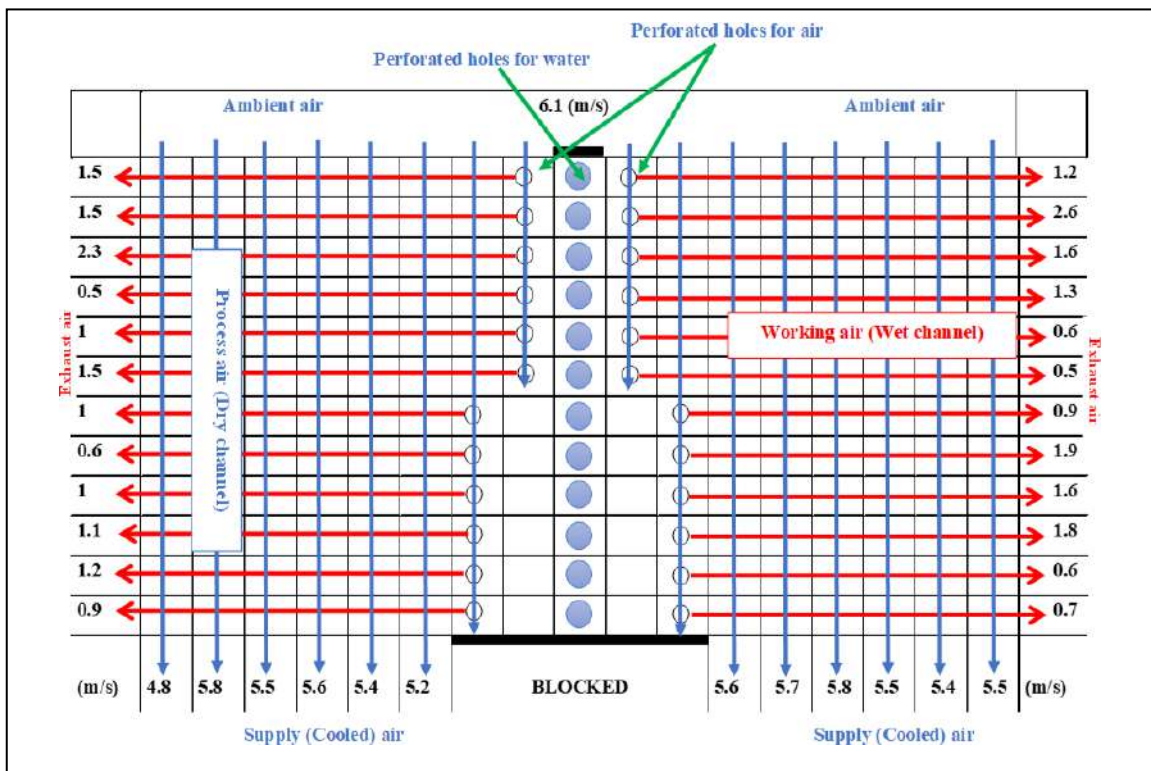


Figure 4.38: Velocity distribution of the process air through channels of DVP 03

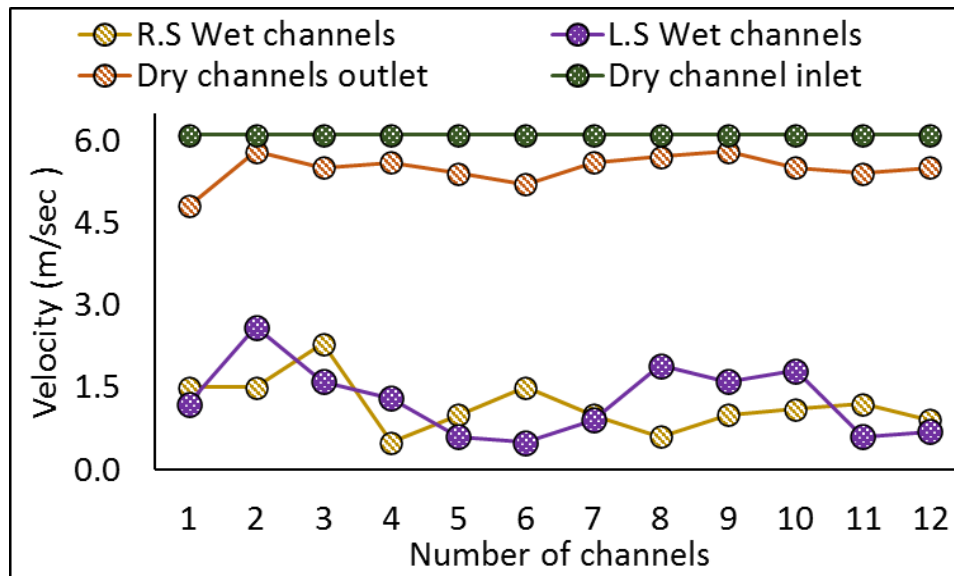


Figure 4.39: The variation of process air velocity through channels of DVP 03

4.10.2. Velocity distribution through channels of the DVP 06

The velocity profile of DVP 06 also shows the process and working air distribution in dry and wet channels as shown in Figure 4.40. In DVP 06, the number of dry channels decreases while the number of wet channels increases. Moreover, one side of the DVP is blocked completely. So, the working air is exhausted from the right side of the system.

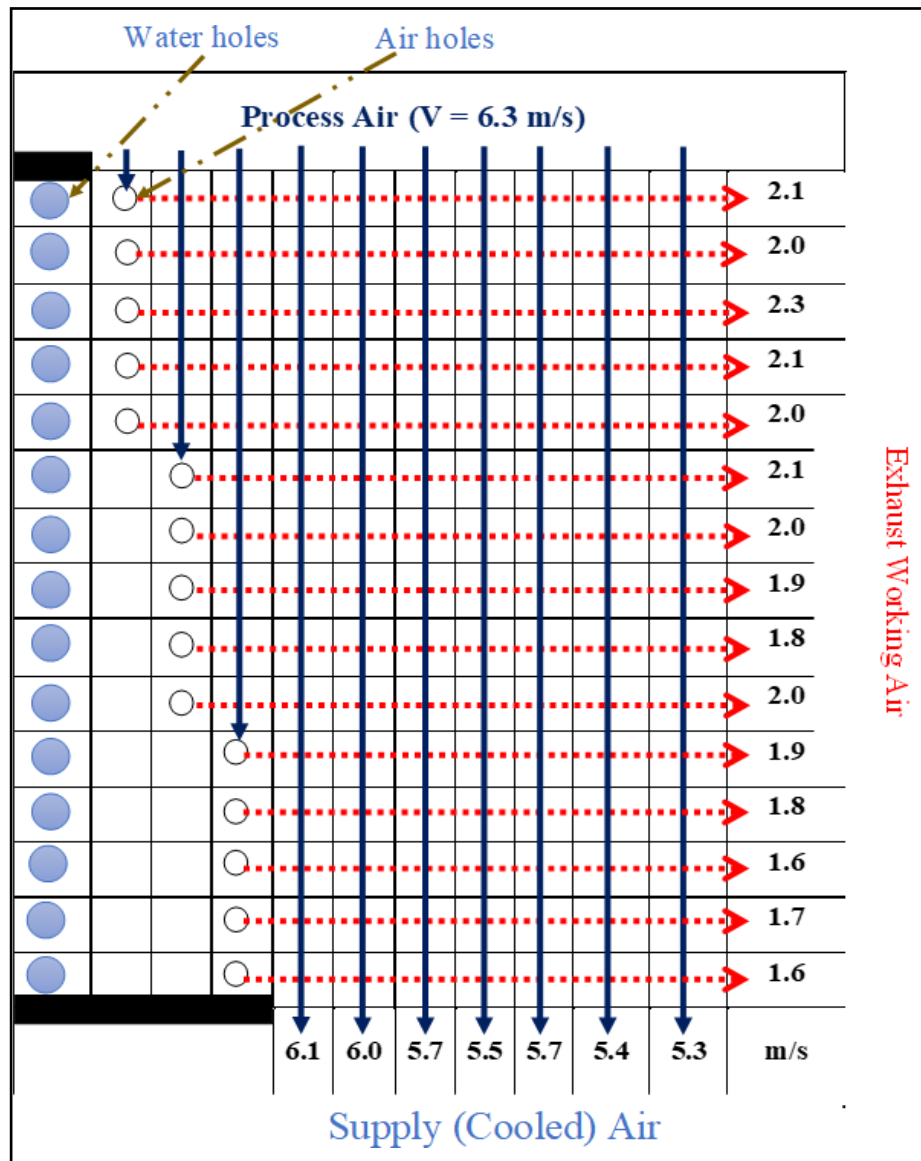


Figure 4.40: Velocity distribution of process air through channels of DVP 06

4.11 Fabrication of Dehumidification Bed

4.11.1. Laser Cutting of Acrylic Sheets to make Ducts

The acrylic sheets of thickness 4 mm are laser cut using a laser cutting machine according to the designed dimensions and then joined using a binding material to make two ducts for making a dehumidification bed as shown in Figure 4.41. Supports were made on the walls of one duct to place the thin Aluminum sheets with Silica gel coating.



Figure 4.41: Ducts with Coated Aluminium Sheets

4.11.2. Silica gel coating on thin Aluminium Sheets using Dip Coating

Method

The coating process begins by preparing the silica gel solution with Polyvinyl Alcohol. The required amount of silica gel powder is measured and slowly added to a container containing a PVA solvent, while continuously stirring. The stirring continues until the silica gel powder is completely dissolved, resulting in a uniform solution. After allowing the solution to rest for a few minutes, ensuring complete dissolution, the next step involves cleaning the aluminum sheet. It is dried using compressed air or a clean cloth.

Once the sheet is cleaned, the dip coating process begins. The prepared silica gel solution is poured into a dip coating container. The cleaned aluminum sheet is immersed in the solution, ensuring that the entire surface is submerged. The sheet is held vertically to allow any excess solution to drip off, and then it is gradually lifted out of the solution at a controlled rate to achieve the desired coating thickness.

The coated sheet is then left to air-dry in a controlled environment, such as a clean and dust-free room, to prevent contamination. After the coating has dried, the next step involves curing and drying

the coated aluminum sheet. The sheet is placed in an oven at a specified temperature. The

recommended curing and drying time are followed, considering factors such as coating thickness and desired properties. Proper ventilation is ensured during the curing process to eliminate any potential fumes or vapors.

Quality assurance and testing are important aspects of the process. The coated aluminum sheet as shown in Figure 4.42 is inspected for any visible defects or inconsistencies in the coating. Once the coating process is complete, the coated aluminum sheets are carefully handled, packaged, and stored to prevent damage or contamination. Detailed documentation of the coating process is maintained, including information such as the silica gel solution concentration, coating thickness of 1 mm, curing parameters, and test results. Compliance with relevant regulatory and industry standards is ensured throughout the process.



Figure 4.42: Silica Gel Coating on Aluminium Sheets

4.12. Instrumentation and Measurements

- Used a two-channel digital thermometer shown in Figure 4.43 to measure ambient temperature and supply air temperature.



Figure 4.43: Two-channel digital thermometer

- Used a single channel digital thermometer shown in Figure 4.44 to measure water temperature.



Figure 4.44: Single Channel Digital Thermometer

- Used humidity meter shown in Figure 4.45 to record relative humidity.



Figure 4.45: Relative Humidity Meter

- Used relative humidity and ambient temperature calculated the dry bulb temperature and wet bulb temperature.

4.12.1. Procedure

- Set the position of the HMX according to the objective of the experiment i.e. indoor or outdoor testing.
- Put temperature sensor prob in sump water.
- Put temperature and humidity sensor at before silica beds and take periodic readings.
- Put temperature and humidity sensor at outlet i.e. product air and take periodic readings
- Calculate the weight of the silica beds before and after the experiment to estimate the efficiency of the beds.

4.13. Experimental Setup of Dehumidification Bed

Real time experimentation as shown in Figure 4.46. is done on the dehumidification bed under different actual conditions of ambient air's temperature and humidity in solar lab of energy engineering department at UET Taxila to study and analyze the performance of the setup. Examined the amount of moisture absorbed by the silica gel material into the ambient air as well as the reduction of temperature from the air at the outlet of dehumidification bed.



Figure 4.46: Experimental Setup of Dehumidification Bed

Different types of temperature and humidity sensors were used during the experimentation of the dehumidification bed to ensure the accuracy of the results.

4.14. Experimental Readings of Dehumidification Bed

Table 4.12 includes the values of obtained results at the outlet of dehumidification bed.

Table 4.12: Experimental Readings of Dehumidification Bed

Time	Humidity	Temperature	Dehumidification Capacity	Dehumidified Temperature	Mass Absorbed	Regeneration Temperature
3.333333	6.1	0.03	8.29567	0.29	16.19503	75
6.666667	10.21	0.89	7.33136	4.47	57.24289	72.1
10	16.69379	2.3	5.68602	5.26	101.4466	69.8
13.33333	18.19899	3.5	4.75337	4.72	133.0209	67.2
16.66667	19.05871	4.5	4.00548	4.28	164.5953	64.5
20	19.39849	5.6	3.66674	4.12	188.3699	62.9
23.33333	19.41884	6.55	3.21801	3.71	210.4728	62.2
26.66667	19.79849	6.3	2.91885	3.54	232.5736	62.5
30	19.29771	6.1	2.76928	3.41	249.8468	62.7
33.33333	19.49879	5.7	2.58011	3.15	267.3058	62.9
36.66667	19.33459	5.2	2.32055	2.94	283.0929	63.2
40	19.89376	4.99	2.24576	2.85	300.3662	63.8
43.33333	19.19879	4.2	2.13138	2.68	312.9975	64.3
46.66667	19.99671	4.01	2.0214	2.49	327.2986	64.8
50	19.89821	3.89	2.05659	2.31	339.928	65.4
53.33333	19.71889	3.76	1.87182	2.25	354.0433	65.9
56.66667	19.49821	3.18	1.72224	2.19	365.1887	66.3
60	19.39179	2.91	1.72224	2.01	376.1462	66.7
63.33333	19.19847	2.81	1.57267	1.83	384.1317	67.1
66.66667	19.09199	2.69	1.72224	1.65	396.763	67.7
70	19.29849	2.52	1.57267	1.48	406.2345	68.2
73.33333	19.30879	2.41	1.30871	1.31	417.1941	68.8
76.66667	19.39859	2.2	1.3835	1.28	428.3374	69.4
80	19.69521	2.15	1.3835	1.17	437.8088	69.9
83.33333	19.79861	2	1.30871	1.02	444.1245	70.5
86.66667	19.79531	1.92	1.30871	1.07	452.112	70.9
90	19.99999	1.89	1.23392	0.96	459.9117	71.4
93.33333	19.89869	1.79	1.15913	0.99	467.8992	71.9
96.66667	19.82581	1.71	1.12394	0.86	475.6989	72.3
100	19.69879	1.58	1.08434	0.89	483.6863	72.6
	19.53712	1.49	1.00955		485.59	

4.15. Experimental Setup of HMX with Dehumidification Bed

During the final testing of our fabricated experimental setups, HMX is mounted with the dehumidification bed as shown in Figure 4.47 to study the effect of dehumidification bed using with HMX in context of removing the moisture content from the ambient air. Study and analyze the cooling capacity, humidity, and temperature of product air at the out of HMX. The HMX now did not add the already present humidity in the ambient air because the silica gel absorbed the moisture content from the ambient air. Achieved moisture free, cooled air as a final product at the outlet of HMX.



Figure 4.47: Experimental Setup of HMX with Dehumidification Bed

Chapter 5

5.1 Results and Discussion

This chapter shows the experimental results of the proposed design variant prototypes of the dew point indirect evaporative cooler. The performance of the proposed design variant prototypes are discussed, then the real time performance of selected prototypes are presented.

5.2 The effect of the ambient air temperature on performing indicators

An extensive experimentation of DVP 01, 02, 03, 05, and 06 are performed to analyze the effect of ambient air temperature on performing parameters. Initially, the experimentation of DVP 01, 02, and 05 are performed under actual climate conditions of Gujranwala, Pakistan. Moreover, the experimentation of DVP 03 is performed under controlled conditions which is created by using the ACLU at Mirpur, Azad Kashmir, Pakistan. While the experimental results of the DVP 04 is not added because the water leakages start from the frontal side of HMX with the passage of time. Finally, the testing of DVP 06 is performed under actual climate conditions of Taxila, Pakistan. All the systems are operated at different air flow rates as given in Table 5.1 and constant water temperature with different parametric conditions like ambient temperature and relative humidity. The overall performance of the systems are presented in terms of effectiveness, cooling capacity, COP, and EER.

Table 5.1: Volumetric flow rates of DVPs

Volumetric flow rate (m ³ /h)	Design variant prototype				
	DVP 01	DVP 02	DVP 03	DVP 05	DVP 06
V	920	920	550	440	440

5.2.1 The effect of ambient temperature on temperature difference

Temperature difference is one of the key parameters. The increment of the temperature difference (ΔT) depends on the ambient air temperature and the relative humidity (RH) while keeping the fix values of water temperature and air velocity. It is observed from Figure 5.1 that the temperature reduction from process side is lowered with increasing the relative humidity (RH) of the inlet. While the temperature at the process side is further decreased with the increase of dry bulb temperature at the inlet. Thus, hot and dry inlet conditions favor the performance of the HMX. This is due to the fact that dry inlet air can hold more moisture before reaching its saturation point at higher process air temperature and lower RH. So, the temperature difference of some design variant prototypes as shown in Figure 5.1.

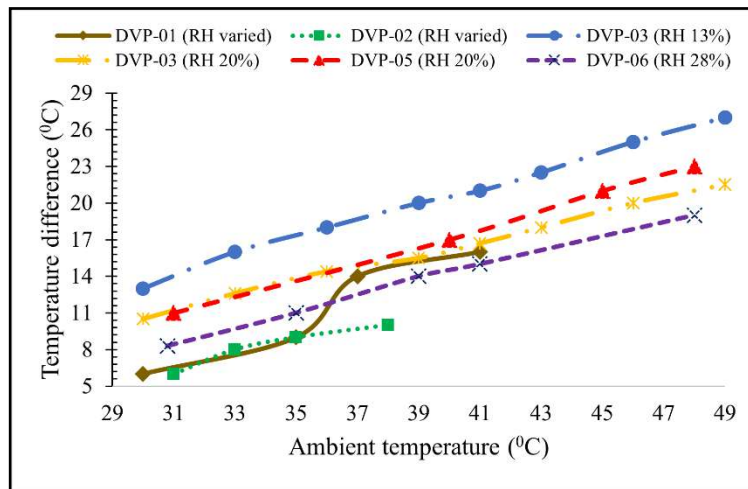


Figure 5.1: Temperature difference in dry channels of various DVPs

5.2.2 The effect of ambient temperature on dew point effectiveness

Dew point effectiveness of the system depends on the dew point temperature of the incoming air that defines how much the hot air would have to be cooled in order to achieve saturation. It is observed that the lower the dew point temperature of ambient air, the higher the dew point effectiveness. The reason is that ambient air is more prone to evaporation. Hence, the dew point effectiveness of the various systems as shown in Figure 5.2. As concluded earlier, dry and hotter inlet air results in higher dew point effectiveness.

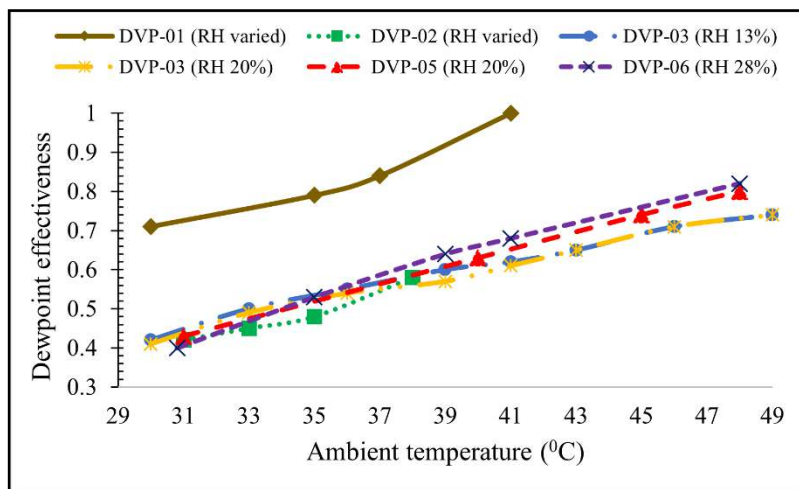


Figure 5.2: Dew point effectiveness of various DVPs

5.2.3 The effect of ambient temperature on wet bulb effectiveness

Wet bulb effectiveness of the system depends on the wet bulb temperature of the incoming air, which defines the adiabatic saturation temperature. It is noted that the wet bulb effectiveness of the system is increased with increasing the ambient air temperature or decreasing the wet bulb temperature. Therefore, the wet bulb effectiveness of the systems varied from 0.53-1.2 as shown in Figure 5.3. Performance of these HMX are

reasonably well, that's why considering that these are better than direct evaporative cooler when operating at high inlet humidity.

5.2.4 The effect of ambient temperature on cooling capacity

It is observed that the CC of the system is related to the effectiveness of the system. While the effectiveness depends on the ambient temperature and the relative humidity. It is due to the fact that with increasing the ambient air temperature and decreasing the relative humidity, the cooling capacity of the system increased. It is also observed that experimental cooling capacity of the system depends on the velocity and the free flow area of the HMX. The air velocity and area of the system are directly proportional to the cooling capacity as shown in Figure 5.4.

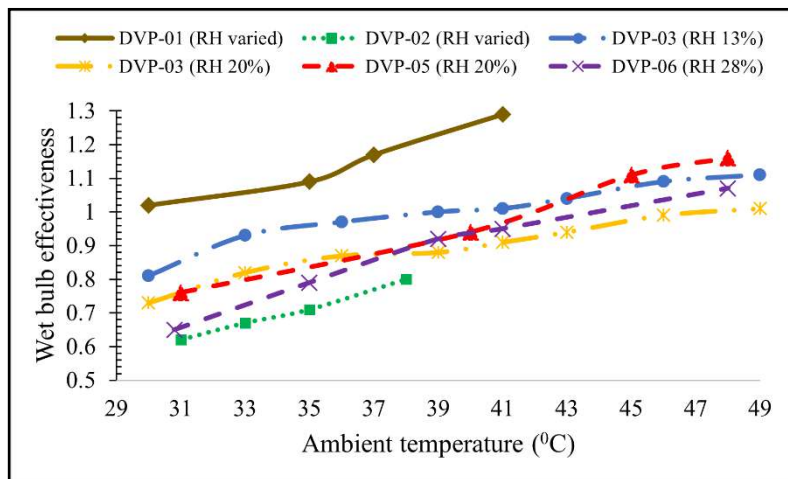


Figure 5.3: Wet bulb effectiveness of the various DVPs

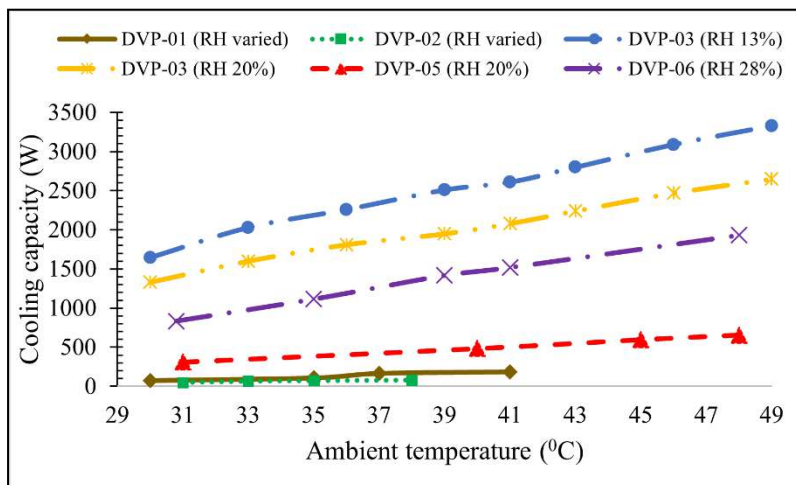


Figure 5.4: Variation of CC with ambient air temperature (T_{in})

5.2.5 The effect of ambient temperature on COP

The coefficient of performance of the system increases as the cooling capacity increases. It is noted that the COP of the system is inversely proportional to the overall power consumption of the system. So, the maximum

value of the COP is calculated at optimum inlet parameters of the DVP 06 i.e., $T_{in}= 48\text{ }^{\circ}\text{C}$, $\text{RH}=28\%$, $V=5.7\text{ m/s}$, and $T_w=20\text{ }^{\circ}\text{C}$ as shown in Figure 5.5 which is strongly influenced by relative humidity and power consumption. The higher air inlet relative humidity results in less evaporation and subsequently decrease cooling capacity along COP.

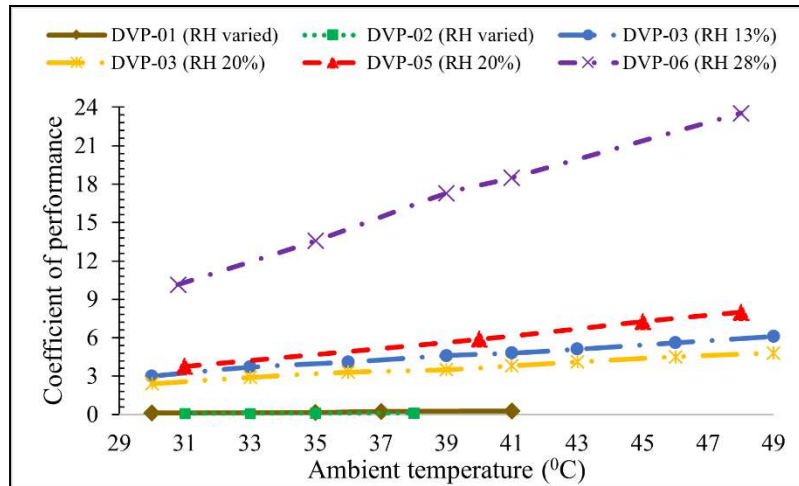


Figure 5.5: Coefficient of performance (COP) variation

5.2.6 The effect of ambient temperature on energy efficiency ratio (EER)

EER is one of the key performance indicators which defines the efficiency of the system. It is observed that the maximum value of EER at $T_{in}= 48\text{ }^{\circ}\text{C}$, $\text{RH}=28\%$, $V_{in}=5.7\text{ m/s}$, and $T_w=20\text{ }^{\circ}\text{C}$ as shown in Figure 5.6. This is due to the fact that the higher value of COP is resulting in higher the EER of the system. Moreover, it was found that a system with an EER rating of 12 or more is considered a better energy efficiency rating [53]. Hence, this system is considered more efficient because the maximum calculated value of EER is 50+.

5.3 Effect of the water temperature on performing indicators

The temperature difference between the ambient air and product air increases by decreasing the water temperature. The reason is that the higher the water temperature, increases its ability to effectually remove the heat from incoming ambient air. So, lower the water temperature resulting in the higher temperature difference as shown in Figure 5.7.

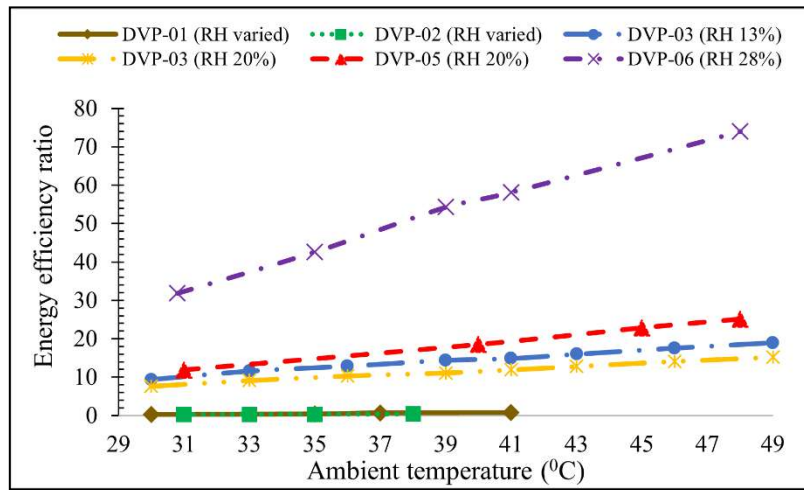


Figure 5.6: Energy efficiency ratio (EER) of the systems

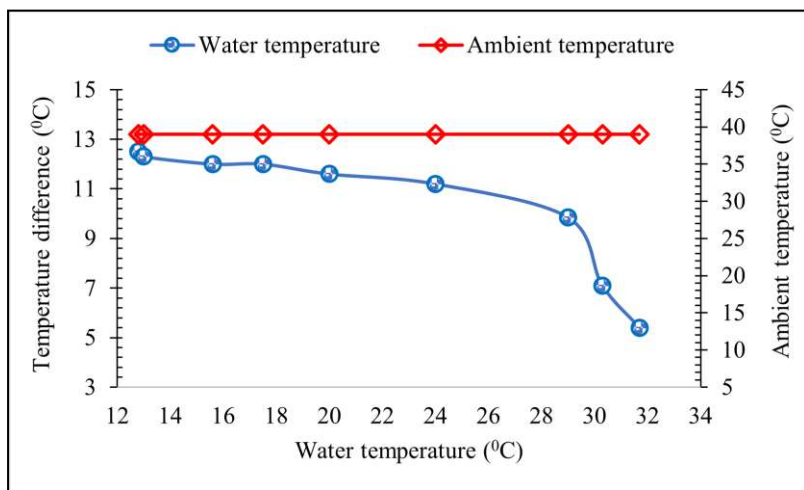


Figure 5.7: Effect of water temperature on temperature difference

Moreover, all remaining indicators are dependent on the temperature differences. So, if the temperature difference is higher than other parameters are also higher. The reason is that temperature difference is directly related to the other parameters like dewpoint and wet bulb effectiveness, CC, COP and EER.

5.4 Effect of the water flow on performing indicators

Water is the key parameters for the evaporation. The evaporation occurs when the water is sprayed onto the wet channels of the HMX. As the water evaporates, the heat of vaporization exerts a cooling effect on the outer walls of the wet channels, which can significantly cool the product air. So, an extensive experimentation of DVP 06 is performed to analysis the effect water flow in wet channels. Primarily, the experimentation of DVP 06 is performed under actual climate conditions of Gujranwala, Pakistan. The system is operated at constant air flow and water temperature with different parametric conditions like temperature and relative humidity. The water is flowing in wet channels for particular time and calculating the performing indicators. After that, the supply of water is cut off and half an hour later calculating the performing indicators again.

5.4.1 The effect of water flow on supply air temperature

Supply air temperature decreases by increasing the ambient temperature and decreasing the relative humidity (RH) at fixed values of water flowing and air velocity. It is observed that the supply air temperature has minor increased after half an hour when the water supply is cut off. So, it is examined that the temperature of the supply air is minor changed within half an hour without the flow of water in wet channels as shown in Figure 5.8.

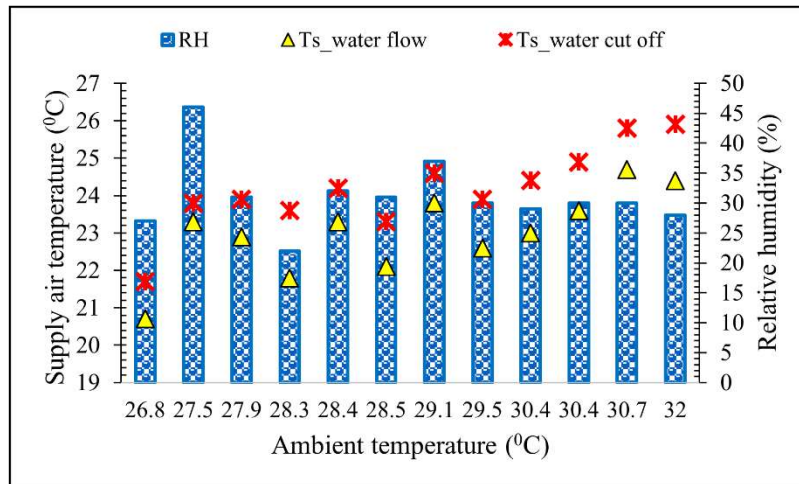


Figure 5.8: Supply air temperature with/without water flow in wet channels

5.4.2 The effect of water flow on working air temperature

The working air temperature decreases due to the evaporation in wet channels by contact with water directly at fixed values of water flowing and air velocity. It is observed that the working air temperature has also been minor increasing after half an hour when the water supply is cut off. So, it is examined that the working air temperature is minor changed within half an hour without the water flow in wet channels as shown in Figure 5.9.

5.4.3 The effect of water flow on the effectiveness of the system

The effectiveness of the system is evaluated at different ambient conditions with water flow in wet channels and compared with effectiveness after the water cut off in wet channels. It is observed that the dew point effectiveness of the system is decreased up to 0.08 without the water flowing in wet channels. Moreover, the wet bulb effectiveness decreased up to 0.14 without water flowing in wet channels as shown in Figure 5.10.

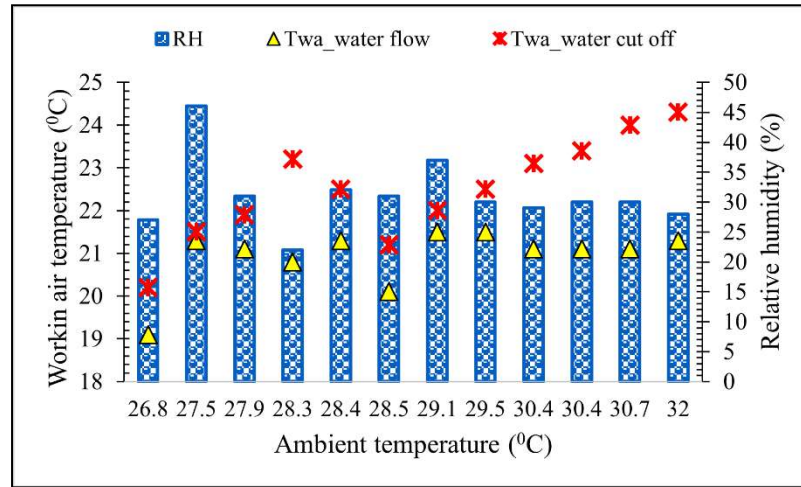


Figure 5.9: Working air temperature with/without water flow in wet channels

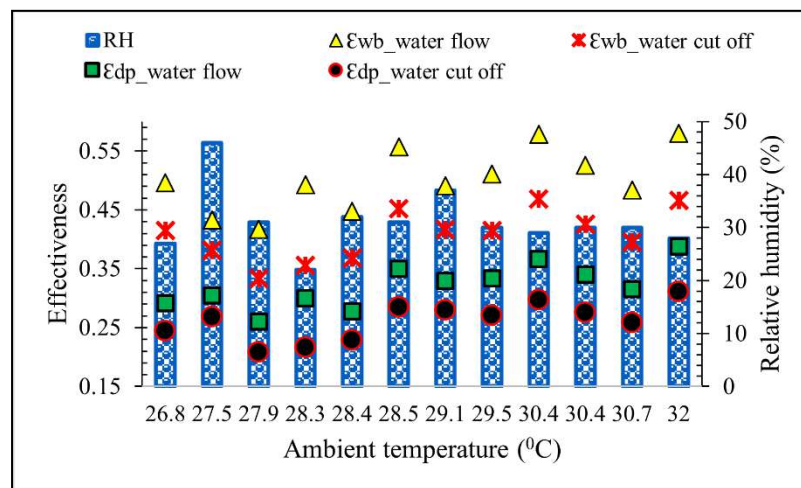


Figure 5.10: Effectiveness of the system with/without water flow in wet channels

5.4.4 The effect of water flow on cooling capacity

Cooling capacity (CC) is measured with water flow in wet channels and compared it the CC results when water is cut off. It is observed that maximum change in cooling capacity is 27 % after the water is cut off in wet channels as shown in Figure 5.11.

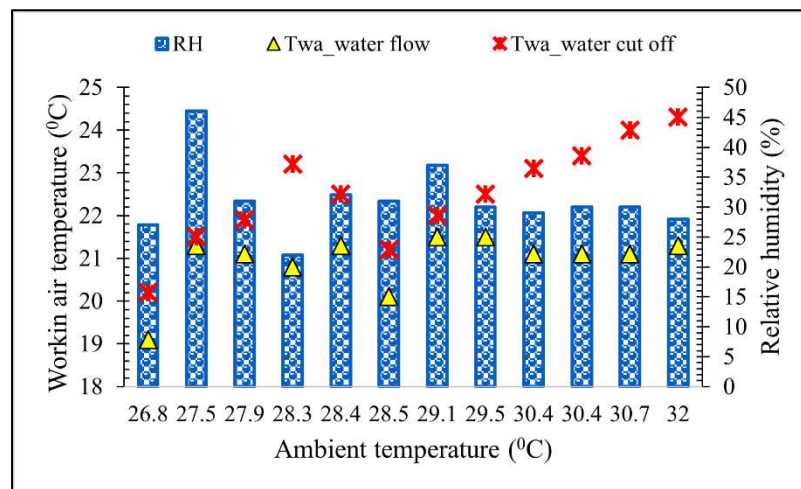


Figure 5.11: Variation in cooling capacity of the system

5.4.5 The effect of water flow on COP

Coefficient of performance is measured with water flow and compared it without water flow in wet channels. It is observed that maximum change in COP of the system is calculated at optimum inlet parameters i.e., $T_{in}=28.3^{\circ}\text{C}$, $\text{RH}=22\%$, $V_{in}=6.3\text{ m/s}$, and $T_w=20^{\circ}\text{C}$. The reason is that lower the RH of ambient air resulting the rapidly absorbed of water droplets in wet channels as shown in Figure 5.12.

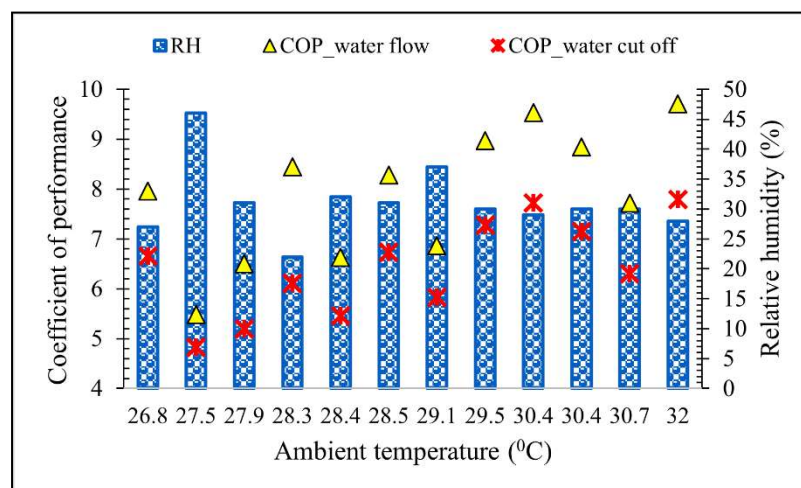


Figure 5.12: COP of the system with/without water flow

5.4.6 The effect of water flow on EER

EER of the system is also measured with water flow in wet channels and compared with without water flow in wet channels of the system. It is observed that the maximum difference of EER occurs at $T_{in}=28.3^{\circ}\text{C}$, $\text{RH}=22\%$, $V_{in}=6.3\text{ m/s}$, and $T_w=20^{\circ}\text{C}$ as shown in Figure 5.13. This is due to the fact that lower the RH of ambient air resulting in the swiftly absorbed of water droplets in wet channels.

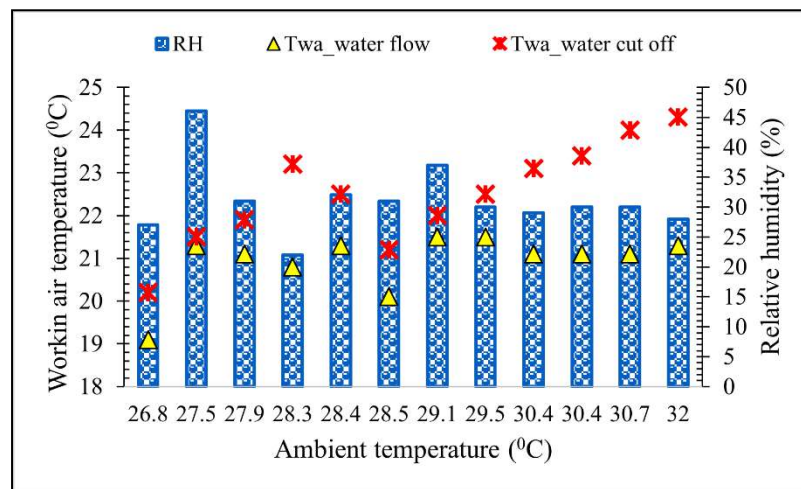


Figure 5.13: Energy efficiency ratio of the system

5.5 Water Recovery

5.5.1 Water consumption of the system

Water consumption is also a key parameter. The water consumption of the system is increased by increasing the ambient air temperature and decreasing the relative humidity (RH) at fixed values of water temperature and air velocity. This is due to the fact that the higher the ambient temperature and lower the humidity of the incoming air holds the more moisture before reaching its saturation point. Hence, the water consumption of the system as shown in Figure 5.14.

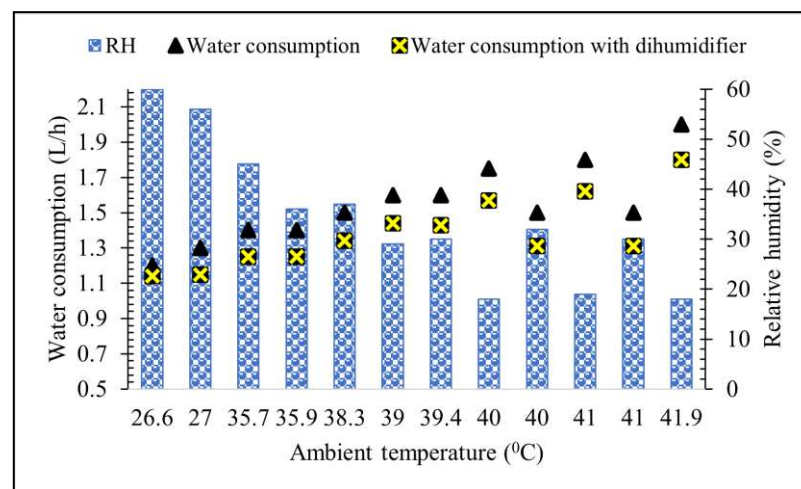


Figure 5.14: Water consumption of the system

5.5.2 Water footprint reduction

The water footprint of the system is reduced by recovery of the water from the exhaust air. The more the water recovers from exhaust air, the lower the water footprint of the system. The water footprint of the system decreases with increasing the relative humidity of the incoming air. The reason is that lower the moisture content required to reach the saturation point. The water recovery from exhaust air increases with increasing the ambient temperature and decreasing the relative humidity as shown in Figure 5.15.

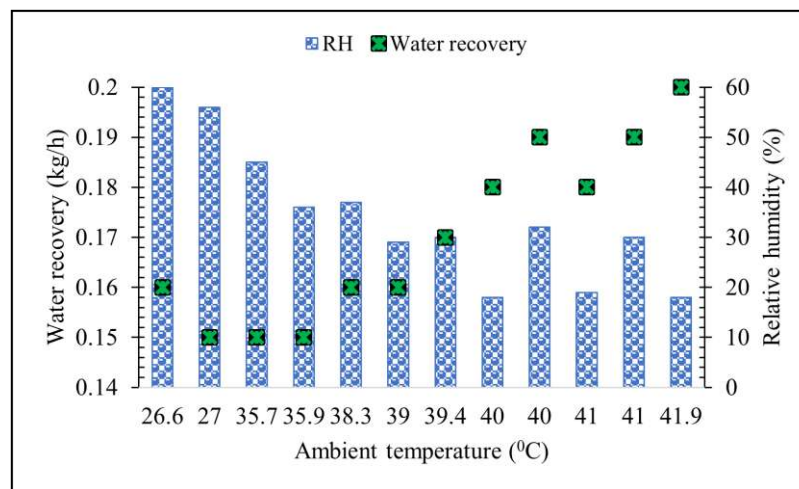


Figure 5.15: Amount of water recovery from exhaust air

5.6. Water Absorbed by Air Using Psychrometric Chart

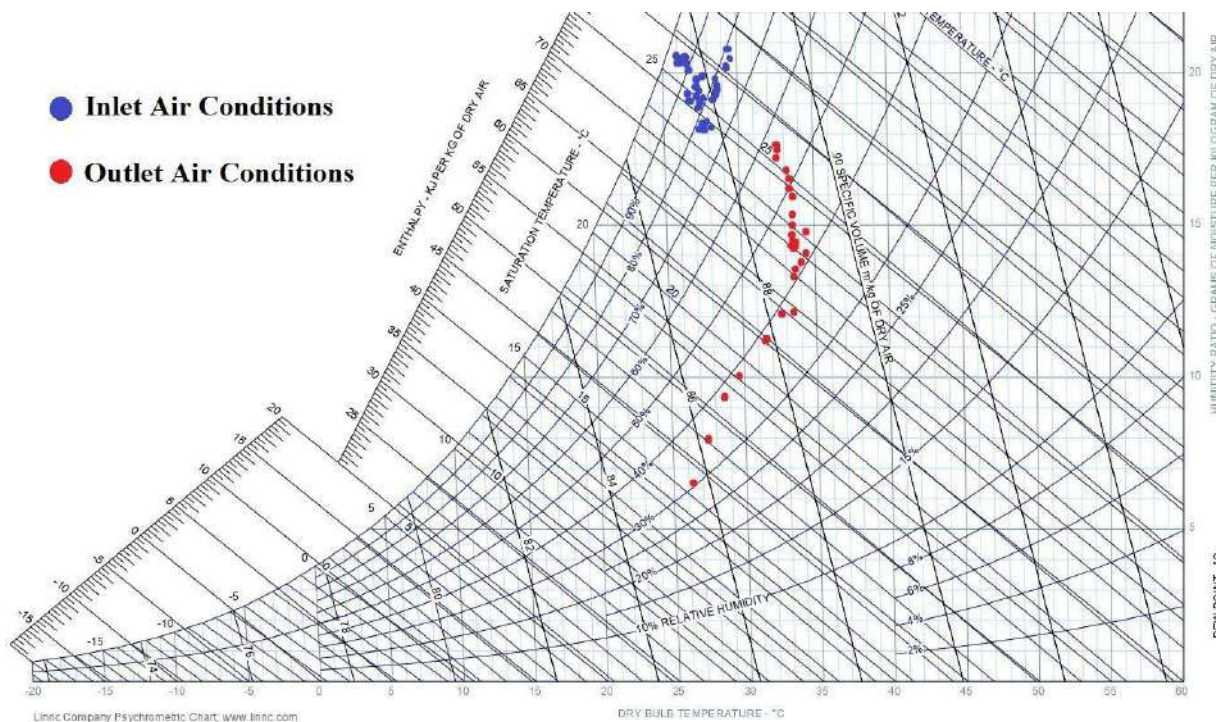


Figure 5.16: Psychrometric Chart Analysis

Humidity ratio of inlet air= 8 g/kg

Humidity ratio of working air= 15.75 g/kg

Amount of Water absorbed= 15.75 g/kg – 8 g/kg

Amount of Water Absorbed= 7.75 g/kg = 8 ml

Percentage absorption of water= $((15.75-8) / 8) \times 100$

Percentage absorption of water= 96.88 %

Chapter 6

6.1 Conclusion and Future Recommendations

6.1.1 Conclusion

In this research, several design variant prototypes of dew point indirect evaporative cooler (DP-IEC) have developed by using the locally available low-cost materials. The performance of some design variant prototypes of DP-IECs have been investigating using optimal design, materials, flow patterns, simulation, and experiments. The experimentation of some DVPs were performed under actual as well as controlled climatic conditions. In experimentation, the ambient parameters have changed under the real climate conditions with a wide range including ambient air temperature and relative humidity.

Some major findings of this thesis are given in the following statements:

1. The performing indicators (effectiveness, CC, COP, and EER etc.) of the dew point indirect evaporative cooler depends mostly on ambient air temperature, relative humidity, length, and width of the channels, working air ratio, and feed water temperature. The energy efficiency ratio of the dew point indirect evaporative cooler is affected by the power consumption of the system. An improved design of heat and mass exchanger (HMX) of the DP-IEC is a compromise dewpoint/wet bulb effectiveness and energy efficiency ratio.
2. A thorough experimental investigation of the design variant prototype 03 was performed under controlled conditions. The inlet parameters like air temperature (33-49 °C) and relative humidity (13% and 20%) were varied under an extensive range of ambient conditions. The comparative investigations were in terms of COP, energy efficiency ratio, the effectiveness of wet bulb, and dry bulb. It has been notified that maximum temperature difference was achieved at $T_{in}=49\text{ }^{\circ}\text{C}$, $\text{RH}=13\%$, $V=6.1\text{ m/s}$, and

$T_w=20$ °C. The higher temperature difference results in extreme values of CC, COP, and EER which vary from 1595-3334 W, 2.9-6.1, and 9.1-19, respectively.

3. A few more detailed experimental investigations of several DVPs were performed under actual climatic conditions. These comparative investigations were in terms of temperature difference, wet bulb and dew point effectiveness, COP, EER, and CC. It was observed that temperature difference increases by increasing the ambient air temperature and decreasing the relative humidity at fixed values of water temperature and air velocity.
4. It has been also found that the dewpoint/wet bulb effectiveness, cooling capacity, and energy efficiency ratio of the dew point indirect evaporative cooler increase with decreasing the water temperature. The lower temperature of the feed water improves the cooling surface of the outer wall of well channels. So, it absorbs more heat from ambient air of dry channels.
5. For the design variant prototype 06, the minimum supply air temperature is achieved at $T_{in}=45$ °C, RH=27% at fixed values of air flow rate ($V=6.3$ m/s) and water temperature ($T_w=20$ °C). Its dew point effectiveness varied from 0.5 to 0.61 while the wet bulb effectiveness varied from 0.5 to 0.73 under actual climatic conditions. Although higher values of temperature difference causing extreme values of COP, EER, and CC which vary between 8.9-18.8, 30.3-64, and 729.4-1537.6 W respectively.
6. Wettability in wet channels has a significant impact on the performance of the DP-IEC. For the design variant prototype 06, it is found that the efficiency of the system was decreased about 27% when the feed water supply was cut off for a half hour.
7. For the design variant prototype 04, the pressure losses were measured with U-tube barometer. The experimental pressure losses of the DP-IEC were approximately 213

Pa. These experimental results compared with mathematical calculations. The maximum percentage difference of the pressure losses was just 8.6%.

8. The high capacities and energy efficiencies of the dew point indirect evaporative cooler make it more usable than other evaporative systems or cooling systems. It could be used for domestic as well as industrial cooling purposes. It can absorb latent energy from the air and make it cooler for others.
9. For the final product, dehumidifier was connected with the DP-IEC to extract the water from exhaust working air. The water consumption of the DP-IEC is around 2 litres per hour. While the water recovery by using dehumidifier, is around 0.2 litres per hour.

6.1.2 Future recommendations

Results of this research work shows that design variant prototype is energy savings and less water footprint system. So, it is encouraging the commercialization of design variant prototype as a product. The following recommendations are suggested after the conclusion of present research work:

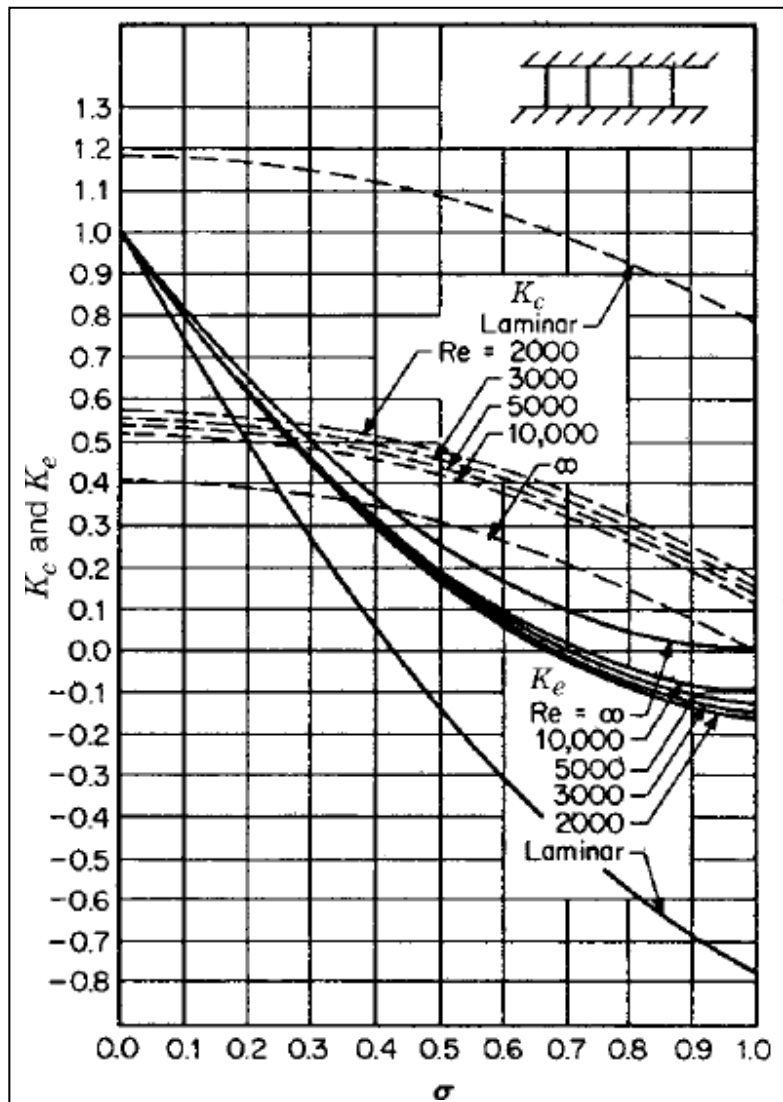
- Optimization of the performance of heat and mass exchanger is the key part of system i.e., increasing effectiveness, coefficient of performance, and energy efficiency ratio of the system.
- Controlling the humidity of the ambient air temperature will be increased the effectiveness of the system.
- Improved the water recovery setup which will be extracted more water from the exhaust air.

Appendix

Appendix A: Design specifications and operating parameters of some design variant prototypes (DVPs)

Parameter	Values					
	DVP-01	DVP-02	DVP-03	DVP-04	DVP-05	DVP-06
HMX width (mm)	17.4	12.4	420	420	300	300
HMX length (mm)	1000	1000	300	300	410	410
HMX height (mm)	500	460	152	300	65	204
Channel height (mm)	04	04	04	04	04	04
Channel width (mm)	25.4	25.4	21.4	21.4	21.4	21.4
Aluminum sheet thickness (mm)	0.3	-	-	-	-	-
Aluminum foil thickness (mm)	-	0.06	-	-	-	-
Polypropylene sheet thickness (mm)	-	-	0.08	0.08	0.08	0.08
Cotton cloth thickness (mm)	0.1	0.1	-	-	-	-
Non-woven fabric thickness (mm)	-	-	0.08	0.08	0.08	0.08
Water holes (mm)	06	06	06	06	06	06
No. of holes in working channel	35	35	30	30	15	15
Air holes (mm)	04	04	04	04	04	04
Total dry channels	01	01	18	36	05	22
Total wet channels	02	02	19	37	06	23
Product to working air ratio (%)	30-70	30-70	40-60	40-60	30-70	30-70
Blower (W)	746	746	-	-	-	-
Axial fan (W)	-	-	550	500	65	70
Water pump (W)	12	12	12	12	25	12

Appendix B: Entrance and exit pressure loss coefficients for multiple square tube core with abrupt contraction and abrupt expansion (Source: kays and London, 1998.)



References

- [1] Dave Marshall-George, “Direct and indirect evaporative cooling strategies,” *Condair*, 2022. <https://www.condair.pk/knowledge-hub/direct-and-indirect-evaporative-cooling-strategies>
- [2] J. GIC, “Indirect evaporative cooling,” *Evapoler*, 2021. <https://www.evapoler.com/product/indirect-evaporative-cooling-decool-4/>
- [3] S. A. Nada, A. Fouda, M. A. Mahmoud, and H. F. Elattar, “Energy & Buildings Experimental investigation of energy and exergy performance of a direct evaporative cooler using a new pad type,” *Energy Build.*, vol. 203, p. 109449, 2019, doi: 10.1016/j.enbuild.2019.109449.
- [4] E. Naderi, B. Sajadi, E. Naderi, and B. Bakhti, “Simulation-based performance analysis of residential direct evaporative coolers in four climate regions of Iran,” *J. Build. Eng.*, p. 101514, 2020, doi: 10.1016/j.job.2020.101514.
- [5] V. Maisotsenko and I. Reyzin, “The maisotsenko cycle for electronics cooling,” *Proc. ASME/Pacific Rim Tech. Conf. Exhib. Integr. Packag. MEMS, NEMS, Electron. Syst. Adv. Electron. Packag. 2005*, vol. PART A, pp. 415–424, 2005, doi: 10.1115/ipack2005-73283.
- [6] J. F. S. J. Alonso, F. J. R. Martínez, E. V. Gómez, and M. A. A. G. Plasencia, “Simulation model of an indirect evaporative cooler,” *Energy Build.*, vol. 29, no. 1, pp. 23–27, 1998, doi: 10.1016/s0378-7788(98)00014-0.
- [7] R. Armbruster and J. Mitrovic, “Evaporative cooling of a falling water film on horizontal tubes,” *Exp. Therm. Fluid Sci.*, vol. 18, no. 3, pp. 183–194, 1998, doi: 10.1016/S0894-1777(98)10033-X.
- [8] P. Finocchiaro, M. Beccali, and B. Nocke, “Advanced solar assisted desiccant and evaporative cooling system equipped with wet heat exchangers,” *Sol. Energy*, vol. 86, no. 1, pp. 608–618, 2012, doi: 10.1016/j.solener.2011.11.003.
- [9] H. Dormido, “These Countries Are the Most at Risk From a Water Crisis,” *Bloomberg*, 2019. <https://www.bloomberg.com/graphics/2019-countries-facing-water-crisis/>
- [10] A. Brunetti, F. Macedonio, G. Barbieri, and E. Drioli, “Membrane condenser as emerging technology for water recovery and gas pre-treatment: current status and perspectives,” *BMC Chem. Eng.*, vol. 1, no. 1, pp. 1–15, 2019, doi:

10.1186/s42480-019-0020-x.

- [11] E. A. Avallone and T. B. Iii, *Marks' standard handbook for mechanical engineers*, vol. 34, no. 06. 1997. doi: 10.5860/choice.34-3330.
- [12] "Acting on Climate Change with HVAC Technology," *Cielo WiGle Inc.*, 2020. <https://cielowigle.com/blog/climate-change/>
- [13] D. H. Gebremeskel, E. O. Ahlgren, and G. B. Beyene, "Long-term evolution of energy and electricity demand forecasting: The case of Ethiopia," *Energy Strateg. Rev.*, vol. 36, no. April, p. 100671, 2021, doi: 10.1016/j.esr.2021.100671.
- [14] L. Pérez-Lombard, J. Ortiz, and C. Pout, "A review on buildings energy consumption information," *Energy Build.*, vol. 40, no. 3, pp. 394–398, 2008, doi: 10.1016/j.enbuild.2007.03.007.
- [15] N. Asim *et al.*, "Sustainability of Heating, Ventilation and Air-Conditioning (HVAC) Systems in Buildings—An Overview," *Int. J. Environ. Res. Public Health*, vol. 19, no. 2, 2022, doi: 10.3390/ijerph19021016.
- [16] E. Sugawara and H. Nikaido, "Properties of AdeABC and AdeIJK efflux systems of *Acinetobacter baumannii* compared with those of the AcrAB-TolC system of *Escherichia coli*," *Antimicrob. Agents Chemother.*, vol. 58, no. 12, pp. 7250–7257, 2014, doi: 10.1128/AAC.03728-14.
- [17] M. Gadalla and M. Saghafifar, "Performance assessment and transient optimization of air precooling in multi-stage solid desiccant air conditioning systems," *Energy Convers. Manag.*, vol. 119, pp. 187–202, 2016, doi: 10.1016/j.enconman.2016.04.018.
- [18] V. Maisotsenko and L. Gillan, "Maisotsenko cycle for air desiccant cooling," *Proc. 2003 4th Int. Symp. Heating, Vent. Air Cond.*, pp. 1011–1020, Jan. 2003.
- [19] A. Pacak and W. Worek, "Review of dew point evaporative cooling technology for air conditioning applications," *Applied Sciences (Switzerland)*, vol. 11, no. 3. pp. 1–16, 2021. doi: 10.3390/app11030934.
- [20] Y. Min, Y. Chen, and H. Yang, "Numerical study on indirect evaporative coolers considering condensation: A thorough comparison between cross flow and counter flow," *Int. J. Heat Mass Transf.*, vol. 131, pp. 472–486, 2019, doi: 10.1016/j.ijheatmasstransfer.2018.11.082.
- [21] Y. Cui, J. Zhu, S. Zoras, and L. Liu, "Review of the recent advances in dew point evaporative cooling technology: 3E (energy, economic and environmental)

- assessments,” *Renew. Sustain. Energy Rev.*, vol. 148, no. June 2020, p. 111345, 2021, doi: 10.1016/j.rser.2021.111345.
- [22] Y. Liu, Y. G. Akhlaghi, X. Zhao, and J. Li, “Experimental and numerical investigation of a high-efficiency dew-point evaporative cooler,” *Energy Build.*, vol. 197, pp. 120–130, 2019, doi: 10.1016/j.enbuild.2019.05.038.
- [23] J. Lin, R. Z. Wang, M. Kumja, T. D. Bui, and K. J. Chua, “Modelling and experimental investigation of the cross-flow dew point evaporative cooler with and without dehumidification,” *Appl. Therm. Eng.*, vol. 121, pp. 1–13, 2017, doi: 10.1016/j.applthermaleng.2017.04.047.
- [24] R. Tariq, C. Zhan, N. A. Sheikh, and X. Zhao, “Thermal performance enhancement of a cross-flow-type maisotsenko heat and mass exchanger using various nanofluids,” *Energies*, vol. 11, no. 10, pp. 1–19, 2018, doi: 10.3390/en11102656.
- [25] R. Tariq, C. Zhan, X. Zhao, and N. A. Sheikh, “Numerical study of a regenerative counter flow evaporative cooler using alumina nanoparticles in wet channel,” *Energy Build.*, vol. 169, pp. 430–443, 2018, doi: 10.1016/j.enbuild.2018.03.086.
- [26] A. Pakari and S. Ghani, “Regression models for performance prediction of counter flow dew point evaporative cooling systems,” *Energy Convers. Manag.*, vol. 185, pp. 562–573, 2019, doi: 10.1016/j.enconman.2019.02.025.
- [27] D. Pandelidis, S. Anisimov, K. Rajski, and E. Brychcy, “Performance comparison of the advanced indirect evaporative air coolers,” *Energy*, vol. 135, pp. 138–152, 2017, doi: 10.1016/j.energy.2017.06.111.
- [28] M. K. Shahzad, M. Ali, N. A. Sheikh, G. Q. Chaudhary, M. S. Khalil, and T. U. Rashid, “Experimental evaluation of a solid desiccant system integrated with cross flow,” *Appl. Therm. Eng.*, no. September, 2017, doi: 10.1016/j.applthermaleng.2017.09.105.
- [29] O. Khalid, M. Ali, N. A. Sheikh, H. M. Ali, and M. Shehryar, “Experimental analysis of an improved Maisotsenko cycle design under low velocity conditions,” *Appl. Therm. Eng.*, vol. 95, pp. 288–295, 2016, doi: 10.1016/j.applthermaleng.2015.11.030.
- [30] M. Ali, W. Ahmad, N. A. Sheikh, H. Ali, R. Kousar, and T. ur Rashid, “Performance enhancement of a cross flow dew point indirect evaporative cooler with circular finned channel geometry,” *J. Build. Eng.*, vol. 35, p. 101980, 2021,

doi: 10.1016/j.jobe.2020.101980.

- [31] S. Anisimov, D. Pandelidis, A. Jedlikowski, and V. Polushkin, "Performance investigation of a M (Maisotsenko) -cycle cross- fl ow heat exchanger used for indirect evaporative cooling," *Energy*, pp. 1–14, 2014, doi: 10.1016/j.energy.2014.08.055.
- [32] B. Rianguvilaikul and S. Kumar, "An experimental study of a novel dew point evaporative cooling system," vol. 42, pp. 637–644, 2010, doi: 10.1016/j.enbuild.2009.10.034.
- [33] R. Kousar, M. Ali, N. A. Sheikh, S. Ihtsham, and S. Khushnood, "Energy for Sustainable Development Holistic integration of multi-stage dew point counter fl ow indirect evaporative cooler with the solar-assisted desiccant cooling system : A techno-economic evaluation," *Energy Sustain. Dev.*, vol. 62, pp. 163–174, 2021, doi: 10.1016/j.esd.2021.04.005.
- [34] E. Zanchini and C. Naldi, "Energy saving obtainable by applying a commercially available M-cycle evaporative cooling system to the air conditioning of an office building in North Italy," *Energy*, vol. 179, pp. 975–988, 2019, doi: 10.1016/j.energy.2019.05.065.
- [35] B. Zheng, C. Guo, T. Chen, Q. Shi, J. Lv, and Y. You, "Development of an experimental validated model of cross-flow indirect evaporative cooler with condensation," *Appl. Energy*, vol. 252, no. 26, p. 113438, 2019, doi: 10.1016/j.apenergy.2019.113438.
- [36] S. Delfani and M. Karami, "Transient simulation of solar desiccant / M-Cycle cooling systems in three different climatic conditions," *J. Build. Eng.*, vol. 29, no. December 2019, p. 101152, 2020, doi: 10.1016/j.jobe.2019.101152.
- [37] R. Boukhanouf, O. Amer, H. Ibrahim, and J. Calautit, "Design and performance analysis of a regenerative evaporative cooler for cooling of buildings in arid climates," *Build. Environ.*, vol. 142, pp. 1–10, 2018, doi: 10.1016/j.buildenv.2018.06.004.
- [38] J. P. Harrouz, K. Ghali, and N. Ghaddar, "Integrated solar – Windcatcher with dew-point indirect evaporative cooler for classrooms," *Appl. Therm. Eng.*, vol. 188, no. February, p. 116654, 2021, doi: 10.1016/j.applthermaleng.2021.116654.
- [39] Z. Duan, "Investigation of a novel dew point indirect evaporative air conditioning system for buildings," no. September, 2011.

- [40] Q. Liu, C. Guo, X. Ma, Y. You, and Y. Li, "Experimental study on total heat transfer efficiency evaluation of an indirect evaporative cooler," *Appl. Therm. Eng.*, vol. 174, no. January, p. 115287, 2020, doi: 10.1016/j.applthermaleng.2020.115287.
- [41] J. Lin, K. Thu, T. D. Bui, R. Z. Wang, K. C. Ng, and K. J. Chua, "Study on dew point evaporative cooling system with counter-flow configuration," vol. 109, pp. 153–165, 2016, doi: 10.1016/j.enconman.2015.11.059.
- [42] M. W. Shahzad, M. Burhan, D. Ybyraiymkul, S. J. Oh, and K. Choon, "An improved indirect evaporative cooler experimental investigation," *Appl. Energy*, vol. 256, no. March, p. 113934, 2019, doi: 10.1016/j.apenergy.2019.113934.
- [43] A. Hasan, "Going below the wet-bulb temperature by indirect evaporative cooling: Analysis using a modified ϵ -NTU method," *Appl. Energy*, vol. 89, no. 1, pp. 237–245, 2012, doi: 10.1016/j.apenergy.2011.07.005.
- [44] F. Z. B. Rasikh Tariq, "Mathematical Modelling and Numerical Simulation of Maisotsenko Cycle," *ICFTE 2017 19th Int. Conf. Fluids Therm. Eng. Room, Italy*, vol. 4, no. 9, 2017, doi: 10.2495/9781845641603/01.
- [45] Z. Duan, C. Zhan, X. Zhao, and X. Dong, "Experimental study of a counter-flow regenerative evaporative cooler," *Build. Environ.*, vol. 104, pp. 47–58, 2016, doi: 10.1016/j.buildenv.2016.04.029.
- [46] M. Ali, N. A. Sheikh, O. Khalid, S. Manzoor, and H. M. Ali, "Parametric investigation of a counter-flow heat and mass exchanger based on Maisotsenko cycle," *Therm. Sci.*, vol. 22, no. 6, pp. 3099–3106, 2018, doi: 10.2298/TSCI160808296A
- [47] H. Caliskan, A. Hepbasli, I. Dincer, and V. Maisotsenko, "Thermodynamic performance assessment of a novel air cooling cycle: Maisotsenko cycle," *Int. J. Refrig.*, vol. 34, no. 4, pp. 980–990, 2011, doi: 10.1016/j.ijrefrig.2011.02.001.
- [48] X. Zhao, J. M. Li, and S. B. Ri, "Numerical study of a novel counter-flow heat and mass exchanger for dew point evaporative cooling," vol. 28, pp. 1942–1951, 2008, doi: 10.1016/j.applthermaleng.2007.12.006.
- [49] M. Jradi and S. Riffat, "Experimental and numerical investigation of a dew-point cooling system for thermal comfort in buildings," *Appl. Energy*, vol. 132, pp. 524–535, 2014, doi: 10.1016/j.apenergy.2014.07.040.
- [50] G. Heidarinejad, M. Bozorgmehr, S. Delfani, and J. Esmaeliani, "Experimental

investigation of two-stage indirect / direct evaporative cooling system in various climatic conditions,” vol. 44, pp. 2073–2079, 2009, doi: 10.1016/j.buildenv.2009.02.017.

- [51] “UNDERSTANDING COP (COEFFICIENT OF PERFORMANCE),” *Adams Air Conditioning*, 2019. <https://www.adams-air.com/houston/what-is-COP.php>
- [52] B. Purushothama, “Definitions of terms used in humidification engineering,” in *Humidification and Ventilation Management in Textile Industry*, 2009, pp. 227–252. doi: 10.1533/9780857092847.227.
- [53] B. An and A. I. R. Conditioner, “Central air conditioners and heat pumps are rated by the Energy Efficiency Ratio (EER).,” *Pacific Gas Electr. Co.*, p. 2, 2006.
- [54] W. S. Chang and L. W. Swanson, *Fundamentals of heat pipes*. 1994.
- [55] R. Tariq, N. A. Sheikh, J. Xamán, and A. Bassam, “An innovative air saturator for humidification-dehumidification desalination application,” *Appl. Energy*, vol. 228, pp. 789–807, 2018, doi: 10.1016/j.apenergy.2018.06.135.
- [56] Jack P. Holman, *Heat Transfer (Tenth Edition)*. 2013.

Annexure

Annexure (if any) should be placed at the end of the project report.